Galactic Discs as Complex Dynamical Systems

Panos Patsis

RCAAM, Academy of Athens

Structures observed in disk galaxies:

Bars and Spirals

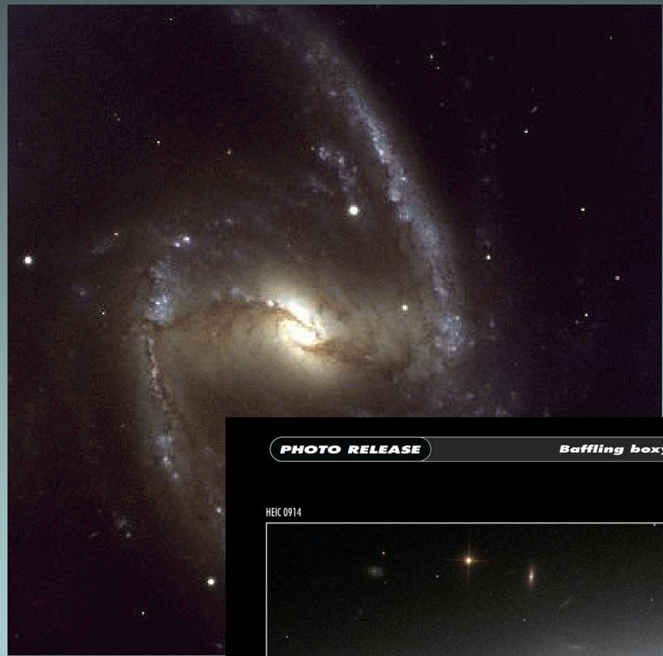

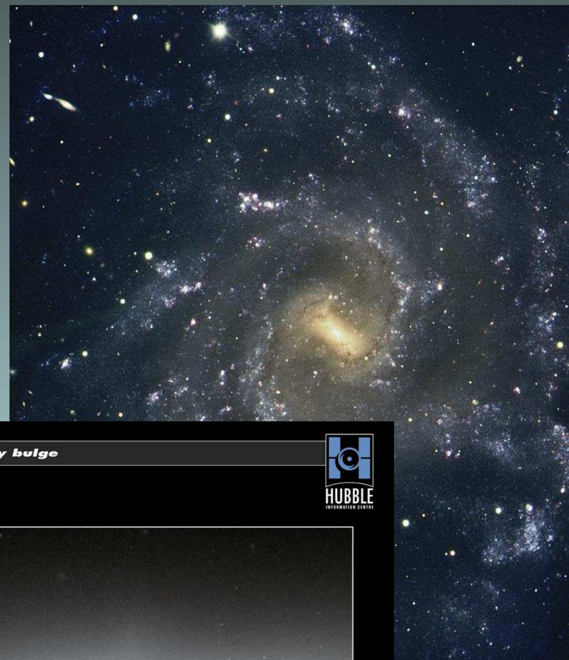

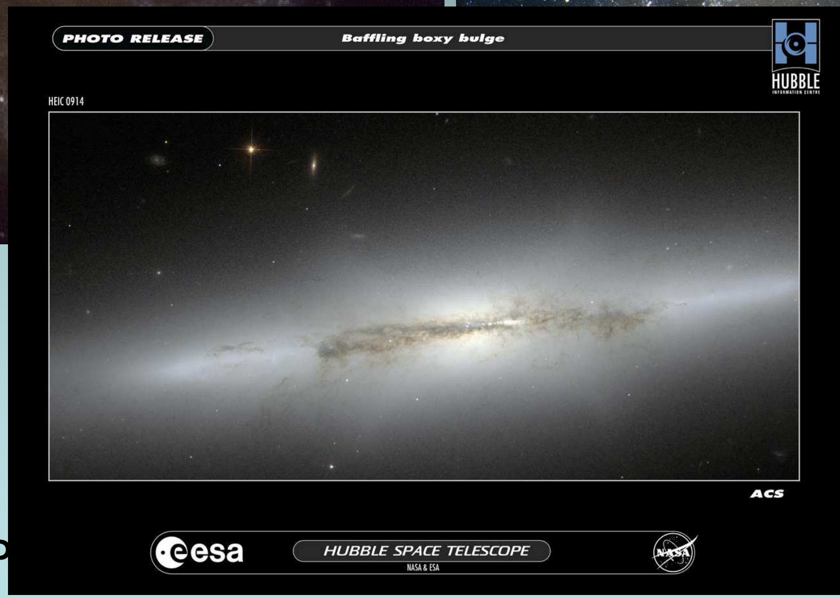

Goal: Understanding the dynamical mechanisms that support the observed structures

(Finding the tools for building galaxies)

"Modeling is neither science nor mathematics; it is the craft that builds bridges between the two."

F. Morrison, "The art of modeling dynamic systems" (1991)

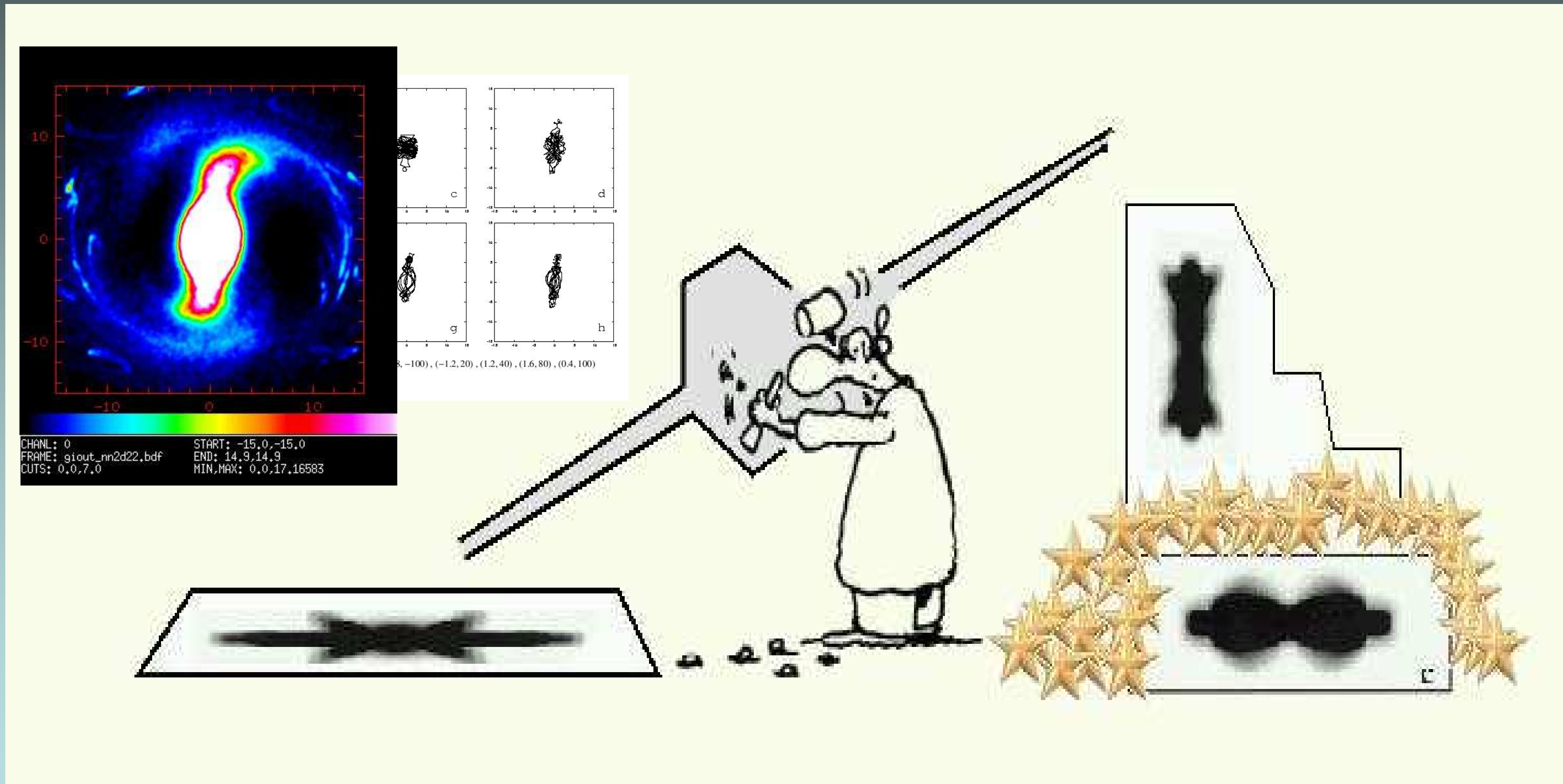

Goal: Understanding the dynamical mechanisms that support the observed structures

What is the dynamical field for our calculations?

Gravitational Potential

$$\Phi=\Phi_0(r) + \Phi_1(r,\theta)$$

A. Analytic potentials. Best: Assumptions based on observational Data (Photometry, Kinematics)

Measured quantities, but "snapshots"

B. Results of self-gravitating N-body simulations

Models; however, evolving in time

Observational input: I. Photometry

- NGC 1300 (VLT, HAWK-I)

NGC 128 (2.3m Aristarchos)

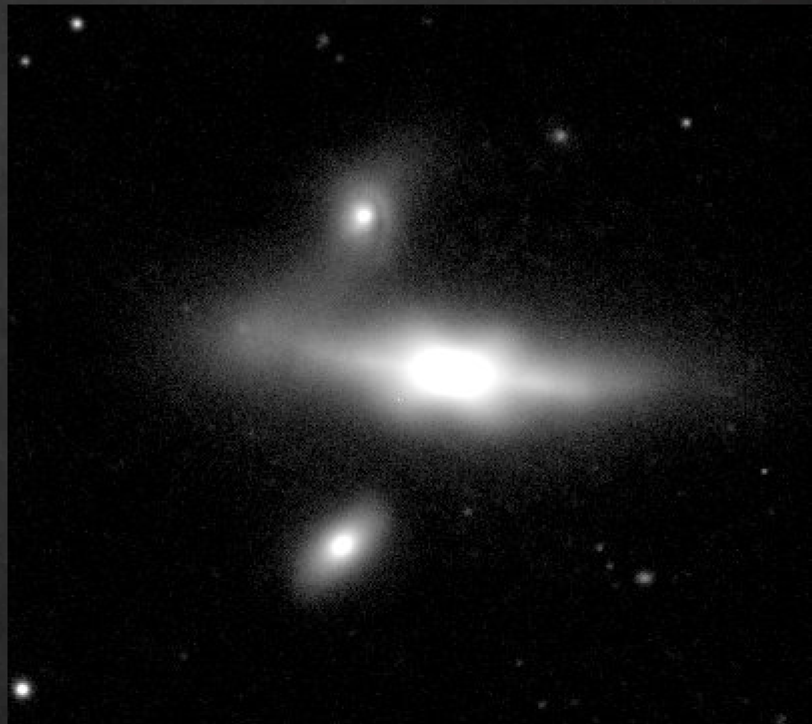

The general morphology

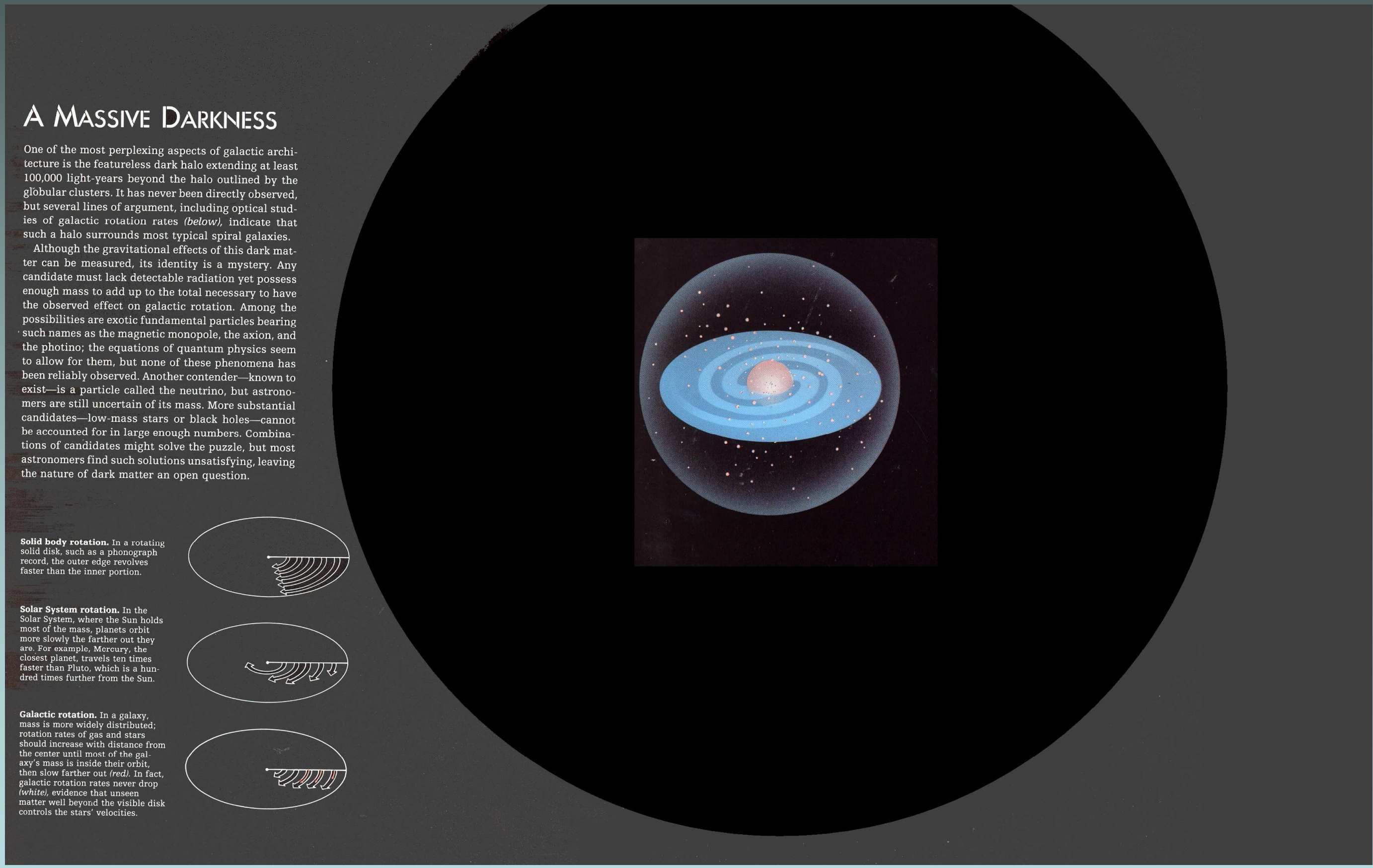

A Massive Darkness

One of the most perplexing aspects of galactic architecture is the featureless dark halo extending at least 100,000 light-years beyond the halo outlined by the globular clusters. It has never been directly observed, but several lines of argument, including optical studies of galactic rotation rates *(below)*, indicate that such a halo surrounds most typical spiral galaxies.

Although the gravitational effects of this dark matter can be measured, its identity is a mystery. Any candidate must lack detectable radiation yet possess enough mass to add up to the total necessary to have the observed effect on galactic rotation. Among the possibilities are exotic fundamental particles bearing such names as the magnetic monopole, the axion, and the photino; the equations of quantum physics seem to allow for them, but none of these phenomena has been reliably observed. Another contender—known to exist—is a particle called the neutrino, but astronomers are still uncertain of its mass. More substantial candidates—low-mass stars or black holes—cannot be accounted for in large enough numbers. Combinations of candidates might solve the puzzle, but most astronomers find such solutions unsatisfying, leaving the nature of dark matter an open question.

Solid body rotation. In a rotating solid disk, such as a phonograph record, the outer edge revolves faster than the inner portion.

Solar System rotation. In the Solar System, where the Sun holds most of the mass, planets orbit more slowly the farther out they are. For example, Mercury, the closest planet, travels ten times faster than Pluto, which is a hundred times further from the Sun.

Galactic rotation. In a galaxy, mass is more widely distributed; rotation rates of gas and stars should increase with distance from the center until most of the galaxy's mass is inside their orbit, then slow farther out *(red)*. In fact, galactic rotation rates never drop *(white)*, evidence that unseen matter well beyond the visible disk controls the stars' velocities.

- Bulge
- Disk
- Halo

Τα άστρα περιστρέφονται γύρω από το κέντρο του γαλαξία σε σχεδόν κυκλικές τροχιές

Observational input: II. Kinematics

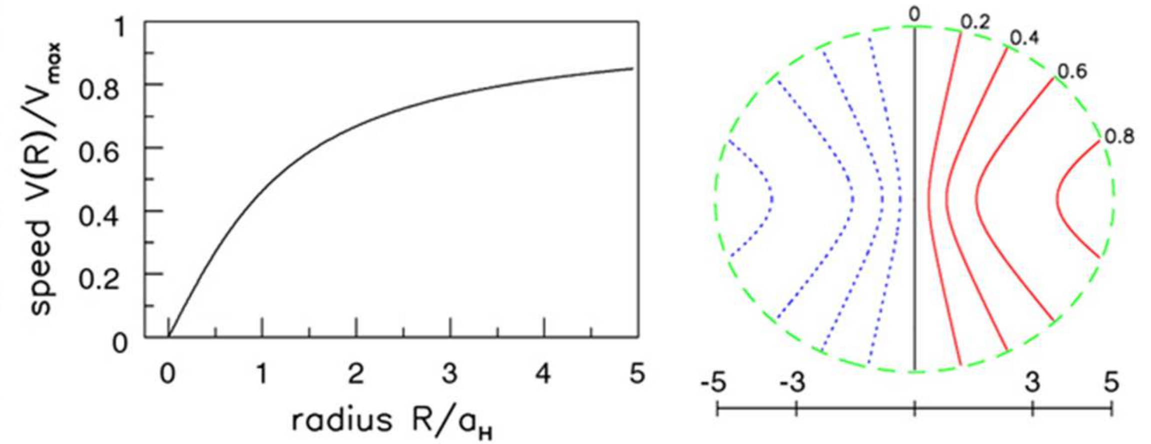

Fig 5.19 'Galaxies in the Universe' Sparke/Gallagher CUP 2007

Kinematics along an axis – Rotation curves

Simplified Rotational Dynamics for Baryonic Disks of Spiral Galaxies - What do we Expect?

$$\frac{GM_G m_s}{r^2} = \frac{m_s v_s^2}{r}$$

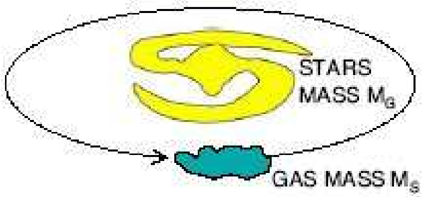

$$v_s = \sqrt{\frac{GM_G}{r}}$$

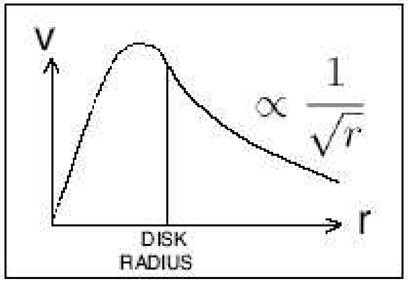

"The test of all knowledge is experiment"

(R. P. Feynmann, The Feynmann Lectures on Physics, volume 1, section 1-1.)

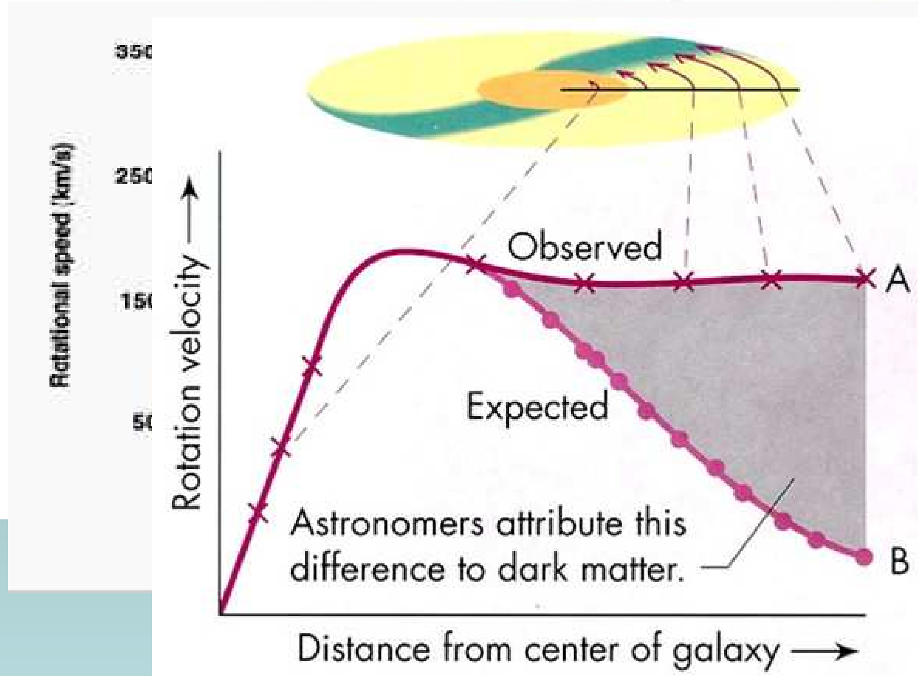

$$\Phi_0(r) = \Phi_D + \Phi_b + \Phi_H$$

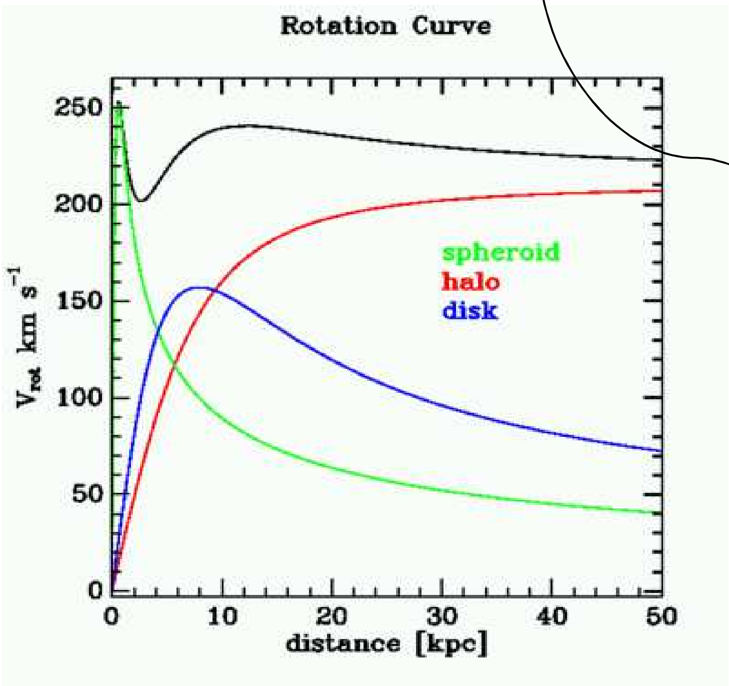

$$v_c^2 = r\frac{d\Phi}{dr}$$

$$V_{tot}^2 = V_D^2 + V_b^2 + V_H^2$$

$\Phi_o(r)$

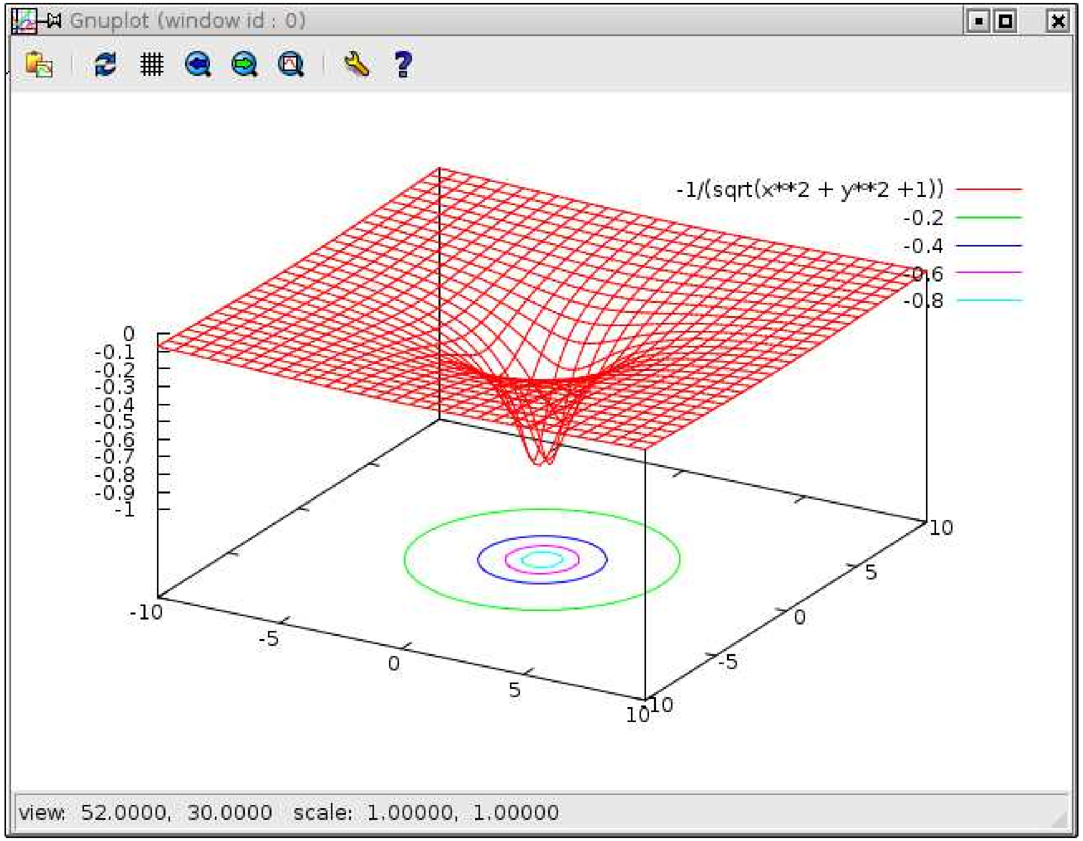
Gnuplot (window id : 0)
-1/(sqrt(x**2 + y**2 +1))
-0.2
-0.4
-0.6
-0.8
0
-0.1
-0.2
-0.3
-0.4
-0.5
-0.6
-0.7
-0.8
-0.9
-1
-10
-5
0
5
10
10
5
0
-5
-10
view: 52.0000, 30.0000 scale: 1.00000, 1.00000

The perturbations (spirals & bars)

$$\Phi = \Phi_0(r) + \Phi_1(r,\theta)$$

Normal, Grand Design Spirals are logarithmic

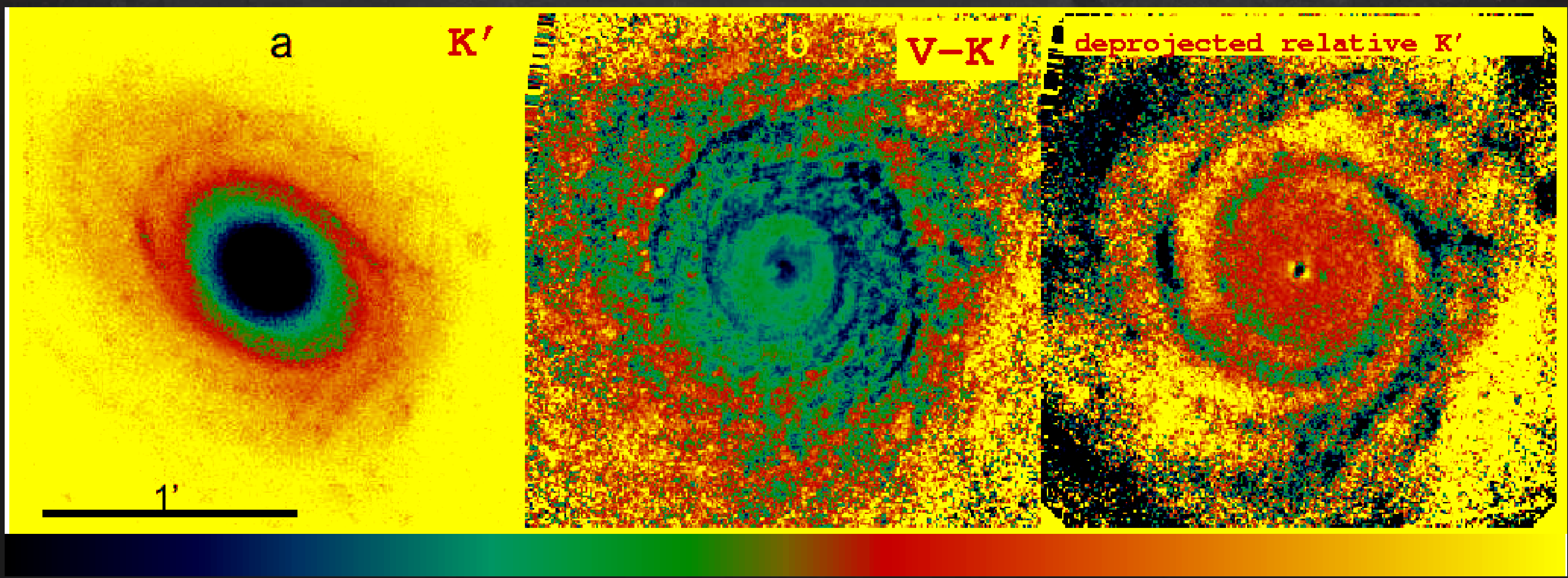

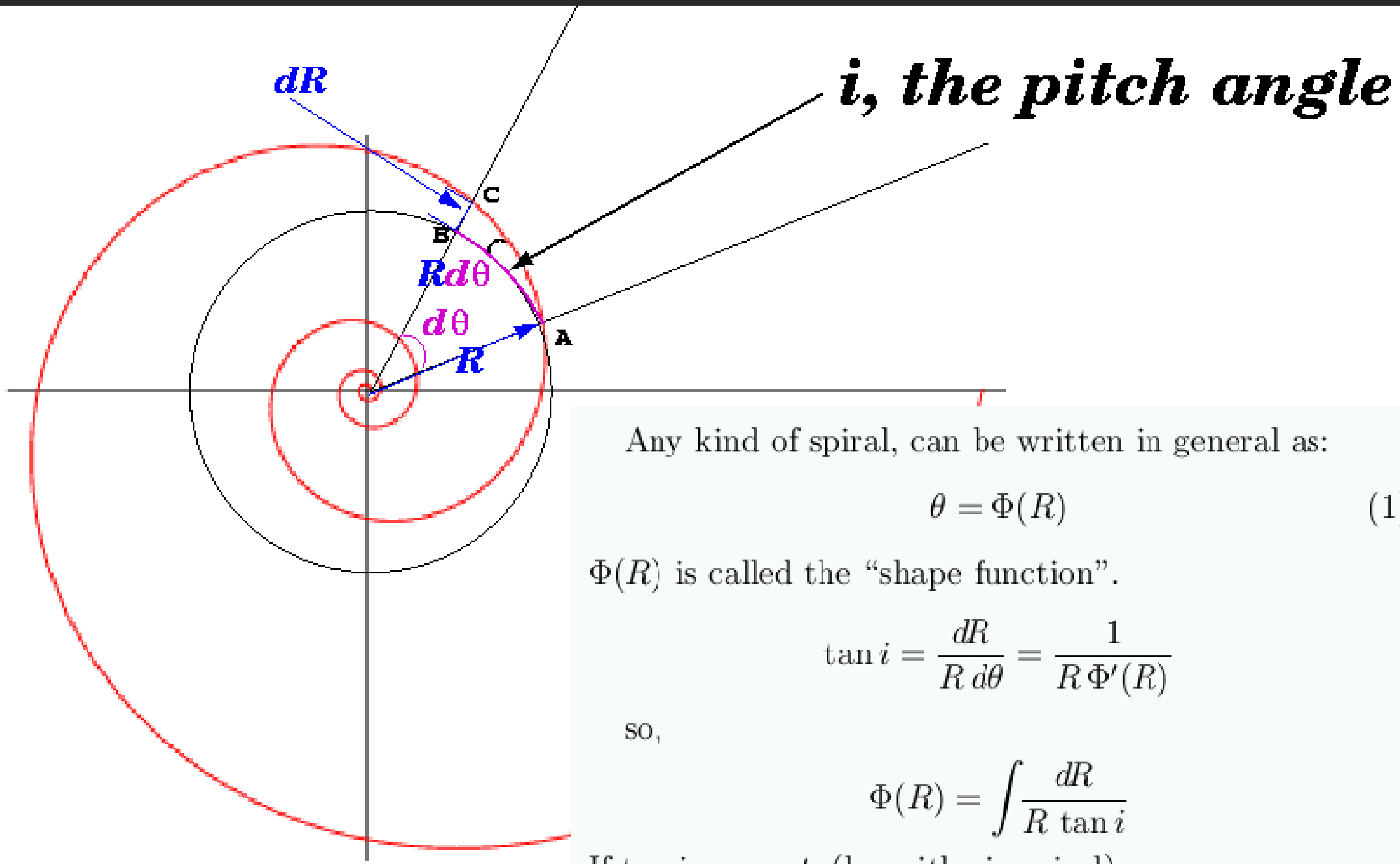

Any kind of spiral, can be written in general as:

$$\theta = \Phi(R) \tag{1}$$

$\Phi(R)$ is called the "shape function".

$$\tan i = \frac{dR}{R\,d\theta} = \frac{1}{R\,\Phi'(R)}$$

so,

$$\Phi(R) = \int \frac{dR}{R\,\tan i}$$

If $\tan i = const.$ (logarithmic spiral),

$$\Phi(R) = \theta = \frac{\ln R}{\tan i} + c = a\,\ln R + c$$

This means, that in a $(\ln R, \theta)$ diagram a logarithmic spiral will appear as a straight line.

Usually it is written:

$$R = e^{a\theta} \tag{2}$$

i=90° is a bar

$$V_1(r,\theta) = Ar\exp(-\varepsilon_s r)\cos(2\ln r/\tan i_0 - 2\theta)$$

Contopoulos & Grosbol 1986

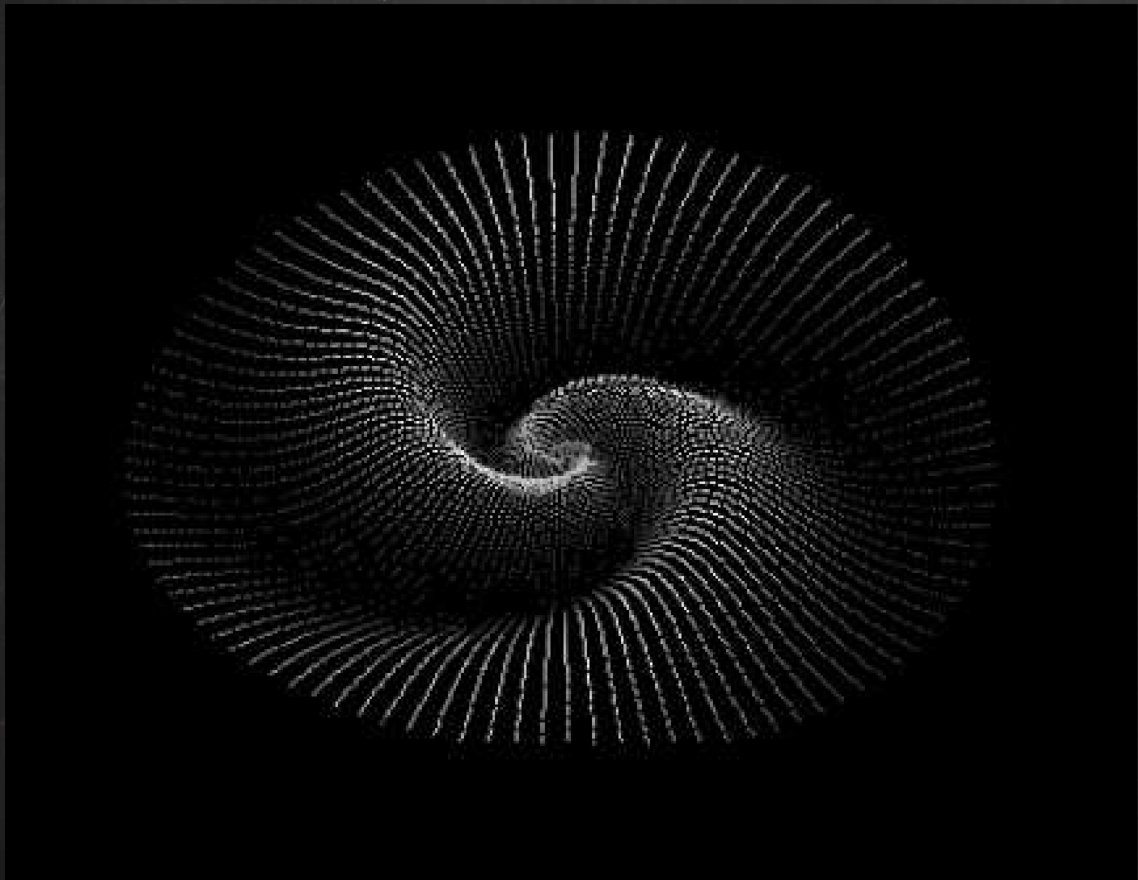

Pitch angle – the angle i at any radius r between the tangent to the arm and the circle at r = constant.

$$\cot i = \left| R \frac{\partial \phi}{\partial R} \right|$$

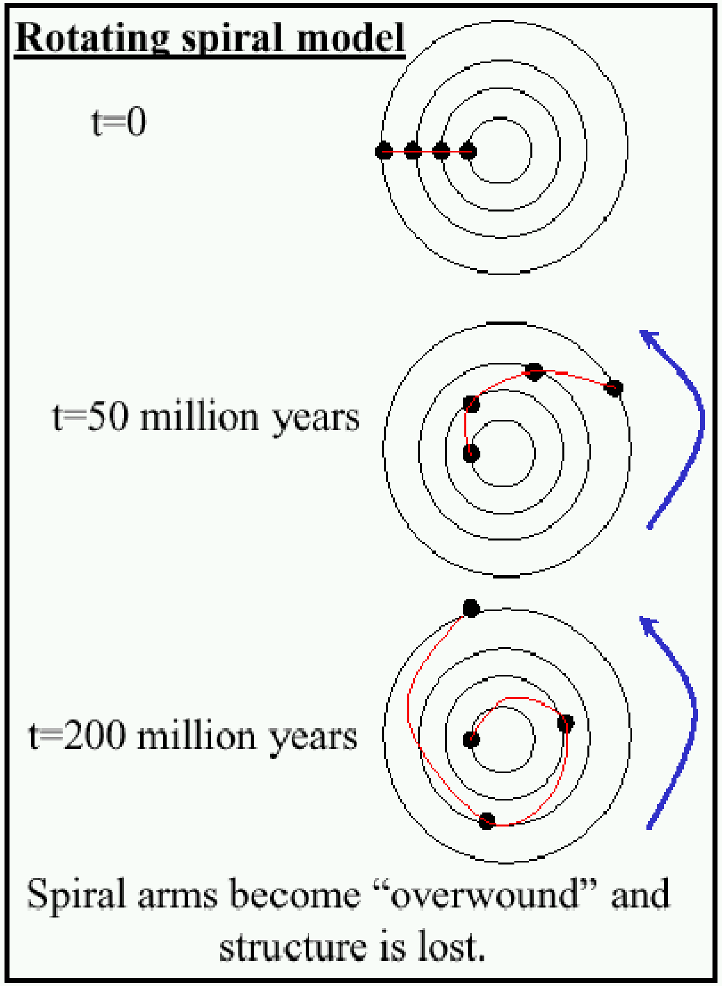

$$\phi(R,t) = \phi_o + \Omega(R)t$$

What happens to out pitch angle with time?

$$\cot i = \left| R \frac{\partial \phi}{\partial R} \right|$$

$$\phi(R,t) = \phi_o + \Omega(R)t$$

$$\cot i = R \left| \frac{\partial \Omega(R)}{\partial R} \right| t = \frac{vt}{R}$$

For v = 220 km/s, R = 10 kpc, and t = 10^{10} yr

i = 0.25 degrees and the inter-arm spacing **D**R = 0.28 kpc.

DW example

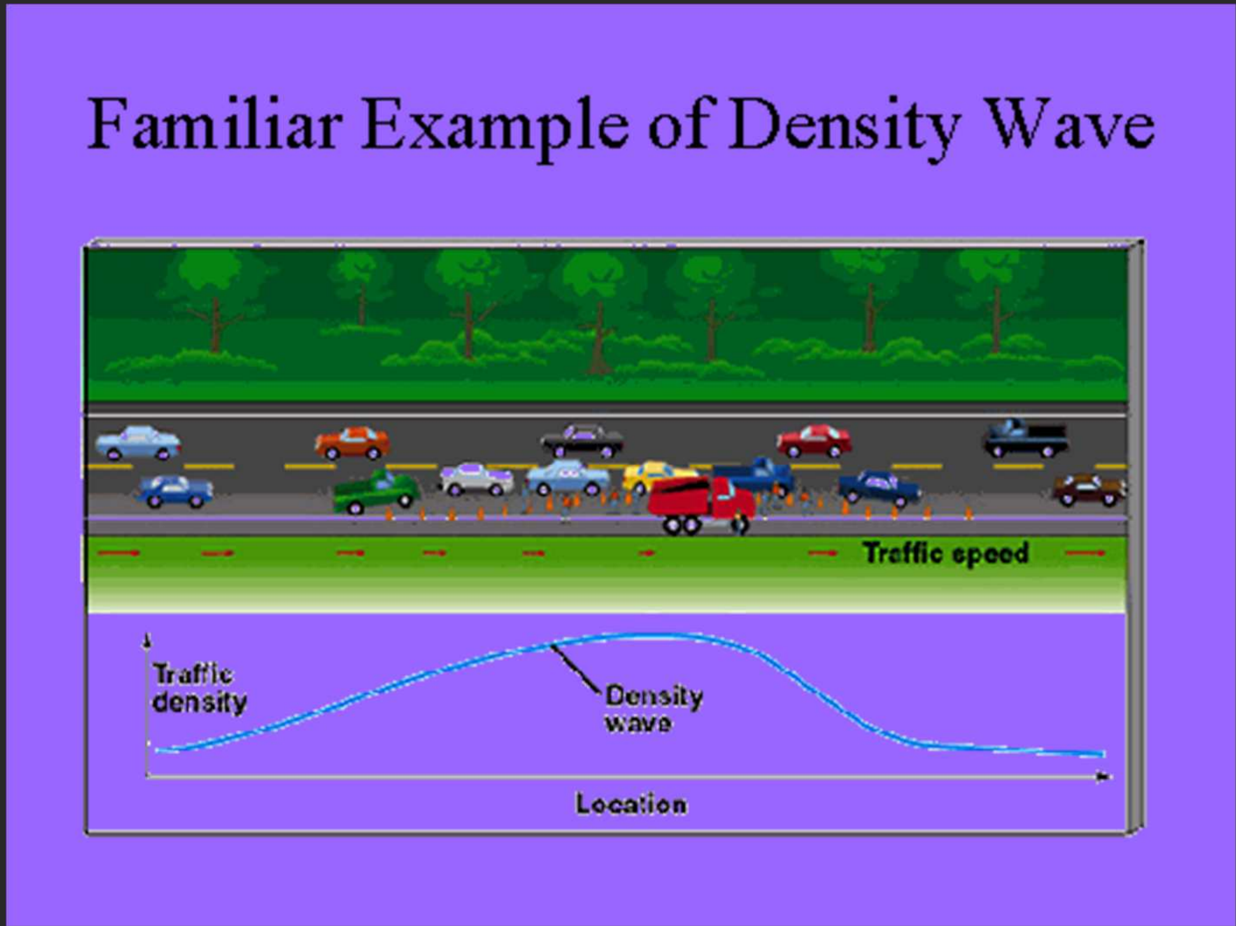
Familiar Example of Density Wave
Traffic speed
Traffic density
Density wave
Location

The standard picture of a density wave
A sketch by Kalnajs (1973), PASA 2, 174

- ...take a number of orbits, make them eccentric, line up their major axes....have created a bar shaped density wave
- ...we can also make spiral waves ...rotate the major axes according to the rule $\theta = -\alpha \log(\text{major axis}) + \text{constant}$.
- ...Thus there will be a systematic inward velocity at the density maximum or arm.

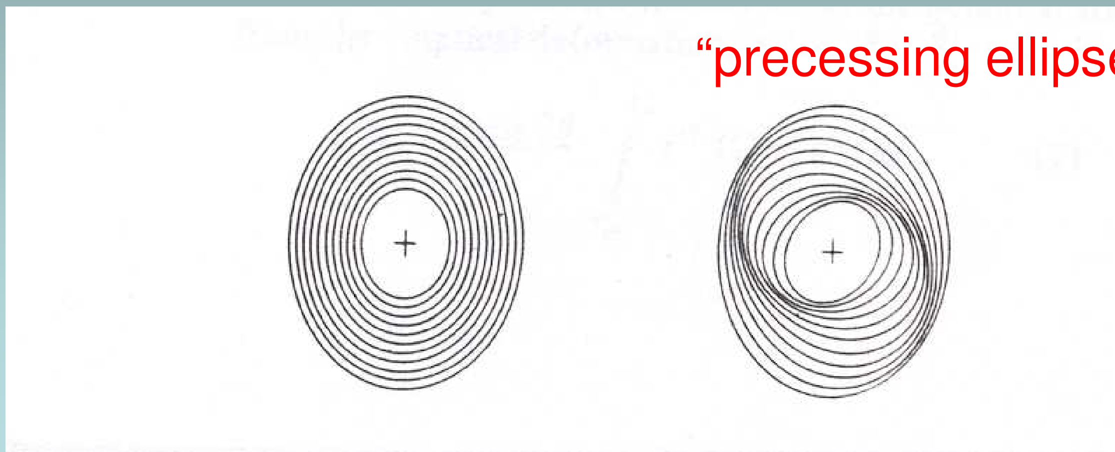

μια τροχιά σαν του Ήλιου

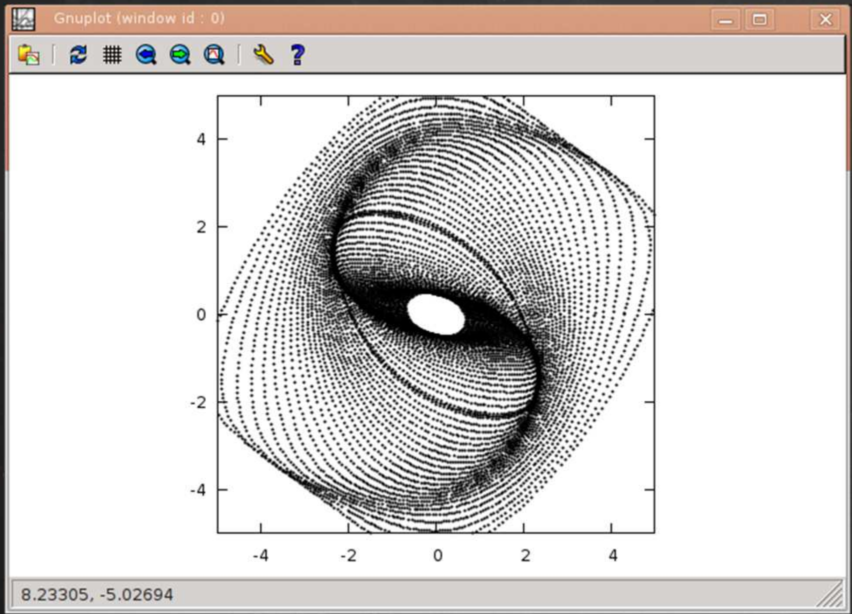

Περίοδος 250 Myr

Εξαφάνιση δεινοσαύρων πριν ~60Myr

Απόσταση μεταξύ κουκίδων ~4Myr

Πρώτοι Homo Sapiens πριν <0.2 Myr

Επίπεδα CO2 πέφτουν σε επίπεδα που δεν μπορεί να γίνει φωτοσύνθεση (Franck et al. 2005, Biog. Dis. 2, 1665) – σε 4 περιόδους από σήμερα.

Στις σπείρες γεννιούνται άστρα

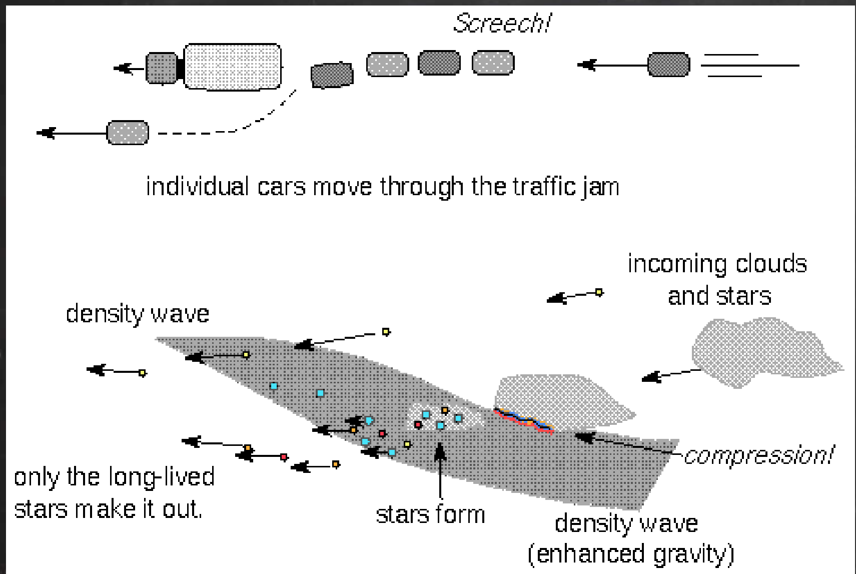

Spiral density waves are like traffic jams. Clouds and stars speed up to the density wave (are accelerated toward it) and are tugged backward as they leave, so they accumulate in the density wave (like cars bunching up behind a slower-moving vehicle). Clouds compress and form stars in the density wave, but only the fainter stars live long enough to make it out of the wave.

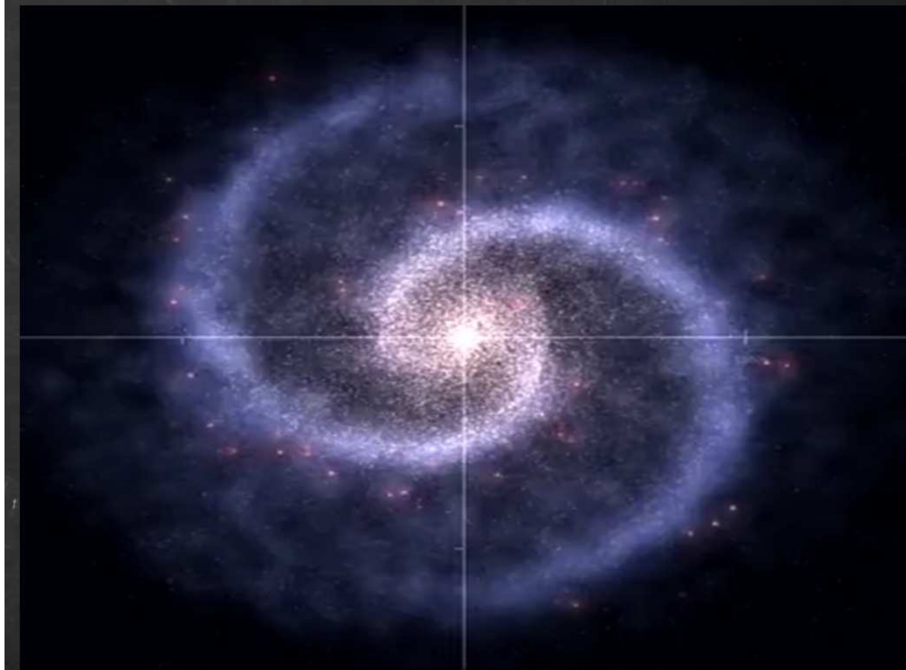

Potentials from N-body simulations

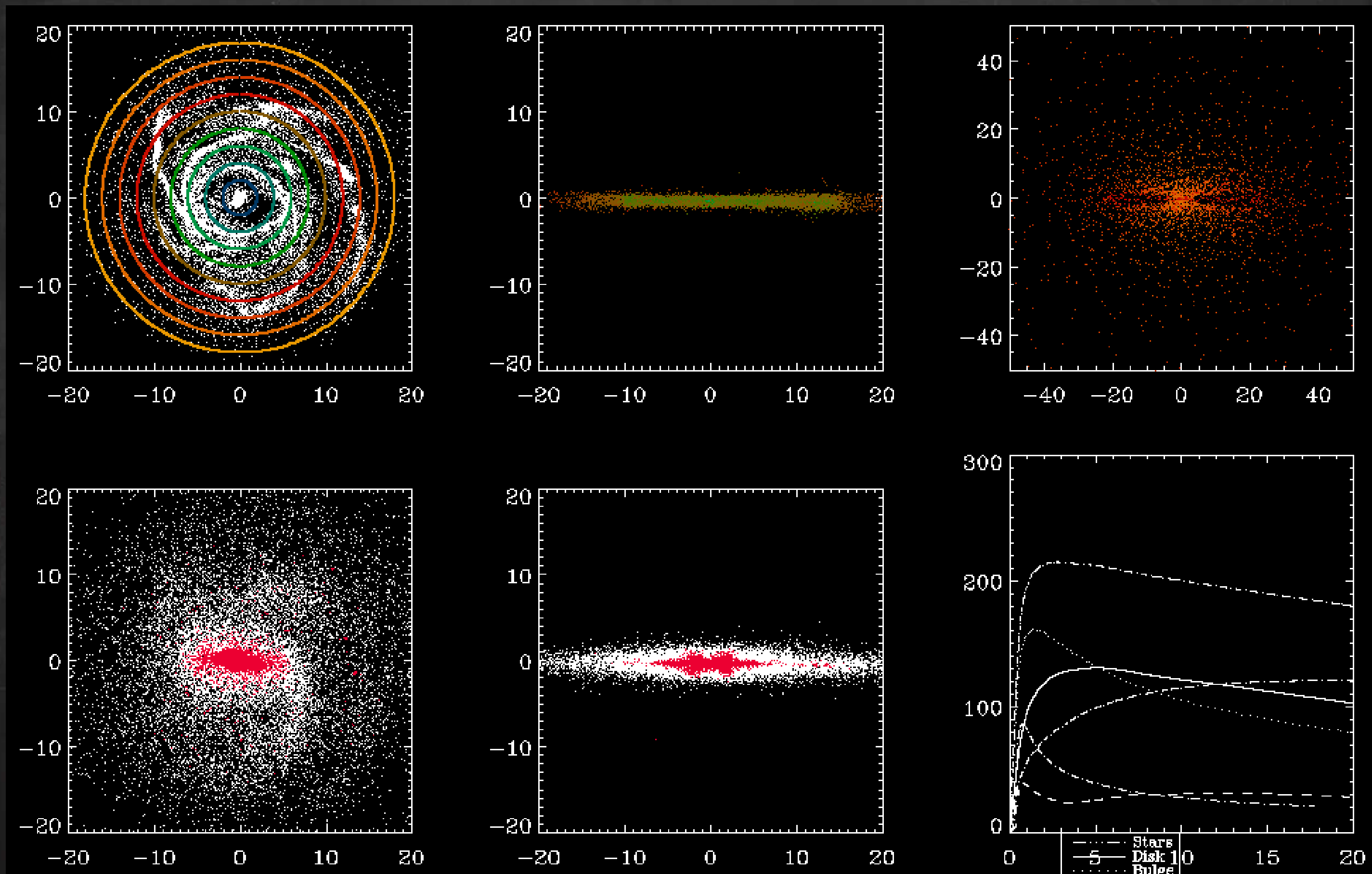

Time independence

- Morphology consistency
- N-body simulations

Structures (especially bars) last for several Gyr. We are legitimated to seek the dynamical mechanisms in time-independent gravitational potentials

Rotating stars and systems

Orbits of stars can be considered as being close but deviating from circular around the center of the system, on the equatorial plane.

This can be described as a combination of circular & epicyclic motion

The pattern (i.e. the system) rotates as well

Ω, Ω_p και κ

Δισκοειδείς γαλαξίες. Περιστρέφονται με γωνιακή ταχύτητα Ω_p . Σε αυτό το σύστημα ο γαλαξίας παραμένει στατικός.

Οι δύο αντίστοιχες, βασικές συχνότητες: $(\Omega - \Omega_p)$ και κ

Ω, Ω_p and κ – RESONANCES

$$\frac{\kappa}{(\Omega - \Omega_p)} = \frac{n}{m}$$

- $n/m = \pm 2/1$ Lindblad Resonances

- $\Omega = \Omega_p$ COROTATION

Συντονισμοί

resonances between the epicyclic frequency κ and the angular velocity in the rotating frame $(\Omega - \Omega_s)$ (where Ω and Ω_s are the angular velocities of the stars and of the spiral pattern), i.e. when

V

$$\frac{\kappa}{\Omega - \Omega_s} = \frac{n}{m} .$$

n/m = 2/1   Inner Lindblad Resonance

= 4/1   Inner 4:1 (UHR)

$\Omega = \Omega_\varsigma$ ***COROTATION***

n/m = –4/1   Outer 4:1

= –2/1   Outer Lindblad Resonance

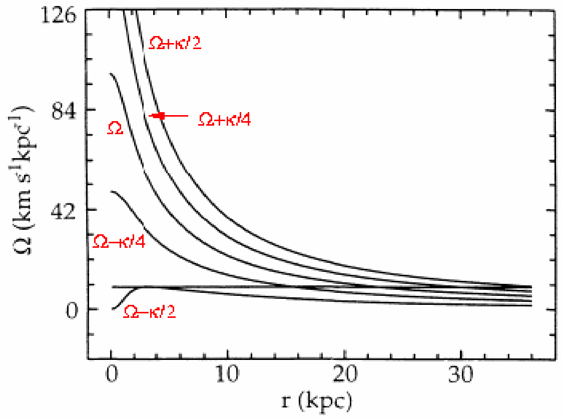

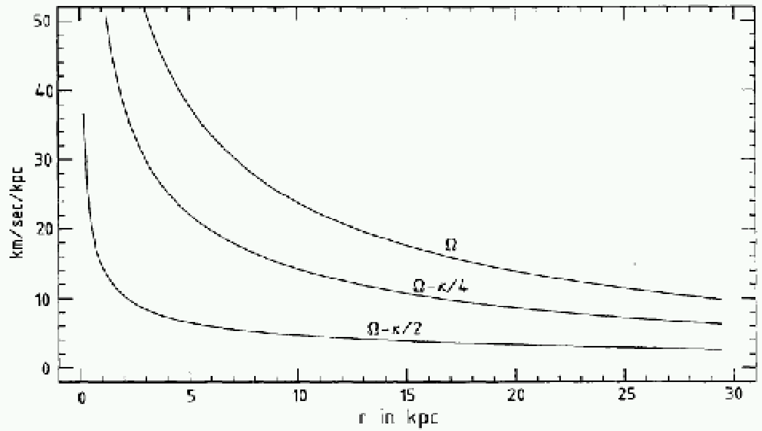

Disk galaxies as autonomous Hamiltonian systems

Orbits in barred/spiral rotating potentials

The equations of motion are derived from the Hamiltonian,

$$H \equiv \frac{1}{2}(\dot{x}^2 + \dot{y}^2) + \Phi(x, y) - \frac{1}{2}\Omega_b^2(x^2 + y^2) = E_J \,, \quad (2)$$

where (x, y) are the coordinates in a Cartesian frame of reference corotating with the bar with angular velocity Ω_b, $\Phi(x, y)$ is the potential in Cartesian coordinates, E_J is the numerical value of the Jacobian integral, and dots denote time derivatives. Throughout this paper E_J is given in (km $\mathrm{s}^{-1})^2$. We use a fourth-order Runge-Kutta integration scheme with a variable step. We find the periodic orbits by

Equations of motion are derived from the Hamiltonian

$$H \equiv \frac{1}{2}\left(\dot{x}^2 + \dot{y}^2\right) + \Phi(x,y) - \frac{1}{2}\Omega_s^2(x^2+y^2) = E_J \qquad (4)$$

where (x, y) are the coordinates in a Cartesian frame of reference corotating with the spiral with angular velocity Ω_s. $\Phi(x, y)$ is the potential in Cartesian coordinates, E_J is the numerical value of the Jacobian integral and dots denote time derivatives.

Effective potential
takes care of Coriolis forces

E_J, the Jacobi integral, is the rotating-frame analog of the total energy

Ενεργό δυναμικό (effective potential)- καμπύλες μηδενικής ταχύτητας

$$E_J = \frac{1}{2}\left|\dot{r}\right|^2 + \Phi_{eff}$$

Επιφάνεια μηδενικής ταχύτητας $\quad \Phi_{eff} = E_J$

Απαγορευμένη περιοχή $\quad \Phi_{eff} > E_J$

The role of periodic orbits

Order +Chaos (2D case)

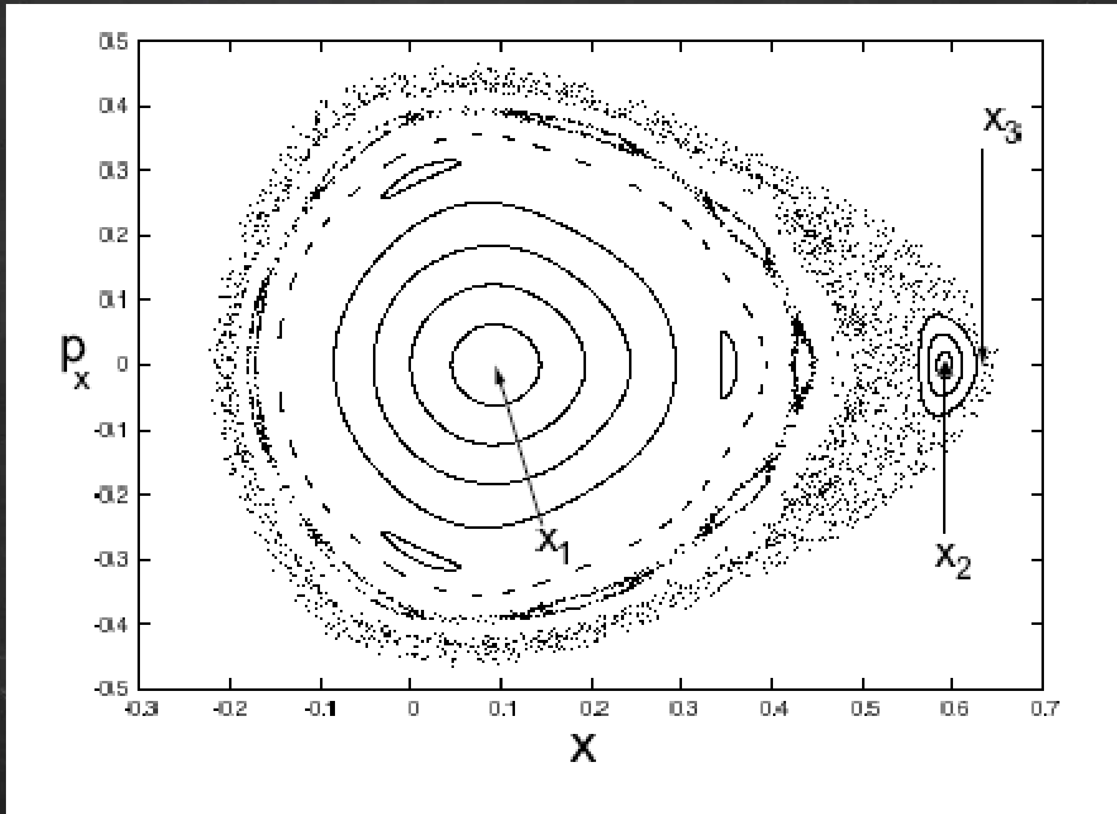

Integration → Finding p.o. → Characteristics

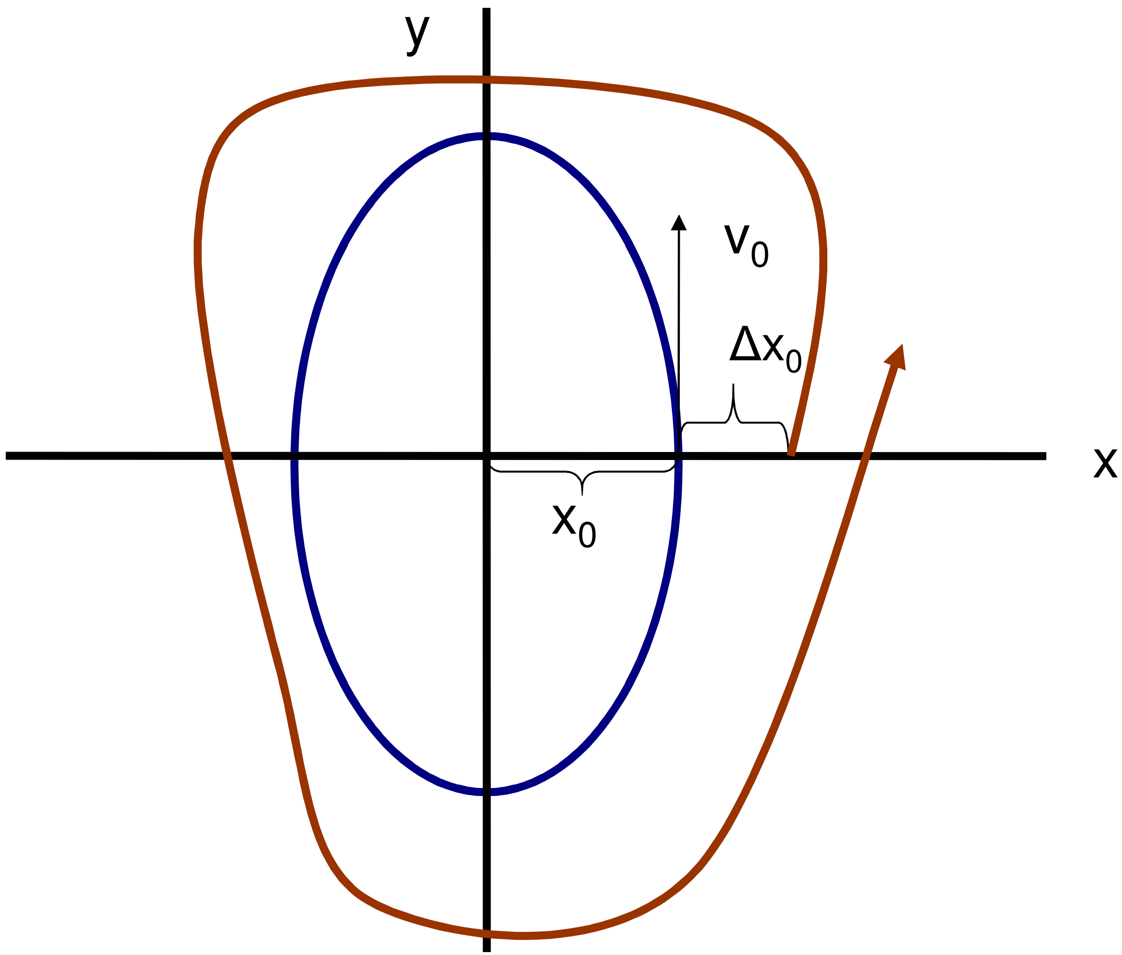

Διατηρητικά συστήματα 2 βαθμών ελευθερίας
– η σημασία των περιοδικών τροχιών

Οικογένεια π.τ.:

$$x_0 = f(x_0, y_0, \varepsilon)$$

$$y_0 = g(x_0, y_0, \varepsilon)$$

- Χαρακτηριστική οικογένειας περιοδικών τροχιών

Η καμπύλη που δίνει το x_0 (ή το y_0) συναρτήσει του ε

Δυναμικό ράβδων

Μέγιστα πυκνότητας→Ελάχιστα δυναμικού

$\Phi(r,\theta)=A(r) * \cos(2\theta+\theta_0)$

π.χ. $A(r) = A$

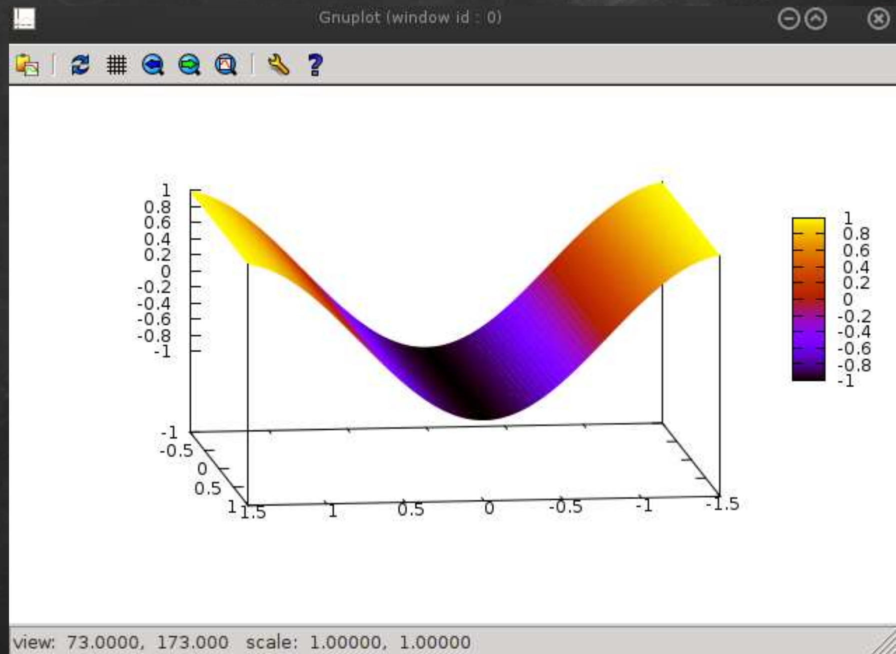

The amplitude of the term cos (2θ) has been taken either of the form (Barbanis and Woltjer 1967)

$$A = \varepsilon r^{\frac{1}{2}}(16 - r), \tag{7}$$

The Ferrers bar has a volume density of

$$\rho(x, y, z) = \begin{cases} \rho_0(1 - g^2)^n & \text{for } g < 1 \\ 0 & \text{for } g \geqslant 1, \end{cases} \tag{3}$$

where $g^2 = x^2/a^2 + (y^2 + z^2)/b^2$, a and b are the semimajor and semiminor axes of the bar ($a > b$), ρ_0 is its central density and (x, y, z) are the Cartesian coordinates in the corotating frame. In our

a Fourier series,

$$\Phi(r, \theta) = \Phi_0(r) + \sum_{m>0} [\Phi_{mc}(r) \cos m\theta + \Phi_{ms}(r) \sin m\theta]$$

NGC 4314 in 2.1μm

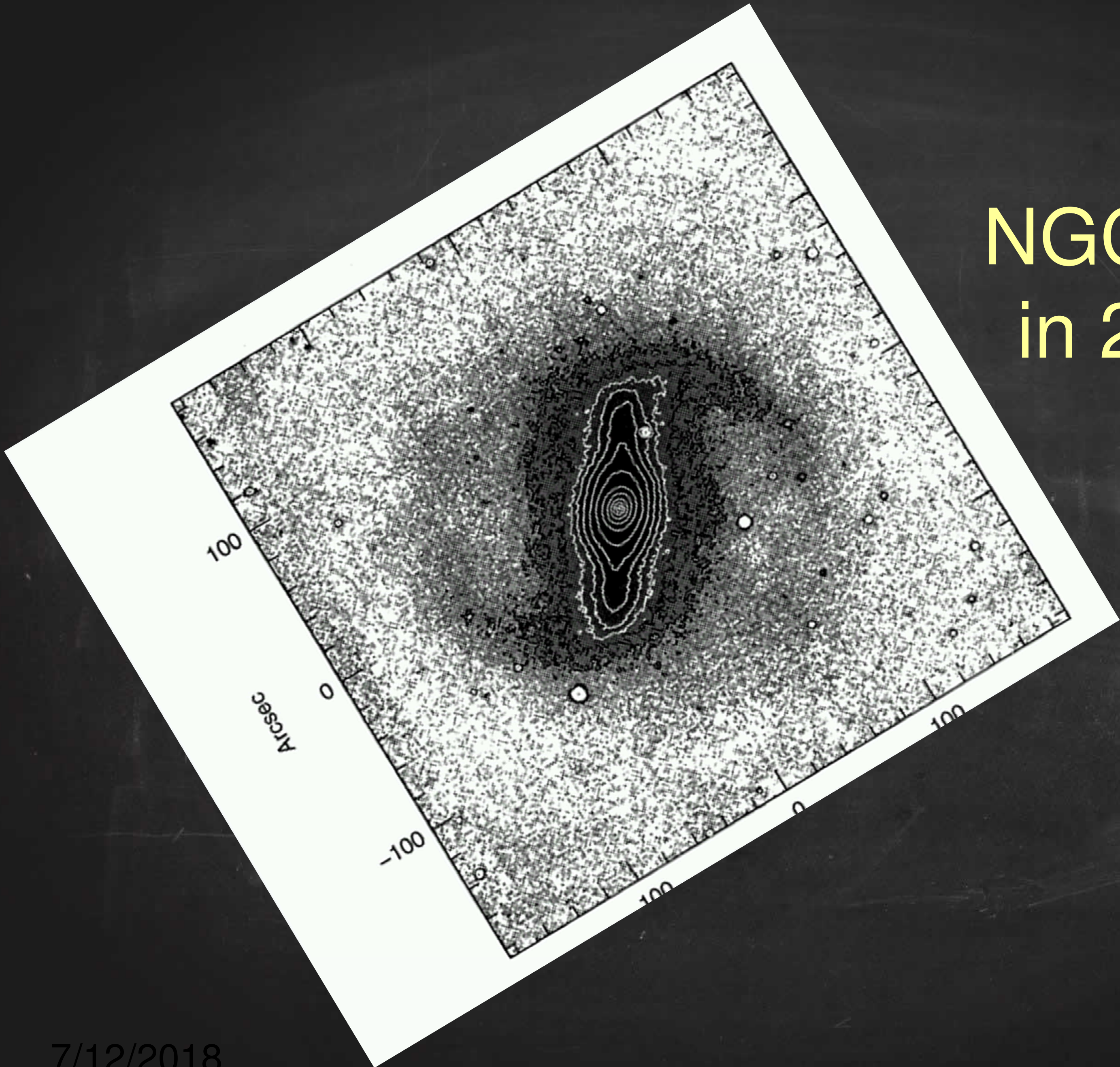

Σημεία ισορροπίας

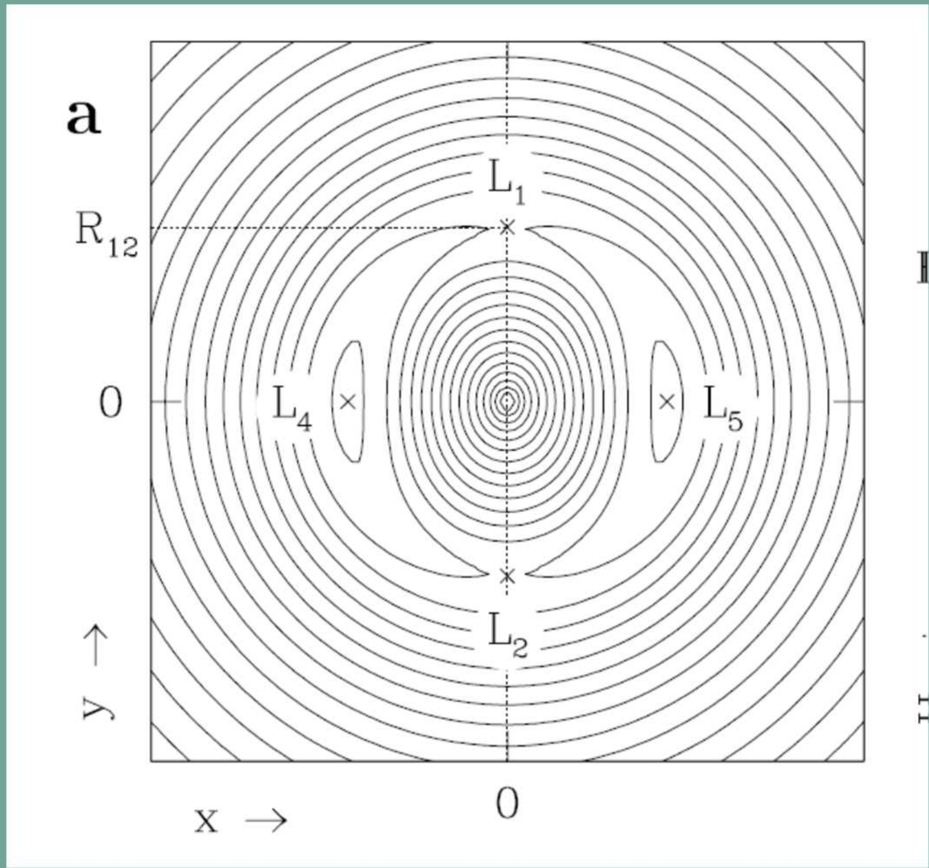

$$\Phi = \Phi_0 + A\cos(2\theta) \quad - \Omega_p J_0$$

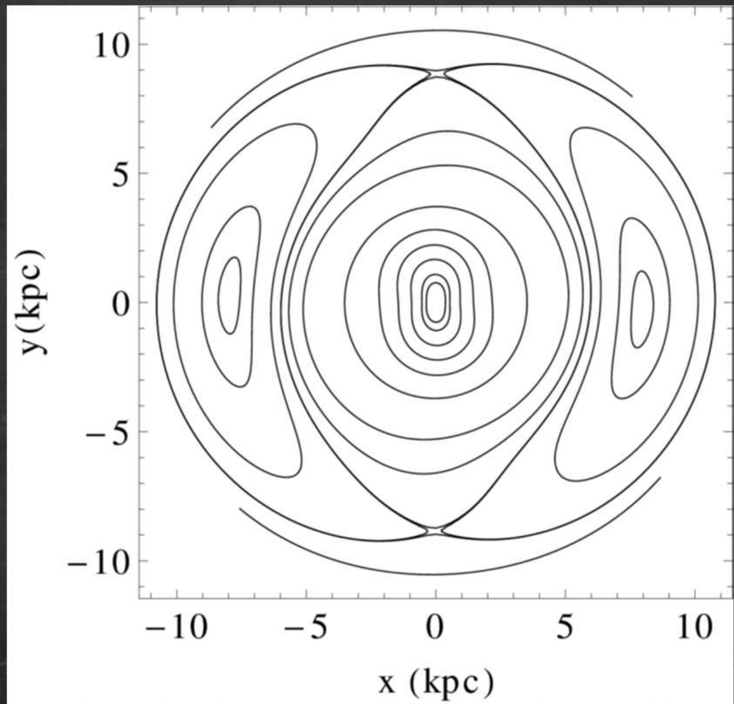

10
5
0
−5
−10
y(kpc)
−10
−5
0
5
10
x (kpc)

Επιφάνεια τομής

- Αυτόνομο Χαμιλτονιανό Σύστημα 2D

$$H \equiv H(x, y, p_x, p_y) \;= h$$

Επιλύουμε π.χ. ως προς p_y

Όλες οι τροχιές με σταθερή ενέργεια h παραμένουν πάνω στην 3D επιφάνεια του 4D φασικού χώρου (x, y, p_x)

Επιφάνεια τομής

Ορίζουμε μια επιφάνεια τομής $y=0$

Poincaré surface of section

Τα σημεία επί της $S(x,y,p_x,p_y)=c$

consequents

Αυτά ορίζουν επί της *S* ένα Poincaré map

Poincaré 1899, Birkhoff 1927

Παράδειγμα

$$H \equiv \frac{1}{2}(\dot{x}^2 + \dot{y}^2) + V(x, y) = h$$

- *V* άρτιο ως προς *y*

Επιφάνεια τομής $y = 0$ δηλ. $(x, \dot{x})$

Τροχιές εντός της ZVC $V(x, y) = h$ με $\dot{y}_0 > 0$

τέμνουν το επίπεδο $y = 0$ άπειρες φορές (αν δεν πρόκειται για τροχιές διαφυγής)

κλειστή CZV

$$\frac{1}{2}\dot{x}^2 + V(x,0) = h$$

Αν το αρχικό σημείο εντός της καμπύλης τότε όλα τα υπόλοιπα θα είναι εντός της ίδιας καμπύλης.

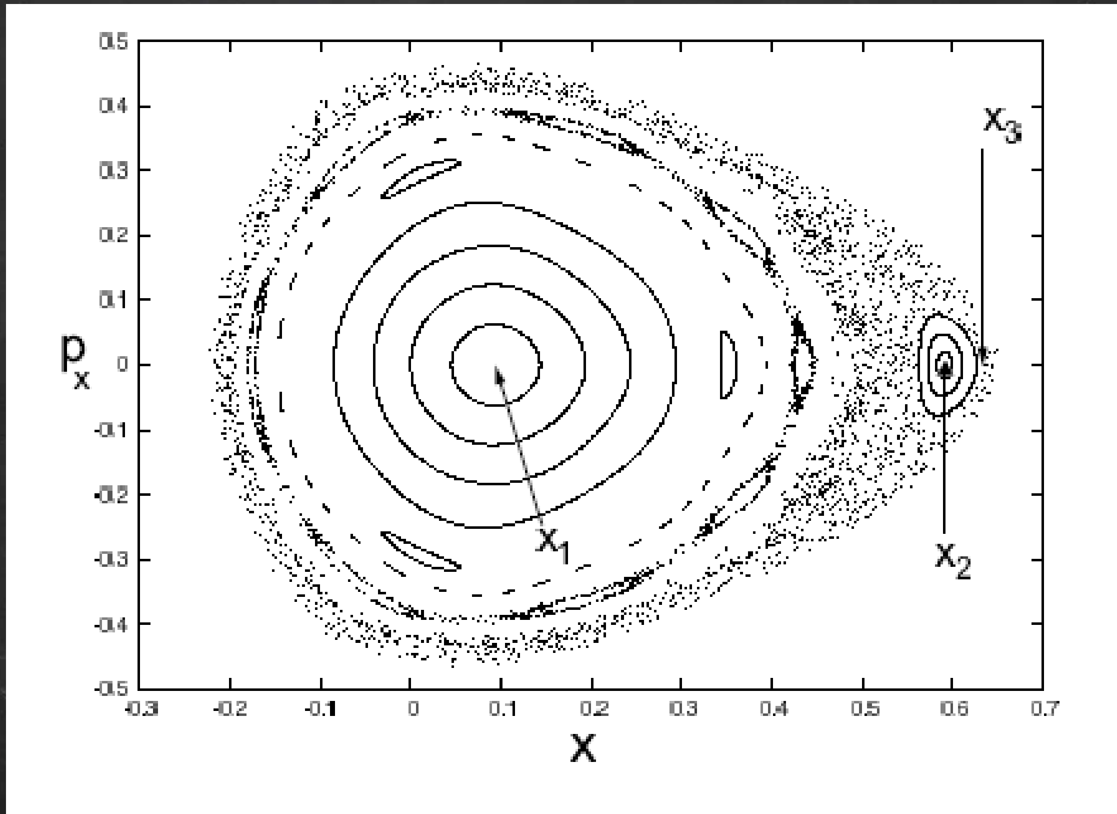

0.5
0.4
0.3
0.2
0.1
0
-0.1
-0.2
-0.3
-0.4
-0.5
-0.3
-0.2
-0.1
0
0.1
0.2
0.3
0.4
0.5
0.6
0.7
p_x
x
x_1
x_2
x_3

κλειστή CZV

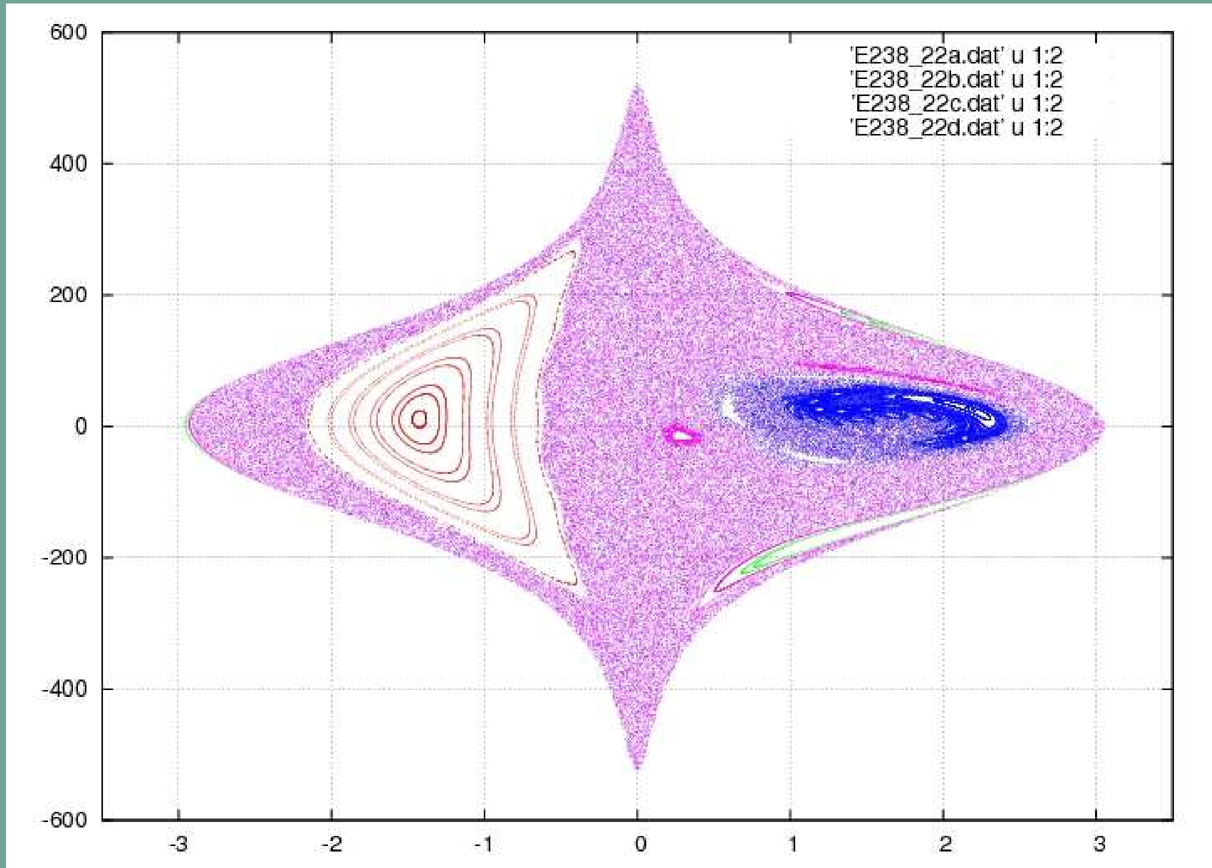

ẋ

x

Order and Chaos on a surface of section

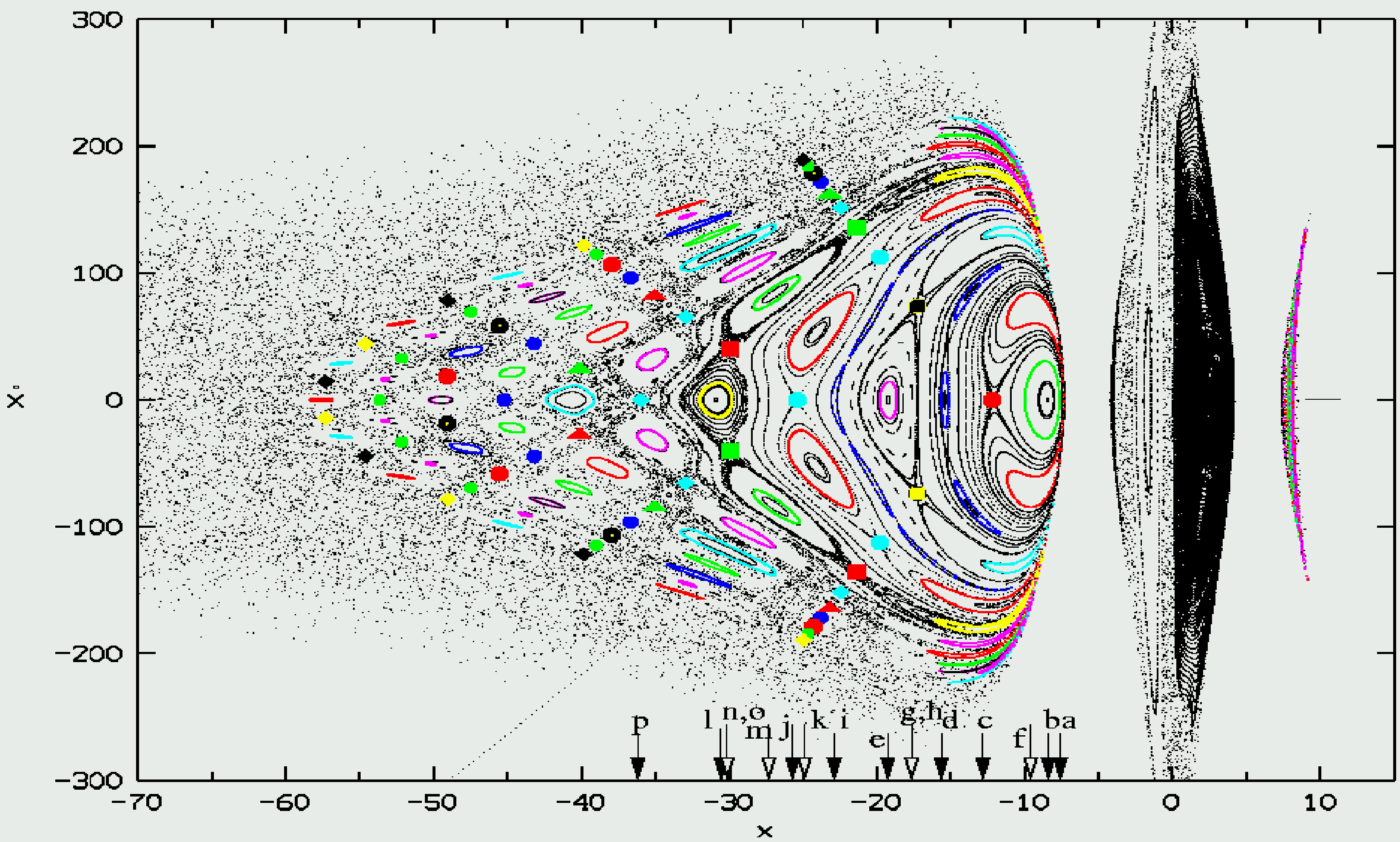

Open CZV

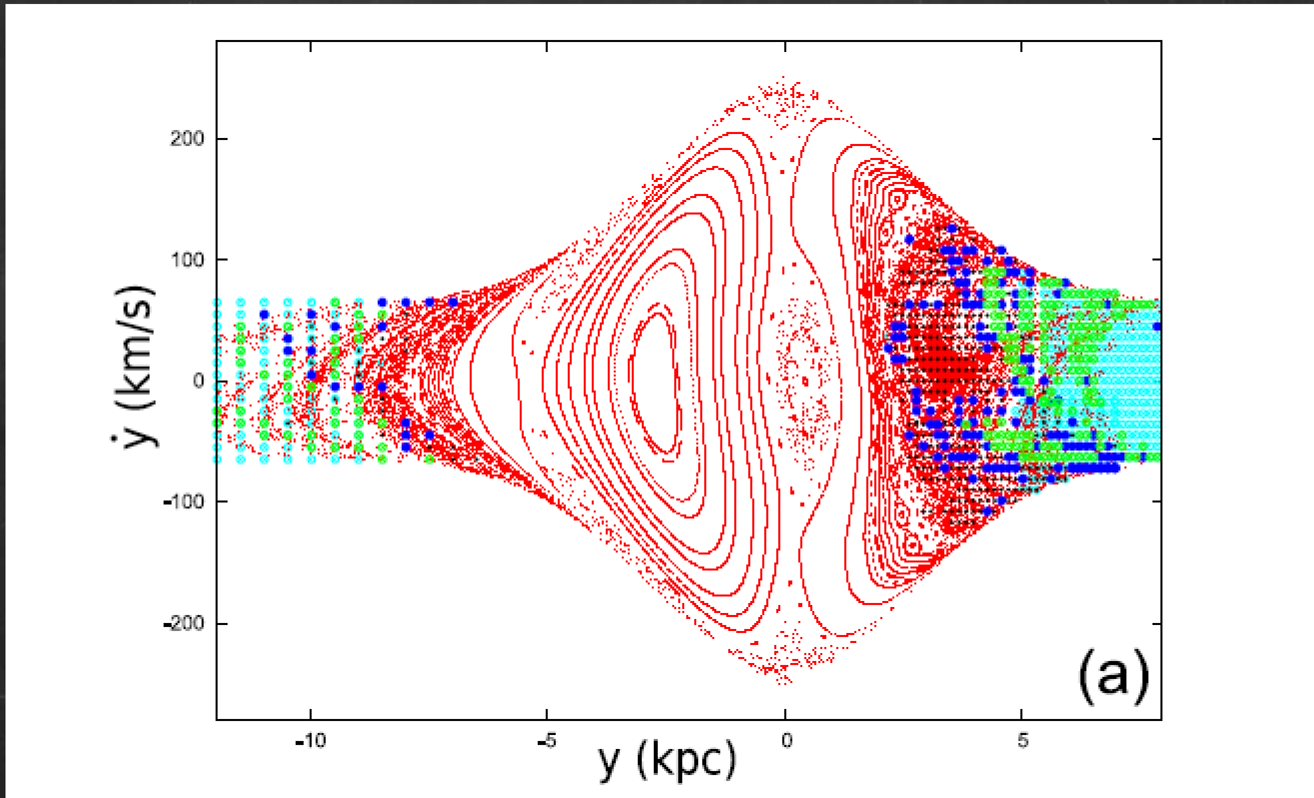

Effective Potential

$\Phi(x, y) \longrightarrow \Phi(x, y) - \frac{1}{2}\Omega_b^2(x^2 + y^2)$

y

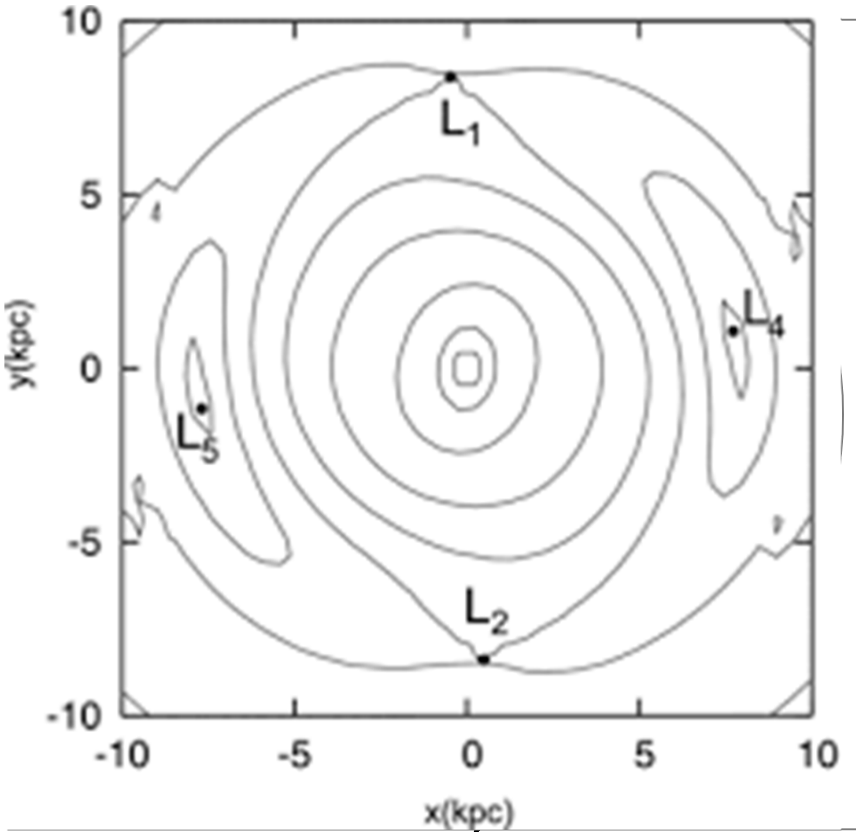

x

Effective potentials

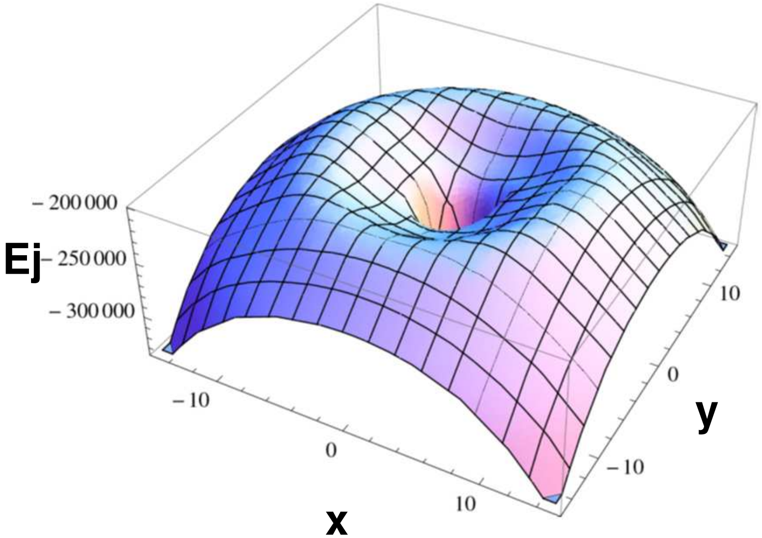

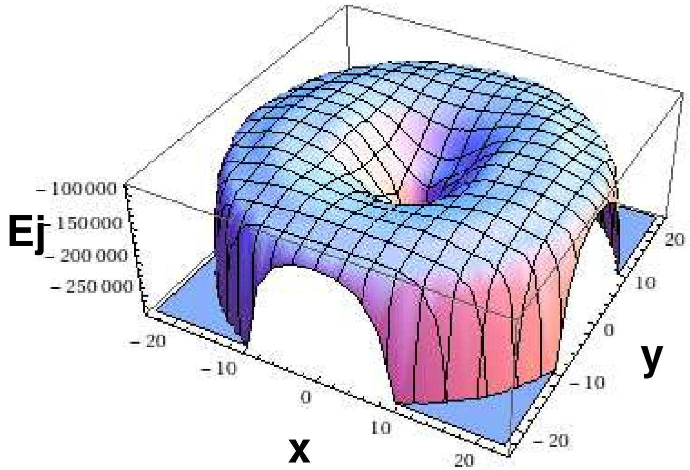

Effective Potential: Different height at different directions

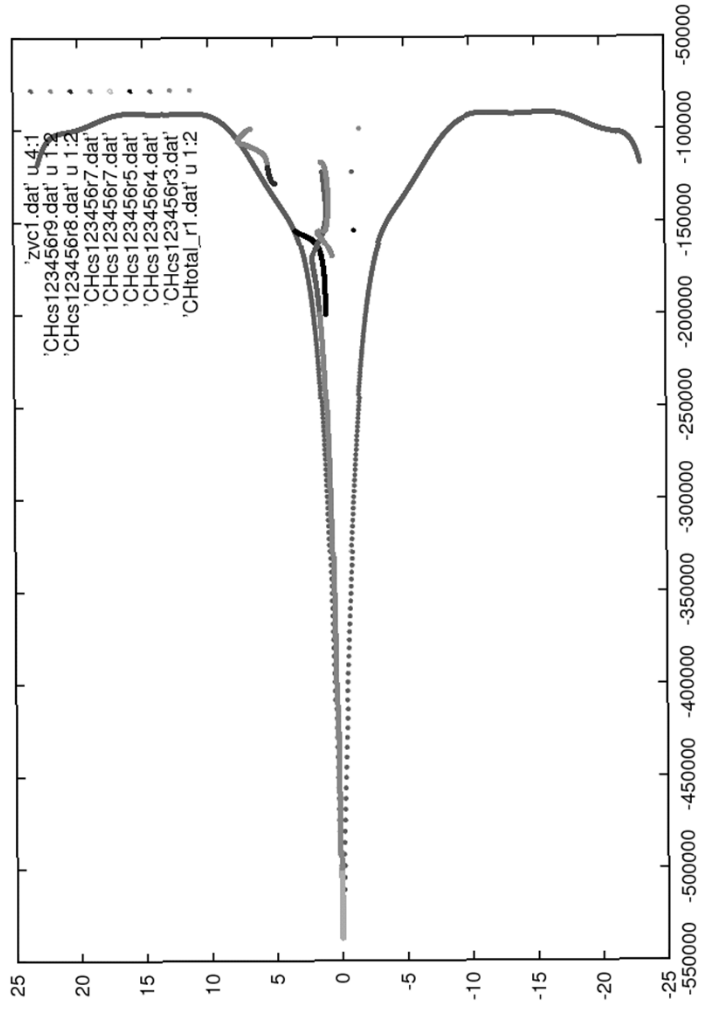

Ej

x ή y

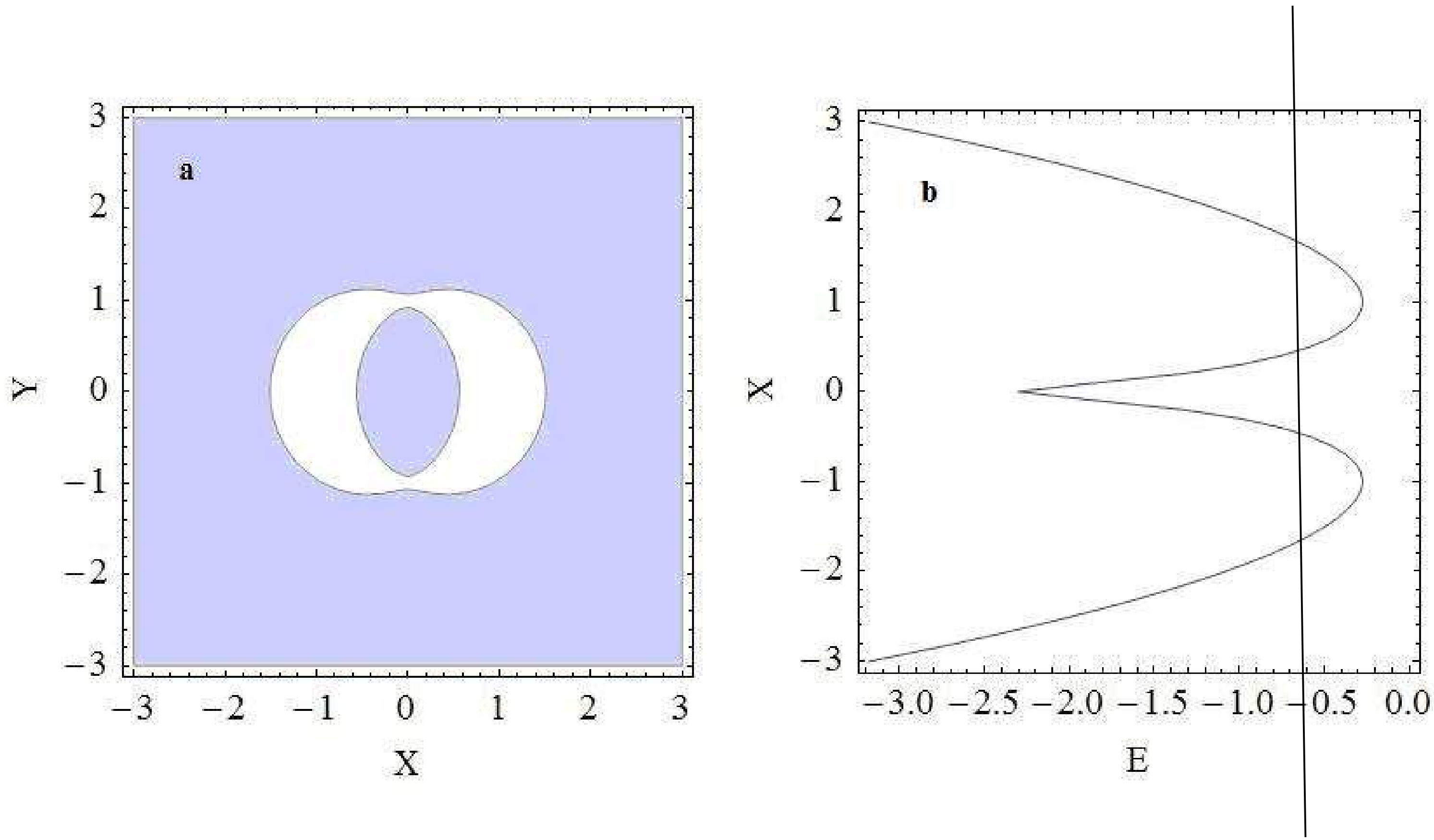
a
b
Y
X
X
E

Μη-ολοκληρώσιμα συστήματα
Τροχιές

Τροχιές: περιοδικές – μη περιοδικές

Περιοδικές τ. : Ευσταθείς - Ασταθείς

$$x = x_0(t) \;\; + \xi$$

Ευστάθεια περιοδικών τροχιών (Hénon 1965)

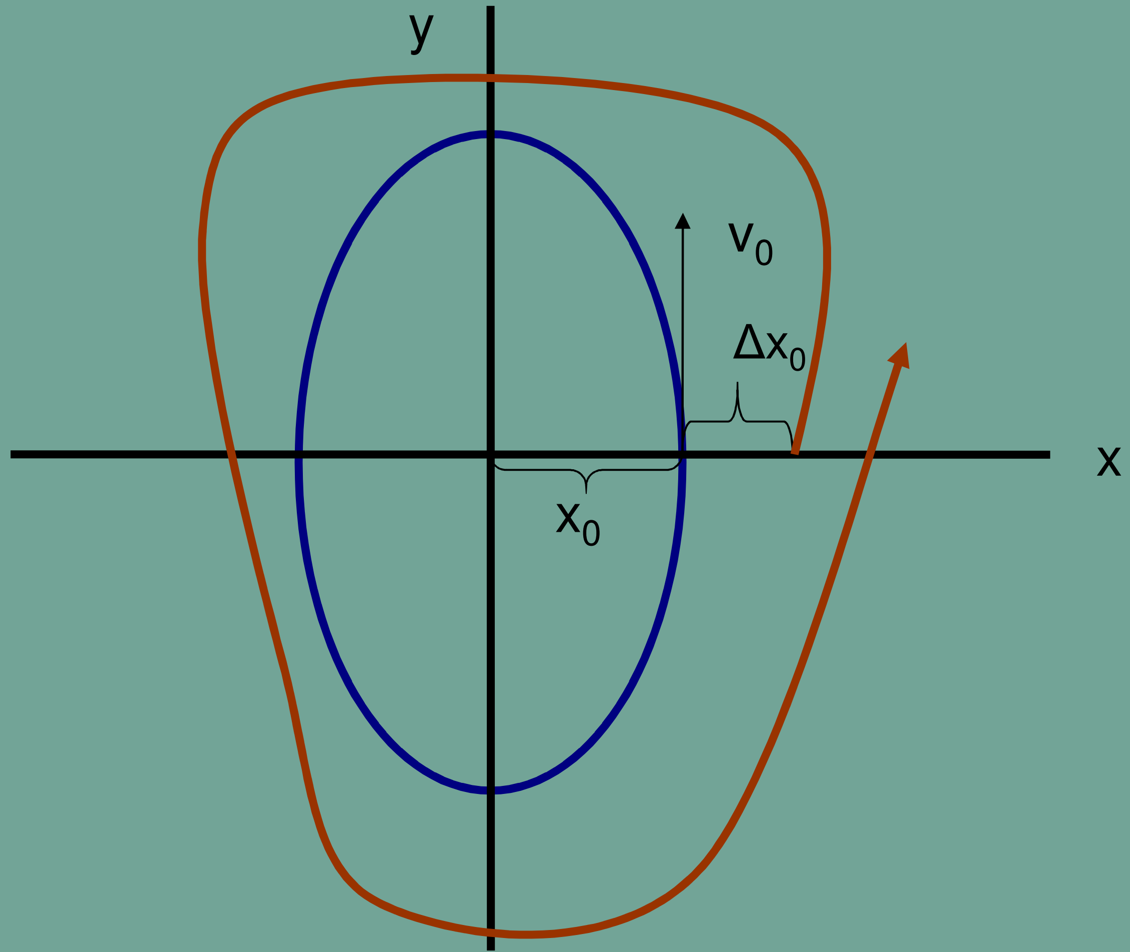

6.1 Ευστάθεια κατά Henón

Η ευστάθεια υπολογίζεται με τη μέθοδο του $Henón$ (1965). Ξεκινώντας από τον τετραδιάστατο χώρο των φάσεων $(x, y, \dot{x}, \dot{y})$, θεωρούμε τις διαδοχικές τομές μιας τροχιάς με τον άξονα $y = 0$, κατά τη διεύθυνση των αυξανόμενων y $(\dot{y} > 0)$. Από τη Χαμιλτονιανή $H = H(x, 0, \dot{x}, \dot{y}) = h$ μπορούμε να λύσουμε ως προς $\dot{y}$ και έτσι ο χώρος των φάσεων περιορίζεται σε δύο αρχικές συνθήκες $(x, \dot{x})$.

Δύο διαδοχικά σημεία τομής στον άξονα $y = 0$ συνδέονται με έναν μετασχηματισμό $\mathbb{R}^2 \to \mathbb{R}^2$. Για την περίπτωση της περιοδικής τροχιάς έχουμε:

$$x_0 = g_1(x_0, \dot{x}_0)$$
$$\dot{x}_0 = g_2(x_0, \dot{x}_0)$$

Εισάγωντας μια μικρή διαταραχή στις αρχικές συνθήκες παίρνουμε μια τροχιά γειτονική της αρχικής $(x_0 + \Delta x_0, \dot{x}_0 + \Delta \dot{x}_0)$. Οι αρχικές και οι τελικές συνθήκες συνδέονται πάλι μέσω του μετασχηματισμού και έχουμε:

$$x_0 + \Delta x_1 = g_1(x_0 + \Delta x_0, \dot{x}_0 + \Delta \dot{x}_0)$$
$$\dot{x}_0 + \Delta \dot{x}_1 = g_2(x_0 + \Delta x_0, \dot{x}_0 + \Delta \dot{x}_0)$$

Αναπτύσσοντας κατά Taylor και κρατώντας όρους μέχρι πρώτης τάξης έχουμε:

$$\Delta x_1 = \frac{\partial g_1}{\partial x}\Delta x_0 + \frac{\partial g_1}{\partial \dot{x}}\Delta \dot{x}_0$$
$$\Delta \dot{x}_1 = \frac{\partial g_2}{\partial x}\Delta x_0 + \frac{\partial g_2}{\partial \dot{x}}\Delta \dot{x}_0$$

ή αναλυτικά:

$$\Delta x_1 = a\Delta x_0 + b\Delta \dot{x}_0$$
$$\Delta \dot{x}_1 = c\Delta x_0 + d\Delta \dot{x}_0$$

όπου $a = \dfrac{\partial g_1}{\partial x}$, $b = \dfrac{\partial g_1}{\partial \dot{x}}$, $c = \dfrac{\partial g_2}{\partial x}$, $d = \dfrac{\partial g_2}{\partial \dot{x}}$

Δεδομένου ότι ο μετασχηματισμός διατηρεί τα εμβαδά, έχουμε

$$ad - bc = 1 \tag{3}$$

Επομένως $\overrightarrow{k}_1 = \mathbf{A}\overrightarrow{k}_0$, όπου $\overrightarrow{k}_1$ είναι το διάνυσμα $(\Delta x_1, \Delta\dot{x}_1)$ και $\overrightarrow{k}_0$ το διάνυσμα $(\Delta x_0, \Delta\dot{x}_0)$.

Εάν $\{\overrightarrow{\delta}_1, \overrightarrow{\delta}_2\}$ η βάση των ιδιοδιανυσμάτων, μπορούμε να γράψουμε:

$$\overrightarrow{k}_0 = A_1\overrightarrow{\delta}_1 + A_2\overrightarrow{\delta}_2$$
$$\overrightarrow{k}_1 = A_1\lambda_1\overrightarrow{\delta}_1 + A_2\lambda_2\overrightarrow{\delta}_2$$

όπου λ_1 και λ_2 οι ιδιοτιμές της Ιακωβιανής $\mathbf{A}$. Η χαρακτηριστική εξίσωση του όπου λ_1 και λ_2 οι ιδιοτιμές της Ιακωβιανής **A**. Η χαρακτηριστική εξίσωση του πίνακα **A**, λόγω της σχέσης (3) είναι

$$\lambda^2 - (a+d)\lambda + 1 = 0$$

Στην περίπτωση που έχουμε $|a+d| < 2$, έχουμε δύο ρίζες μιγαδικές συζυγείς. Σε αυτήν την περίπτωση $|\lambda_1| = |\lambda_2| = 1$, και η τροχιά χαρακτηρίζεται ευσταθής.

Εάν έχουμε $|a+d| > 2$ τότε έχουμε δύο πραγματικές ρίζες, με $\lambda_1\lambda_2 = 1$ και η τροχιά χαρακτηρίζεται ασταθής. Ως δείκτης ευστάθειας ορίζεται ως εκ τούτου η παράμετρος

$$\alpha = \frac{1}{2}(a+d)$$

Για $|a| < 1$ η περιοδική τροχιά είναι ευσταθής, ενώ για $|a| > 1$ είναι ασταθής. Το διάγραμμα που δίνει τον δείκτη ευστάθειας α ως συνάρτηση της ενέργειας ονομάζεται διάγραμμα ευστάθειας.

Henon's index

Characteristic equation:

$$\lambda^2-(a+d)\lambda+1=0$$

$$\alpha=1/2(a+d)$$

$|\alpha|<1$ STABLE

$|\alpha|>1$ UNSTABLE

Ελλειπτικά σημεία

M. Henon (1983)"Numerical exploration of Hamiltonian Systems". In: Chaotic Behaviour of Deterministic Systems, Les Houches, XXXVI. Ed. by G. Iooss, R.H.G. Helleman, and R. Stora. Elsevier, pp. 53–170.

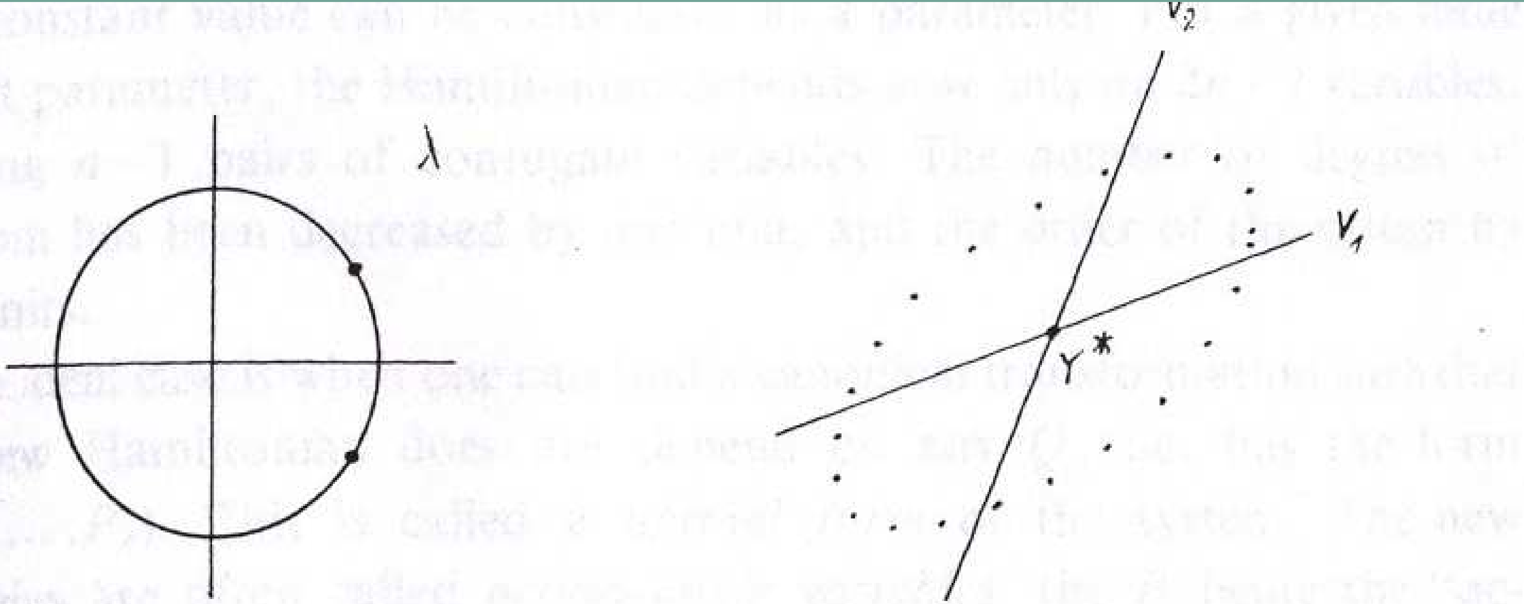

Fig. 8.

(1) $-1<a<1$: the two eigenvalues are complex conjugate, and lie on the unit circle (fig. 8, left). In the linear approximation, the sequence of points

Υπερβολικά σημεία - 1

(2) $a > 1$: the two eigenvalues are real and positive, one being less tha[n] 1 and the other greater than 1. Points of a neighbouring trajectory lie o[n] a branch of hyperbola (fig. 9); V and V' are the eigenvectors. The fixe[d] point is called *hyperbolic*, or *linearly unstable*, since nearby trajectories ru[n] away from it.

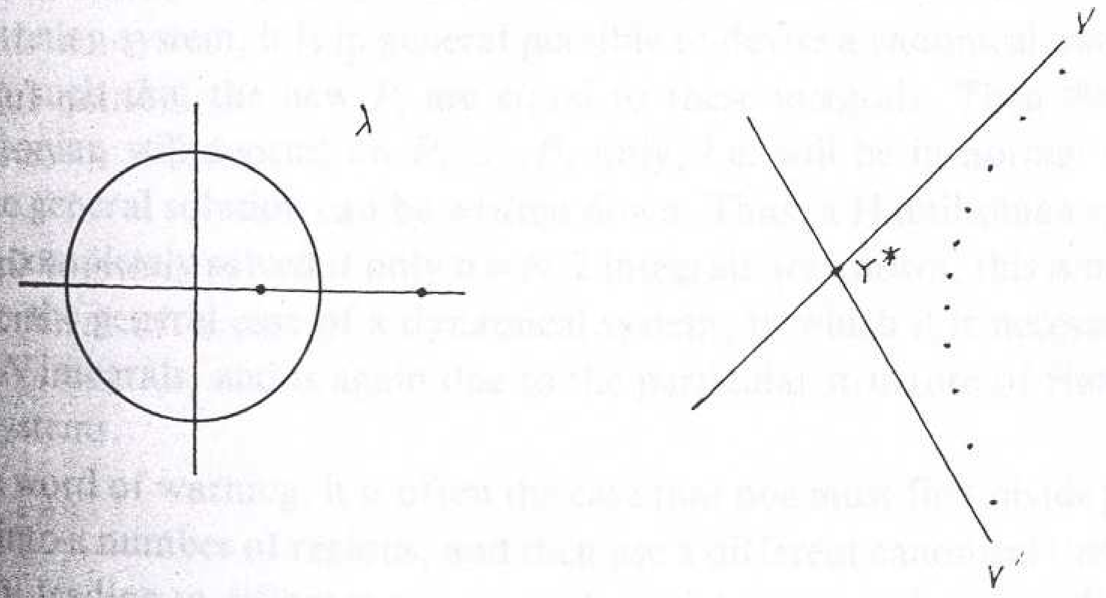

Fig. 9.

Υπερβολικά σημεία – II

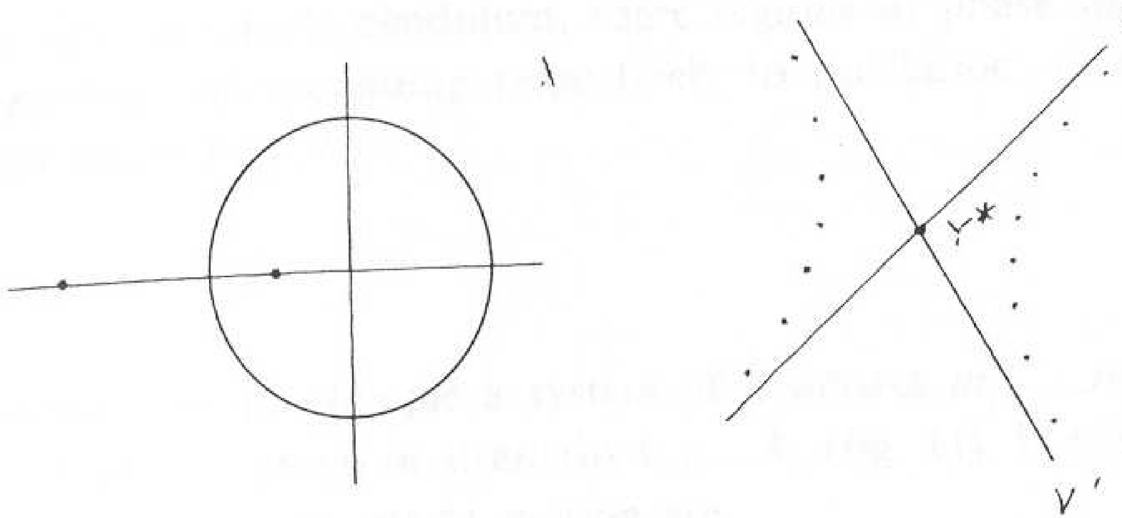

Fig. 10.

(3) $a < -1$: this case is very similar to the previous one. The two eigen-values are real and negative. Points of a neighbouring trajectory now lie on both branches of a hyperbola (fig. 10). The fixed point is again called hyperbolic, or linearly unstable.

Χάος

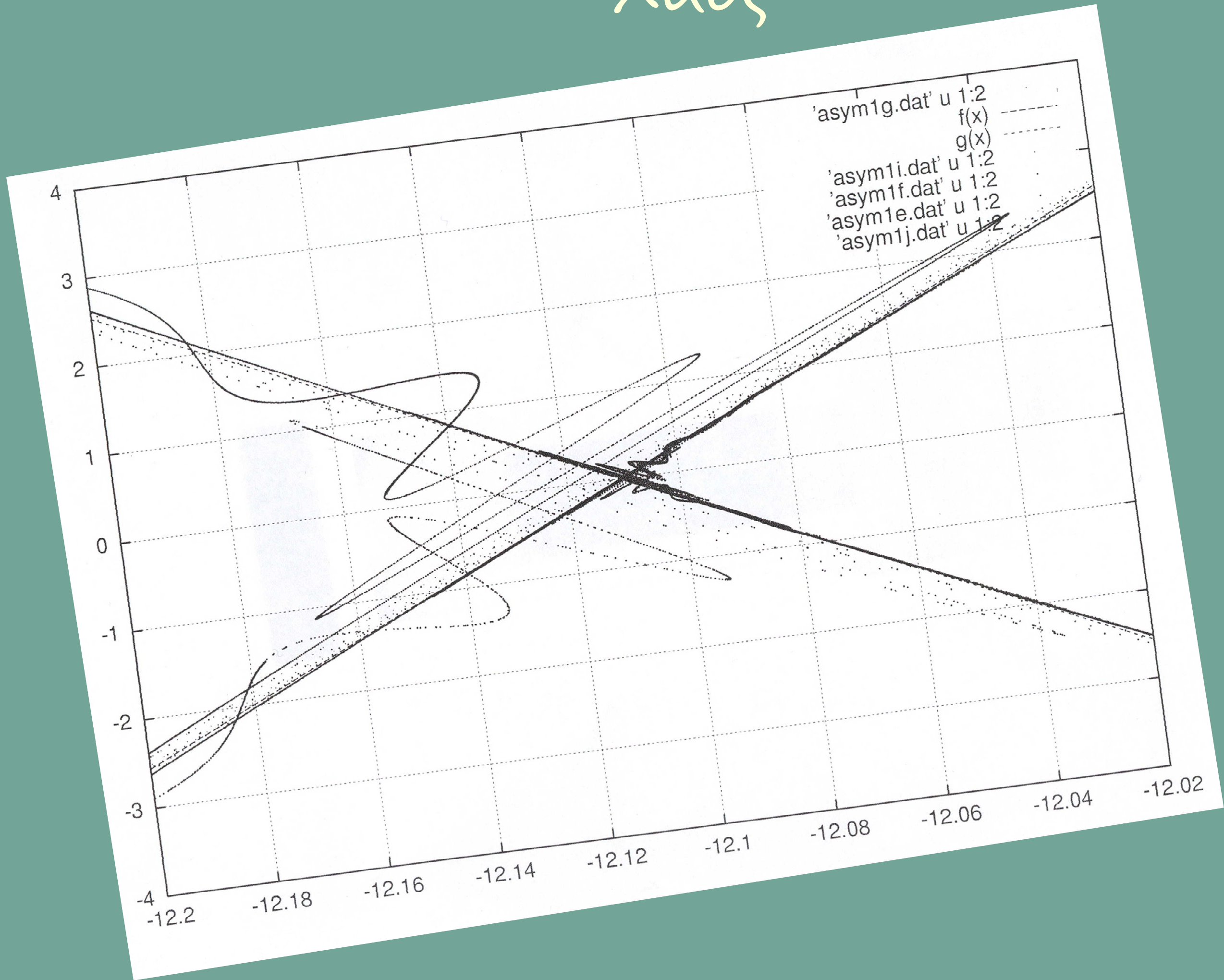

'asym1g.dat' u 1:2
f(x)
g(x)
'asym1i.dat' u 1:2
'asym1f.dat' u 1:2
'asym1e.dat' u 1:2
'asym1j.dat' u 1:2
4
3
2
1
0
-1
-2
-3
-4
-12.2
-12.18
-12.16
-12.14
-12.12
-12.1
-12.08
-12.06
-12.04
-12.02

Stability diagram

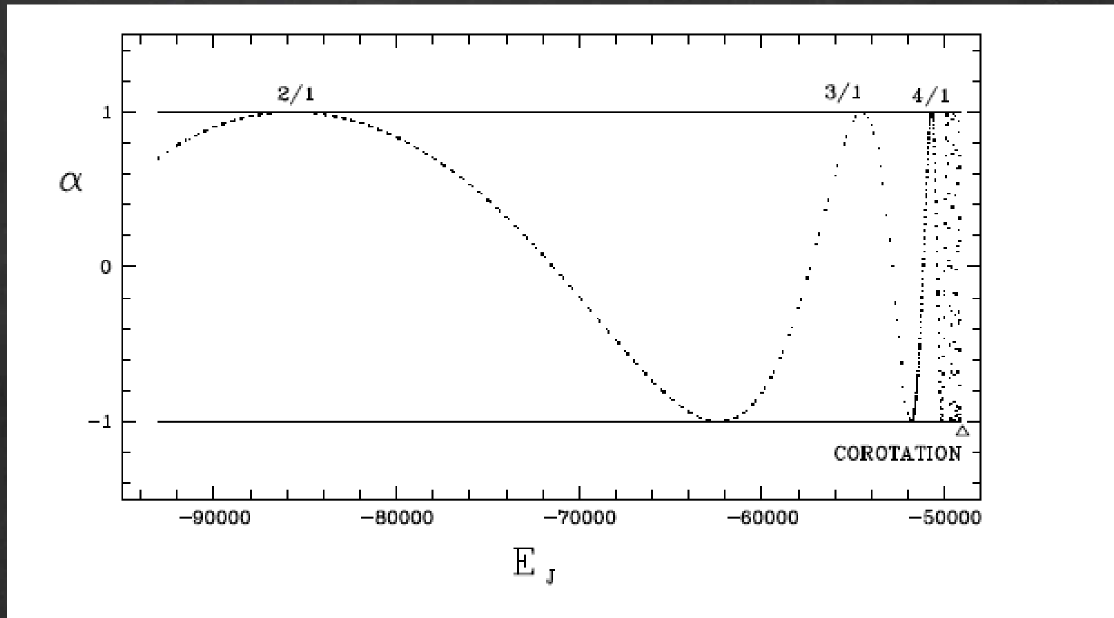

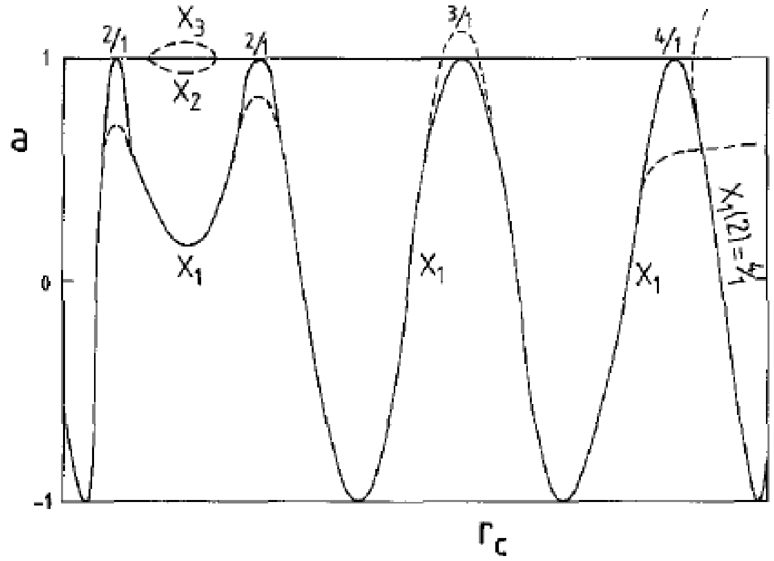

Fig. 5. Stability curves for a model with a double inner Lindblad resonance (schematically). (——) $A=0$ (axisymmetric case), (----) $A \neq 0$

$$\Phi=\Phi_0+\Phi_b$$

Στους άρτιους συντονισμούς έχουμε χάσματα στις χαρακτηριστικές και "οριζόντια" τμήματα στις καμπύλες ευστάθειας.

Στους περιττούς συντονισμους έχουμε ασταθή τμήματα στις χαρακτηριστικές και τομές με τους άξονες $|\alpha|=1$

Διάγραμμα ευστάθειας - διακλαδώσεις

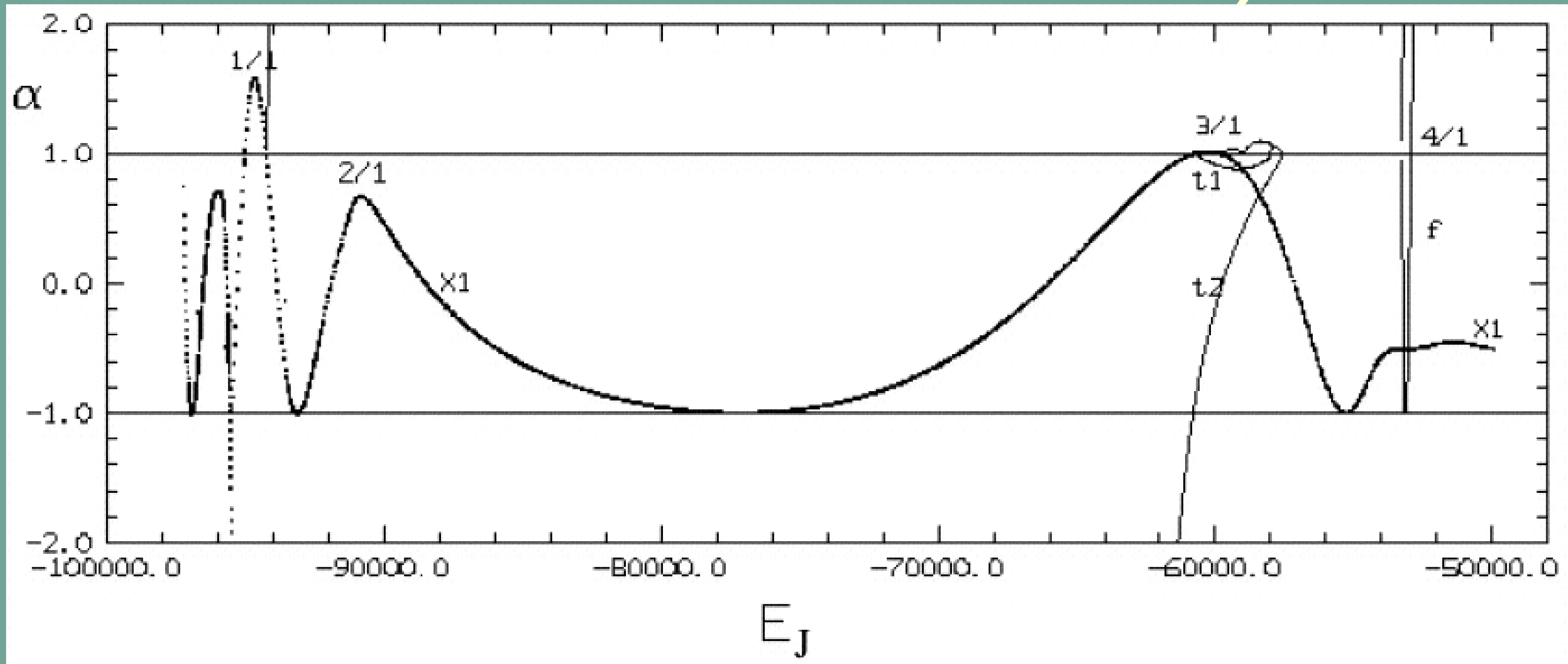

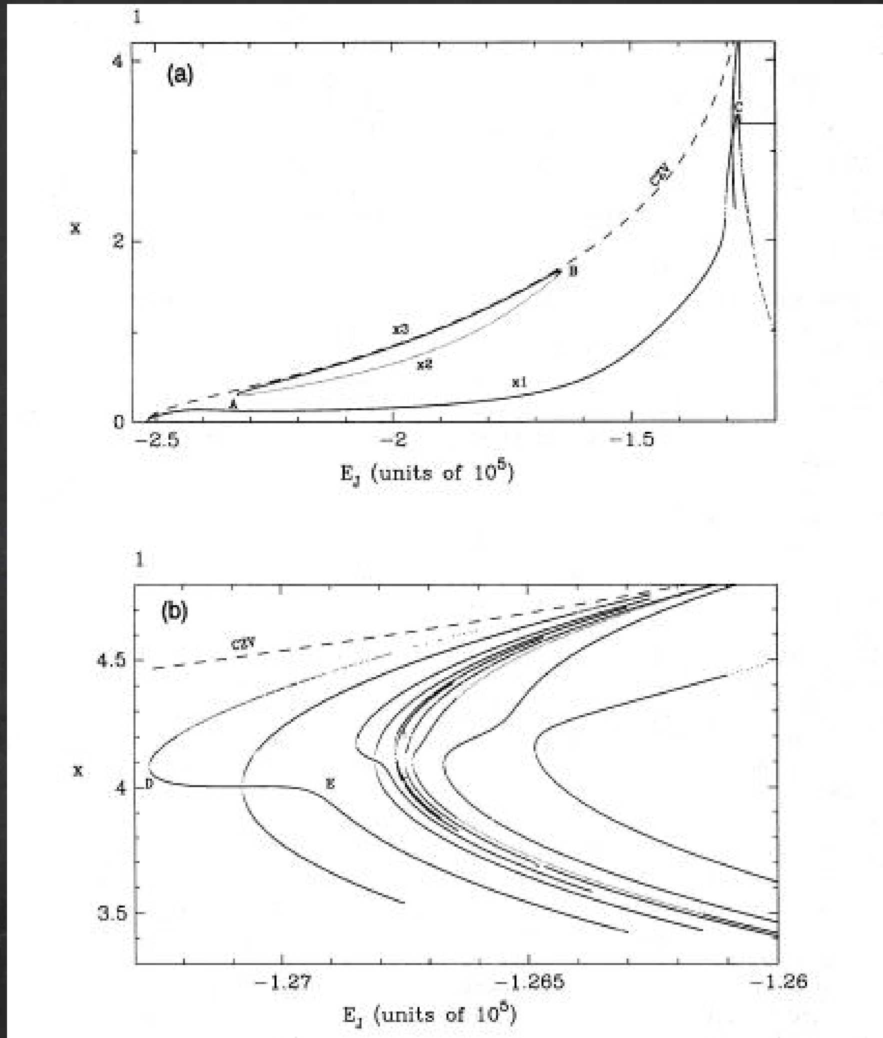

1
(a)
x
4
2
0
CZV
B
C
x3
x2
x1
A
-2.5
-2
-1.5
E_J (units of 10^5)
1
(b)
CZV
4.5
x
4
3.5
D
E
-1.27
-1.265
-1.26
E_J (units of 10^5)

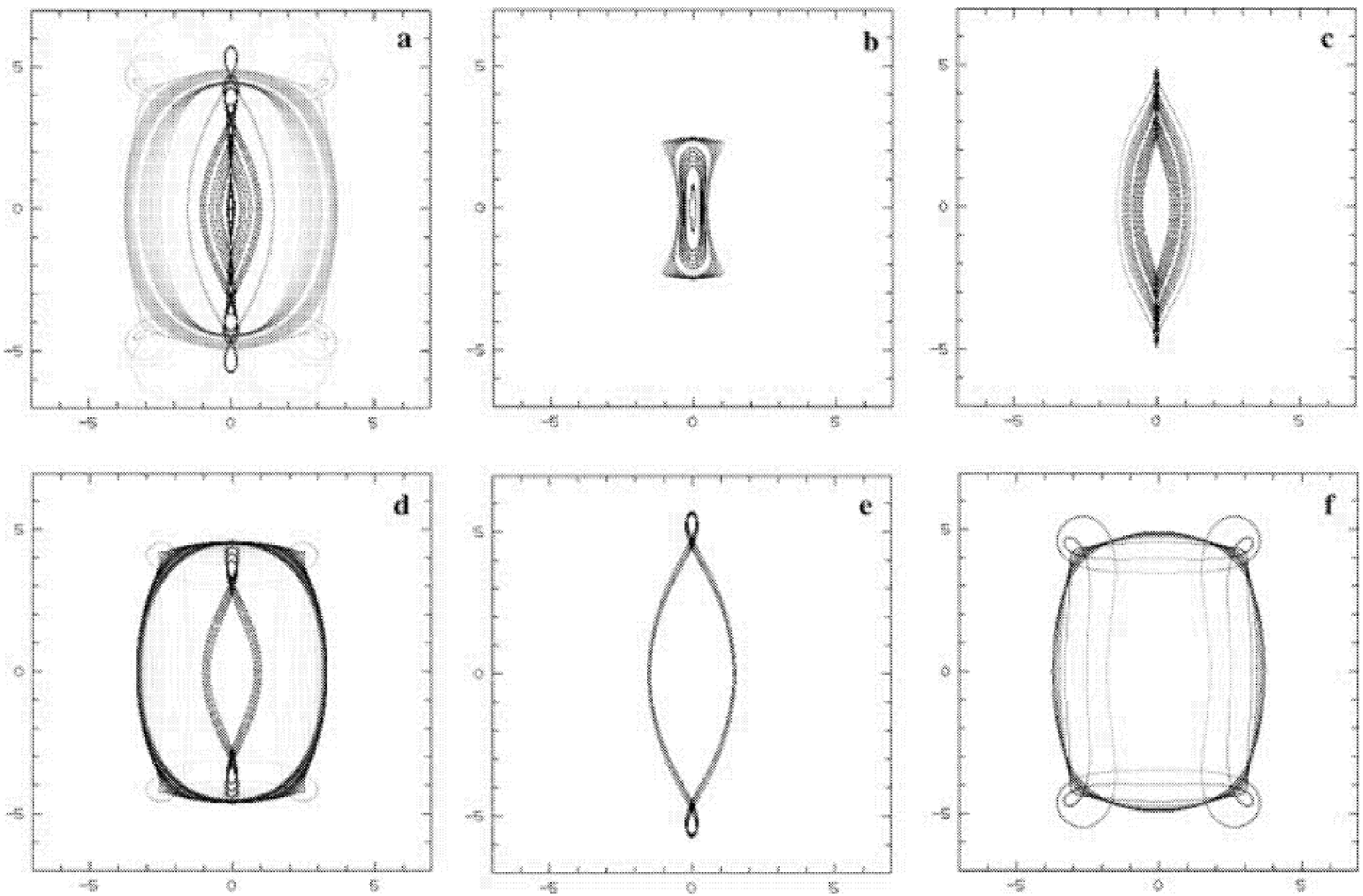
a
b
c
d
e
f

Example: 2D bifurcation's tree of the main family of p.o.

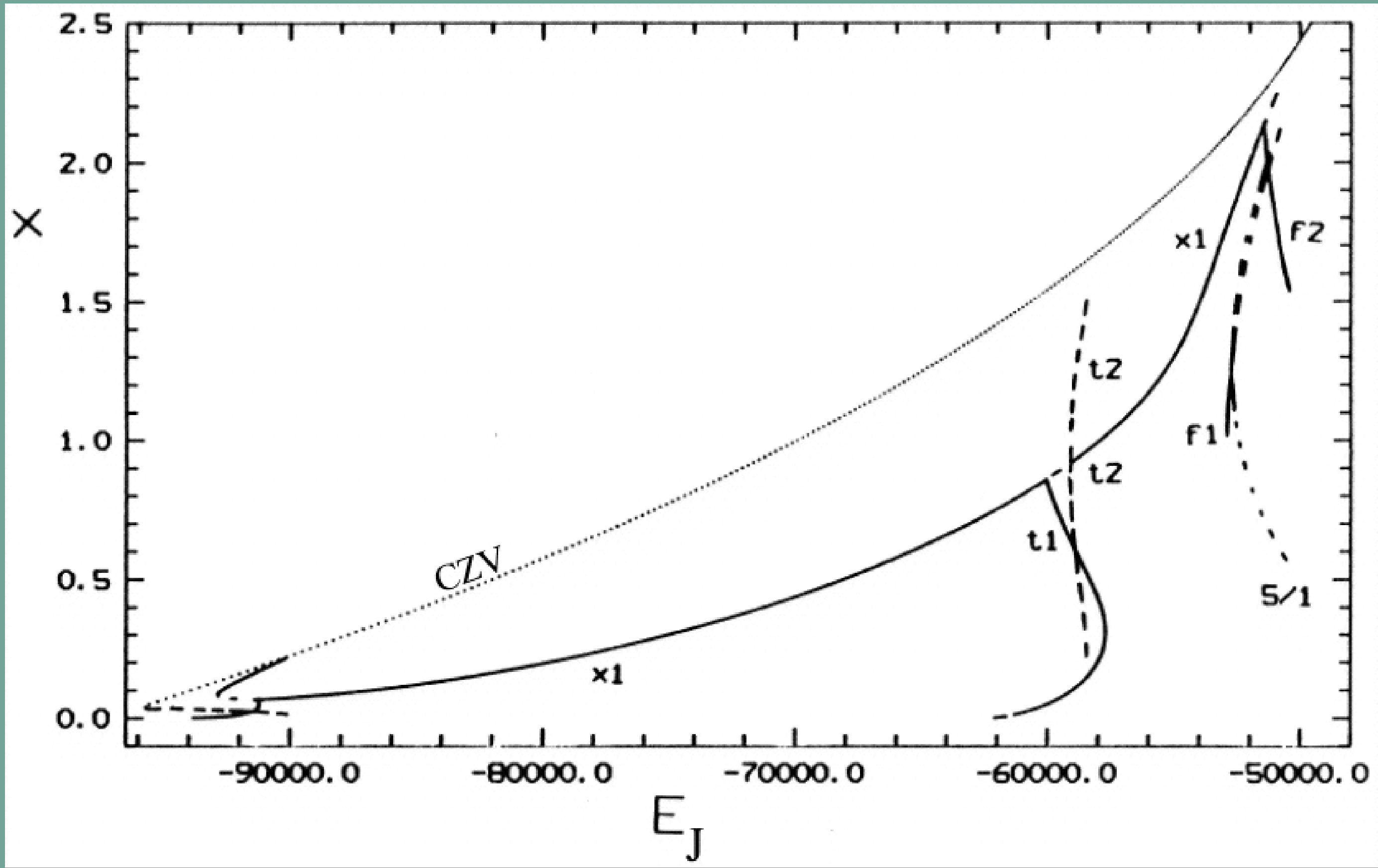

Μορφολογική εξέλιξη τροχιών

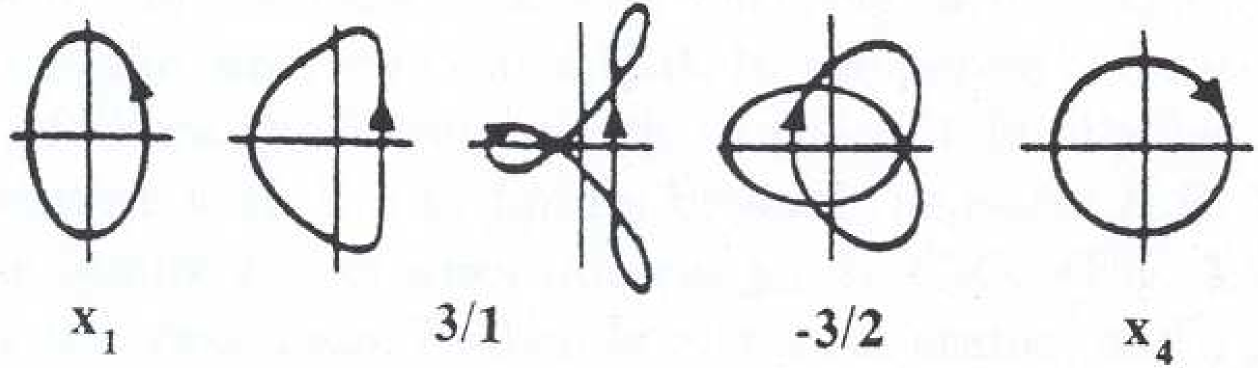

Orbital behavior close to corotation

Chaotic orbit can support observed structures

Patsis, Athanasoula, Quillen 1997

- Chaotic orbits may support observed structures

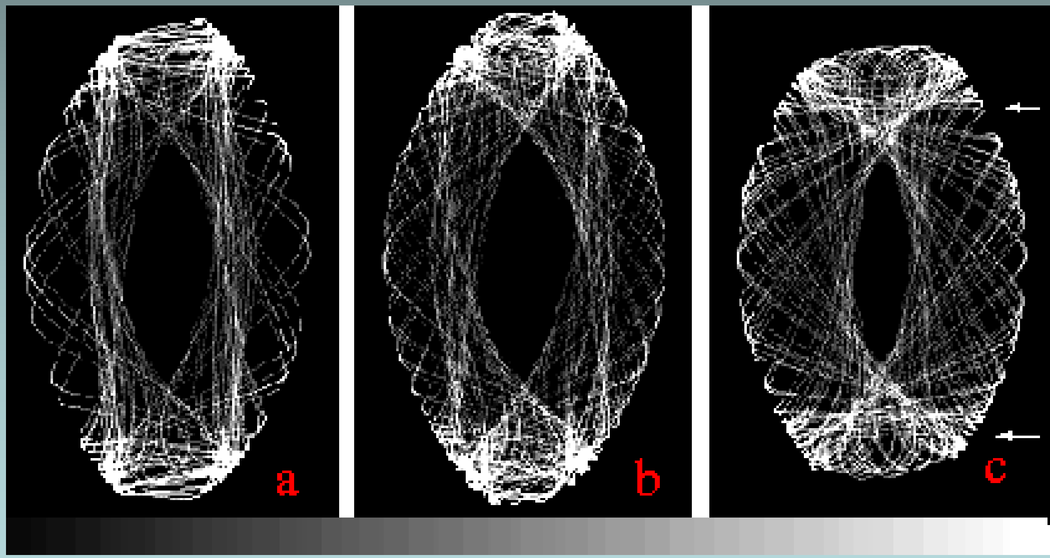

Orbits in barred-spiral galaxies

Contopoulos 1978, A&A 64,323
Kaufmann & Contopoulos 1996, A&A 309, 381
Patsis et al. 1997, ApJ 483, 731

Voglis & Stavropoulos 2005, AIPC 848, 647
Patsis 2006, MNRAS 369L, 56
Voglis et al. 2006, MNRAS 372, 901
Voglis et al. 2006, MNRAS, 373,280
Romero-Gomez et al. 2006, A&A 453,59
Voglis et al. 2007, MNRAS 381, 757
Romero-Gomez et al. 2007, A&A 472, 63
Tsoutsis et al. 2008, MNRAS 387, 1264
"Chaos in Astronomy" 2009, SPRINGER
Athanassoula et al. 2009, MNRAS 400, 1706

- Tsoutsis et al. 2009, A&A 495, 743
- Romero-Gomez et al. 2009, CNSNS 14.4123
- Patsis & Kalapotharakos 2008, MemSAIt, 2011, 18, 83
- Tsigaridi & Patsis 2010 ASPC 424, 382
- Kalapotharakos et al. 2010, MNRAS 403,83
- Kalapotharakos et al. 2010, MNRAS 408, 9
- Patsis et al. 2010b, MNRAS 408, 22
- Patsis et al. 2010c, MNRAS 409L, 94
- Chatzopoulos et al., 2011, MNRAS 416, 479
- Harsoula et al., 2011, MNRAS 411, 1111

(see also Danby 1965, ApJ 70, 501)

Response models of barred galaxies (the collective effect)

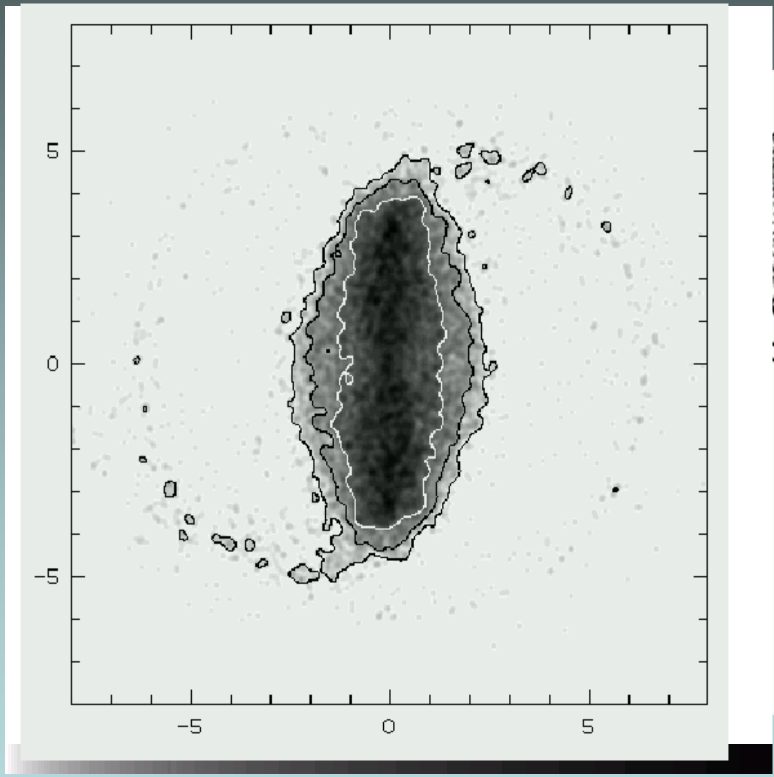

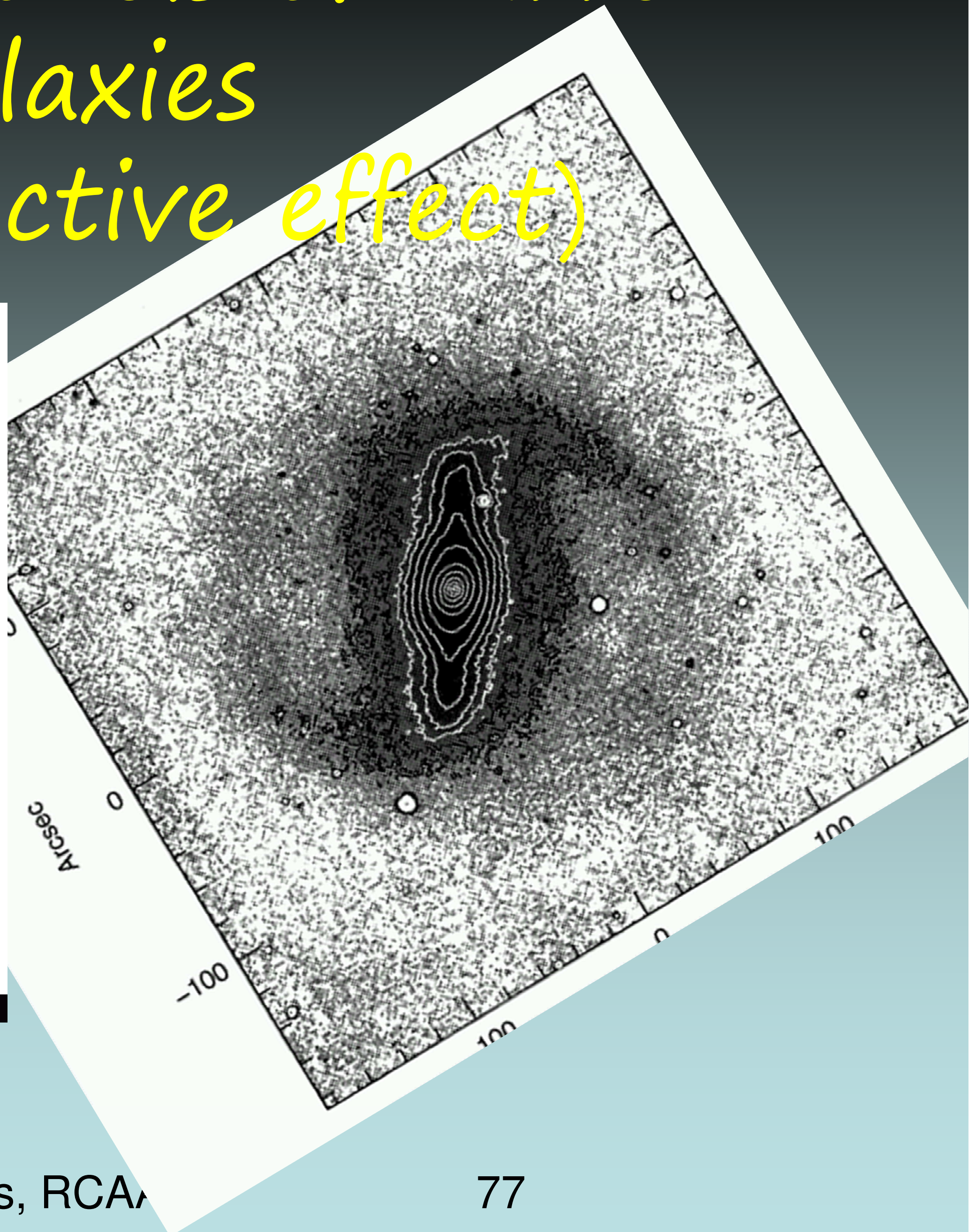

4:1 resonance-type chaotic orbits. NGC 4314 – an early type barred galaxy

1. We isolate the particles found on the response spirals (or in the outer envelope of the bar)

2. We perform statistics on their Jacobi constants (Ej)

3. We realize that they belong to a narrow ΔEj interval, where chaos dominates on the surfaces of section

includes the characte-ristic of 4:1 family and L1,L2

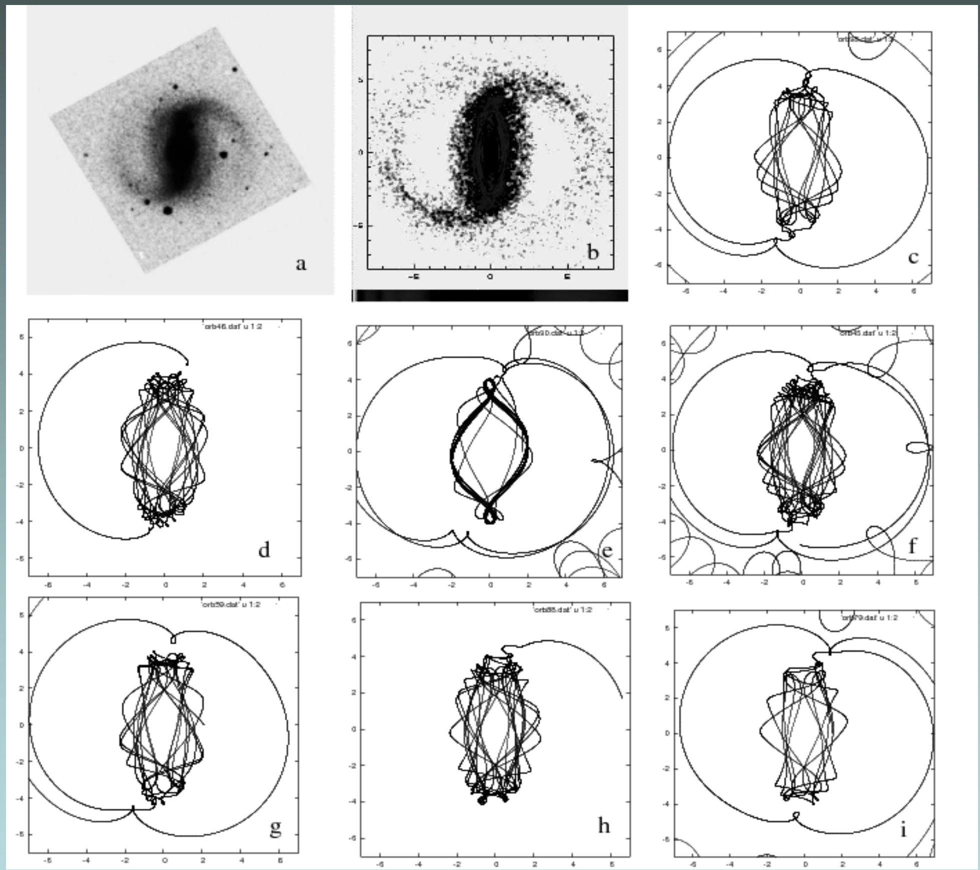

Orbits supporting the boxy bar

Chatzopoulos, Patsis, Boily 2011, MNRAS 416, 479

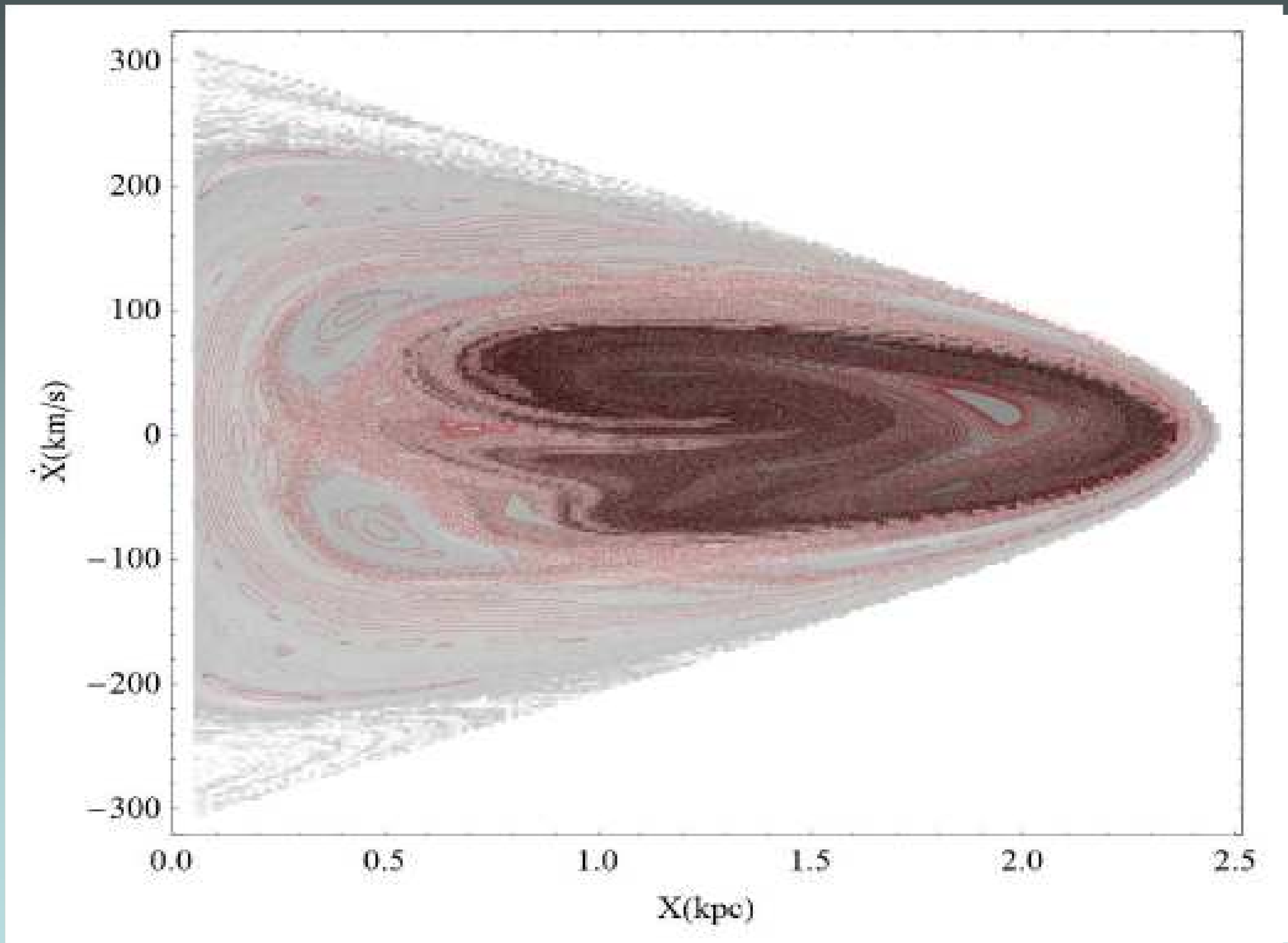

NGC 1300
+C. Kalapotharakos, P. Grosbol

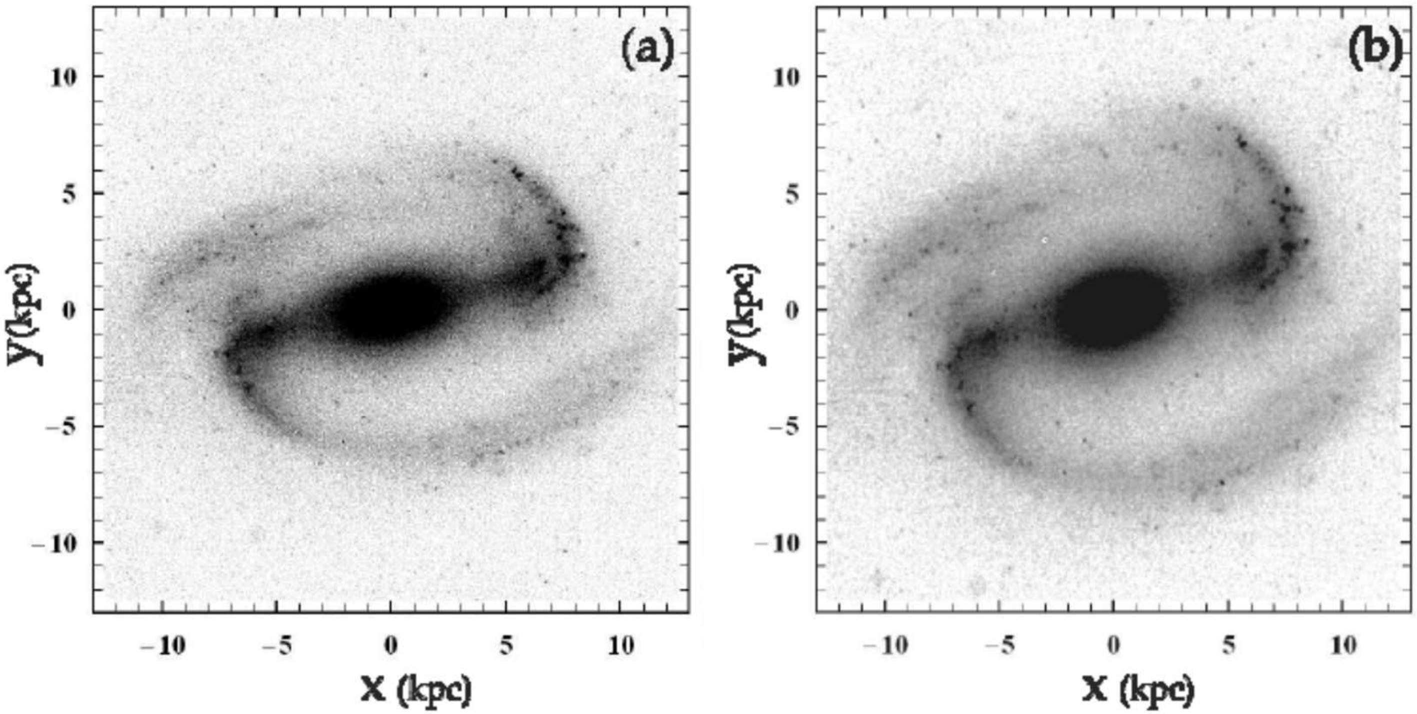

Figure 1. (a) The observed K band image of NGC 1300. (b) The deprojected K band image of NGC 1300 using (PA, IA)=(87°, 35°). The galaxy was observed with SOFI at the 3.5 m NTT telescope at ESO La Silla. The units on the axes are in kpc, assuming a distance to the galaxy D = 19.6Mpc. The images are in linear intensity scale.

2D response $\Omega_p = 22$ km s^{-1} kpc^{-1}

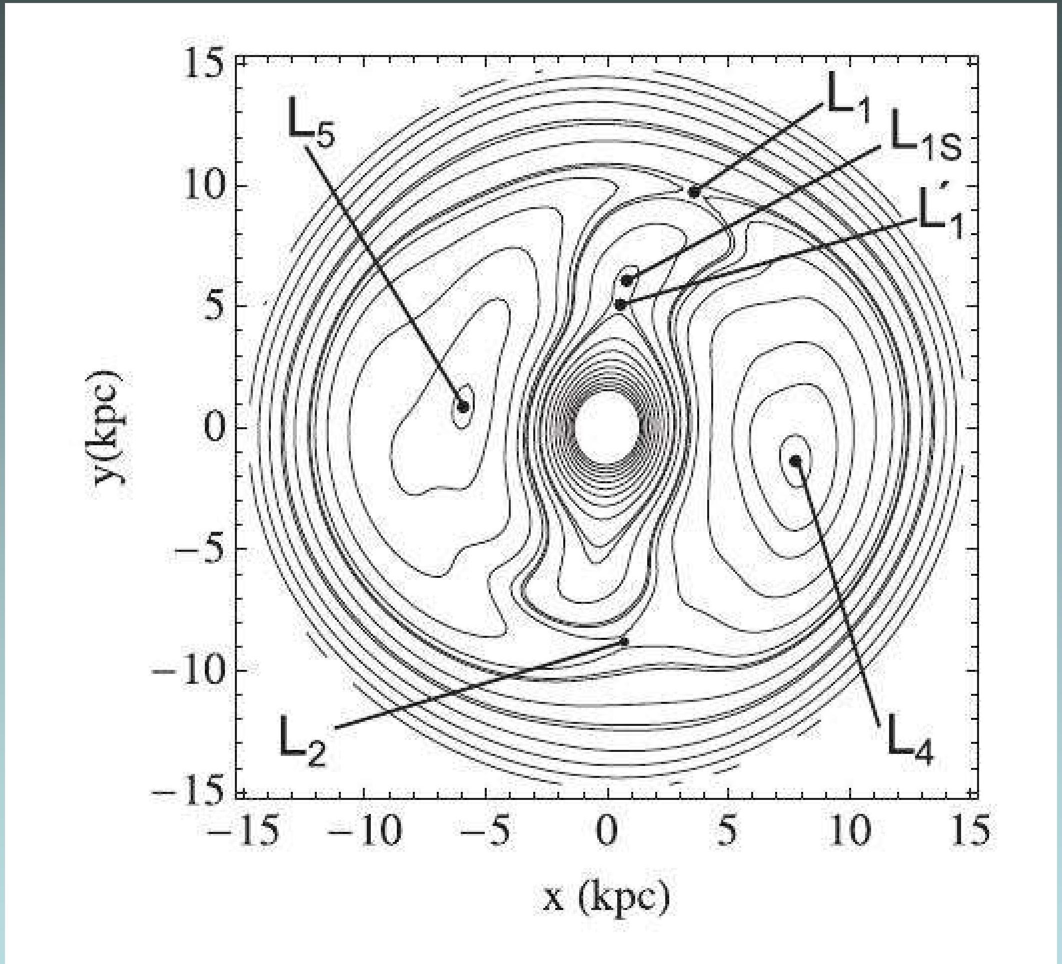

2D response $\Omega_p = 22$ km s^{-1} kpc^{-1}

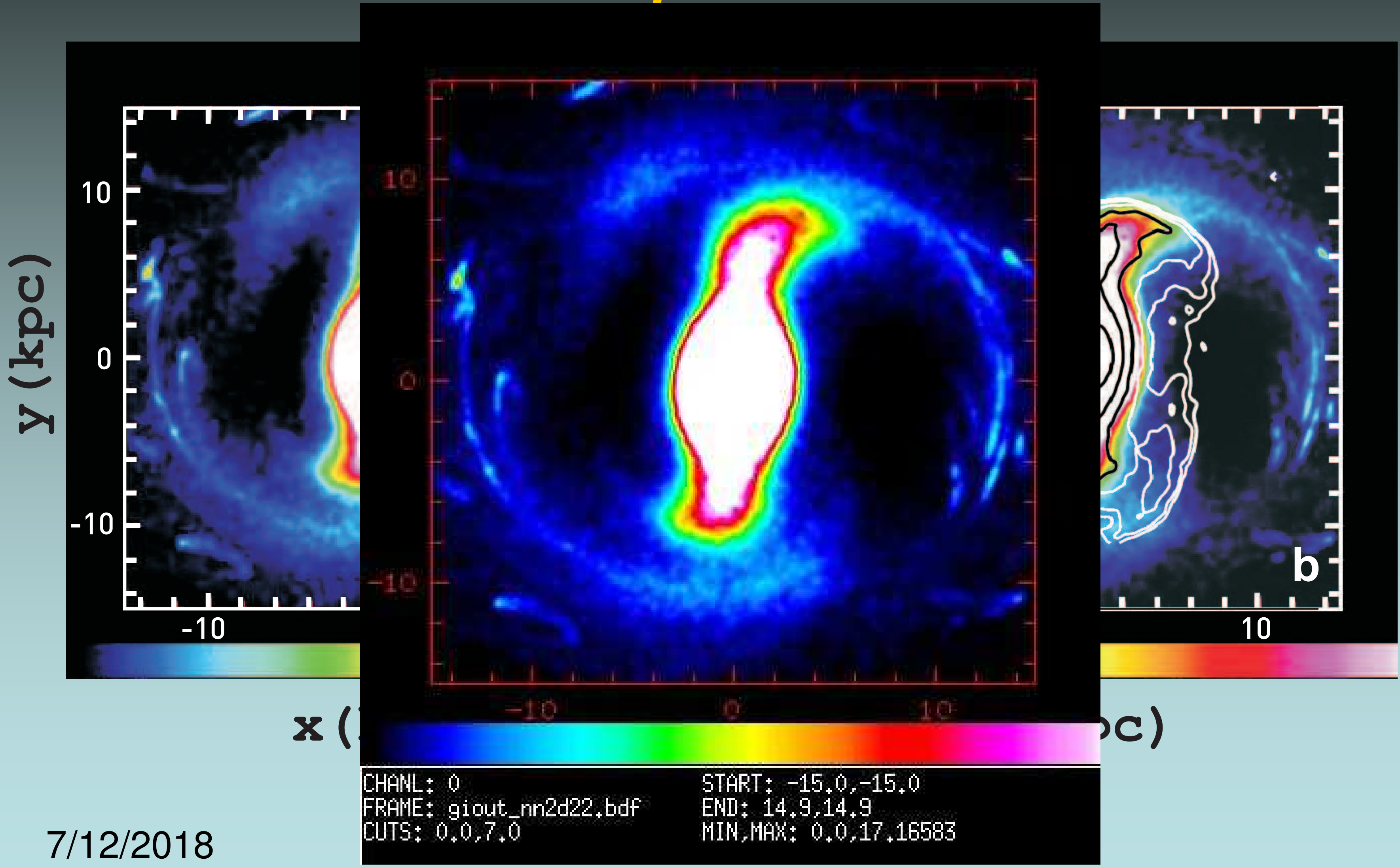

2d22: histograms

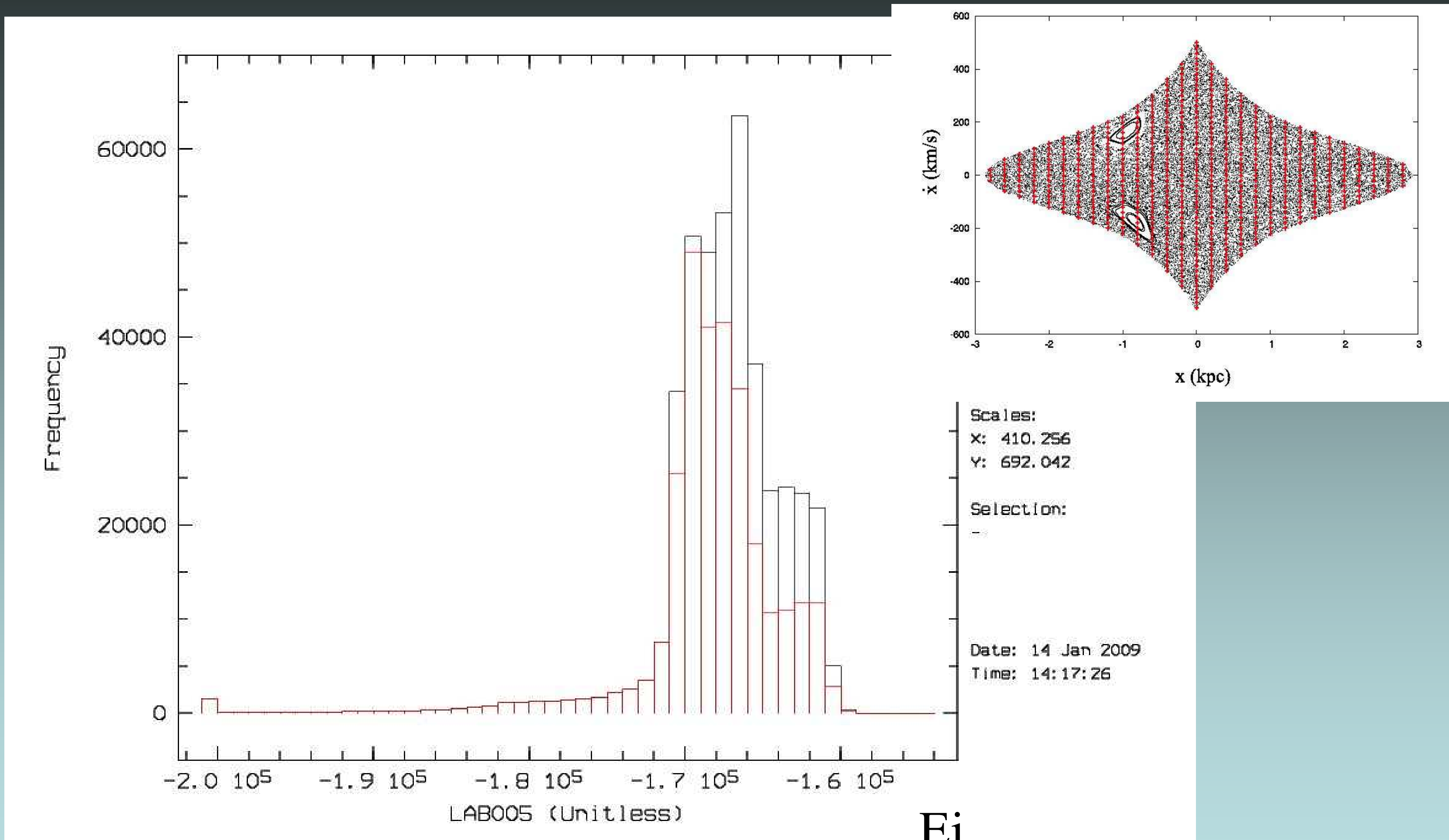

Ej

2d22: stable periodic orbits

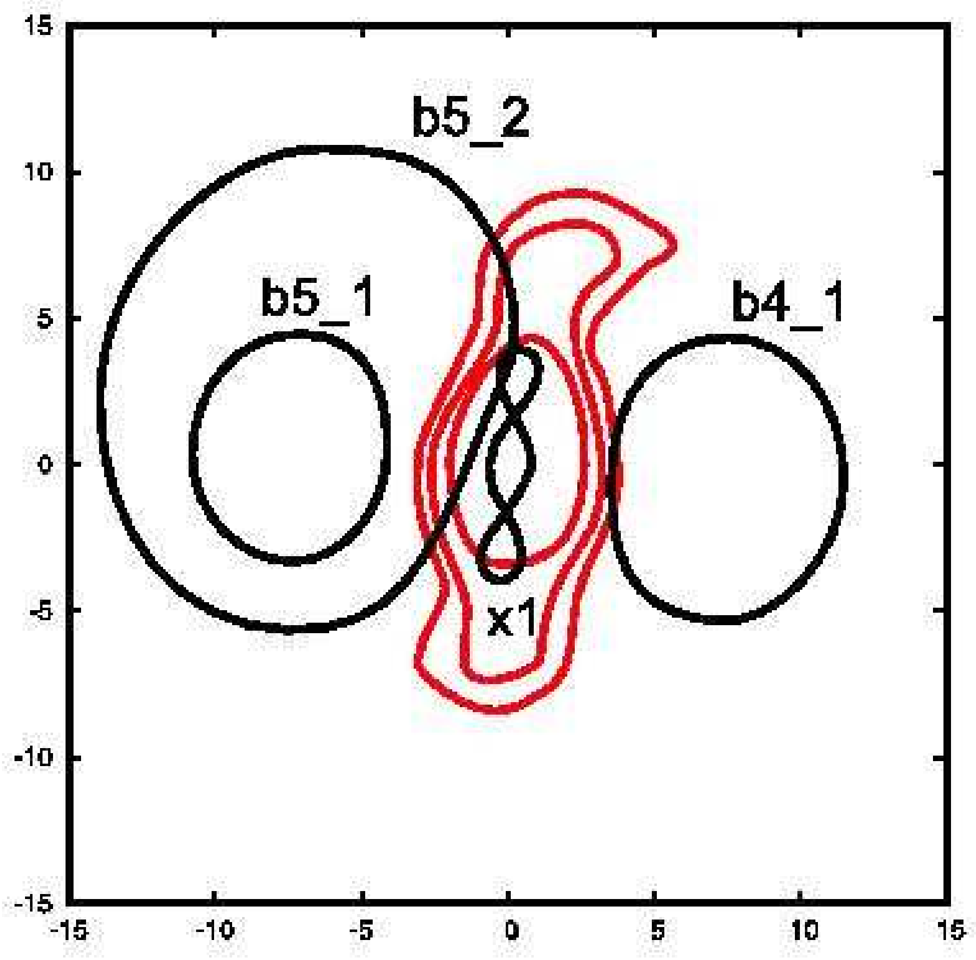

"chaotic" spirals

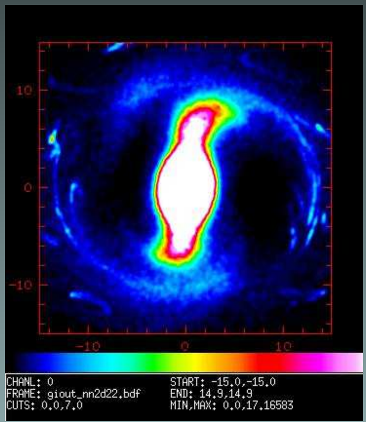

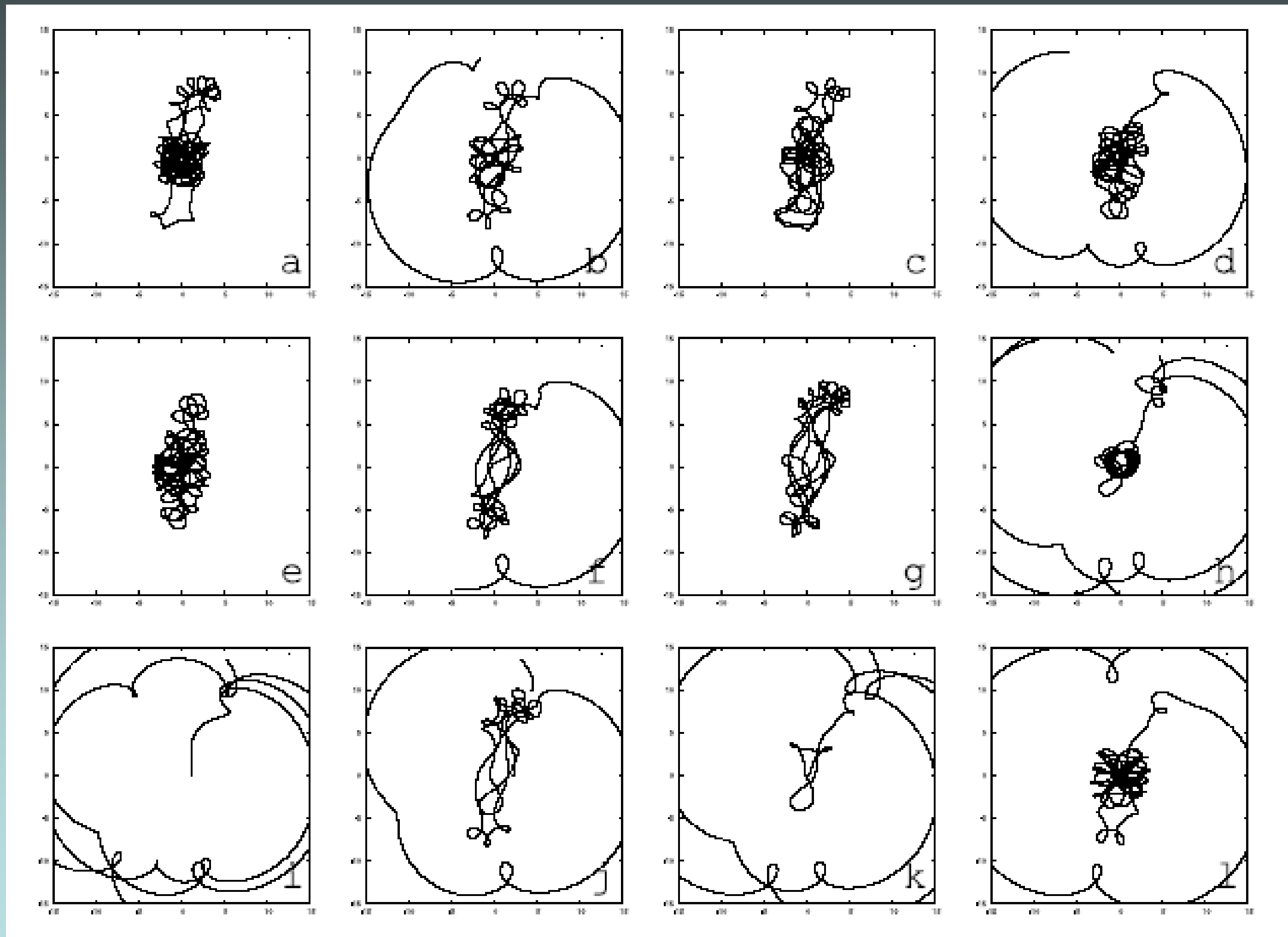

Regular motion is not the only way to build structures in galaxies

3D systems

Φ=Miyamoto disk + Plummmer sphere + 3D Ferrers bar

$$H = \frac{1}{2}(p_x^2 + p_y^2 + p_z^2) + \Phi(x, y, z) - \Omega_b(xp_y - yp_x),$$

with

$$\Phi(x, y, z)_{eff} = \Phi(x, y, z) - \Omega_b(xp_y - yp_x)$$

$$\dot{x} = p_x + \Omega_b y, \qquad \dot{y} = p_y - \Omega_b x, \qquad \dot{z} = p_z$$

$$\dot{p}_x = -\frac{\partial \Phi}{\partial x} + \Omega_b p_y, \quad \dot{p}_y = -\frac{\partial \Phi}{\partial y} - \Omega_b p_x, \quad \dot{p}_z = -\frac{\partial \Phi}{\partial z}$$

$$\Phi(x, y, z) = \Phi_D + \Phi_S + \Phi_B$$

4D space of section, i.c. (x,p_x,z,p_z) in the plane $y=0$ with $p_y>0$

Application in a 3D rotating galactic potential

$$\Phi_D = -\frac{GM_D}{\sqrt{x^2 + y^2 + (A + \sqrt{B^2 + z^2})^2}},$$

- Miy
  B=1

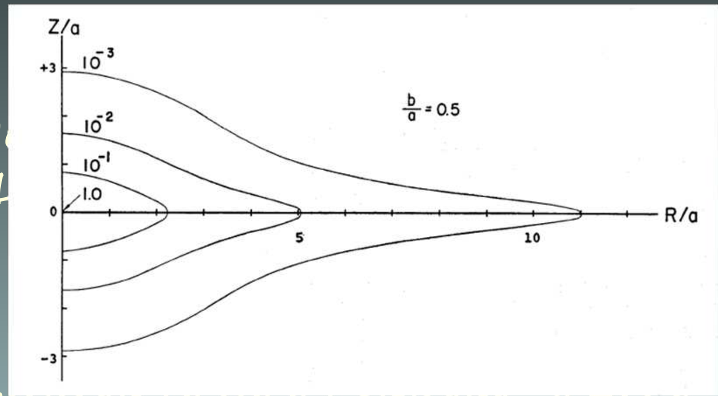

$$\Phi_S = -\frac{GM_S}{\sqrt{x^2 + y^2 + z^2 + \epsilon_s^2}},$$

- Plummer (1911) sphere, ϵ_s=0.4 kpc

$$\rho = \begin{cases} \frac{105 M_B}{32\pi abc}(1 - m^2)^2 & \text{for} \quad m \leqq 1 \\ 0 & \text{for} \quad m > 1 \end{cases},$$

where

$$m^2 = \frac{y^2}{a^2} + \frac{x^2}{b^2} + \frac{z^2}{c^2}, \quad a > b > c,$$

- Ferrers bar, a:b:c = 6:1.5:0.6

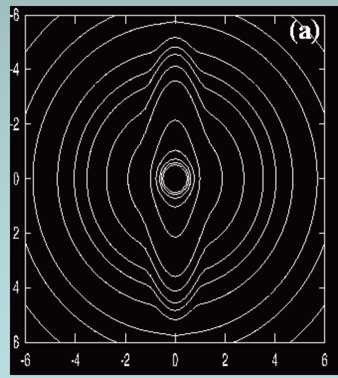

Linear Stability

The relation of the final deviations of this neighboring orbit from the periodic one, with the initially introduced deviations can be written in vector form as: $\vec{\xi} = M\,\vec{\xi}_0$. Here $\vec{\xi}$ is the final deviation, $\vec{\xi}_0$ is the initial deviation and M is a 4×4 matrix, called the monodromy matrix. It can be shown that the characteristic equation is written in the form $\lambda^4 + \alpha\lambda^3 + \beta\lambda^2 + \alpha\lambda + 1 = 0$. Its solutions $(\lambda_i, i = 1, 2, 3, 4)$ obey the relations $\lambda_1\,\lambda_2 = 1$ and $\lambda_3\,\lambda_4 = 1$ and for each pair we can write:

$$\lambda_i, 1/\lambda_i = \frac{1}{2}[-b_i \pm (b_i^2 - 4)^{\frac{1}{2}}],$$

where $b_i = 1/2\,(\alpha \pm \Delta^{1/2})$ and stability indices

$$\boxed{\Delta = \alpha^2 - 4(\beta - 2).}$$

motion is stable when all the roots of (44) are complex conjugate lying on the unit circle, and this happens when the following three inequalities hold:

$$\Delta > 0, \qquad |b_1| < 2, \qquad |b_2| < 2. \tag{49}$$

In all other cases the motion is unstable.

Simple instability

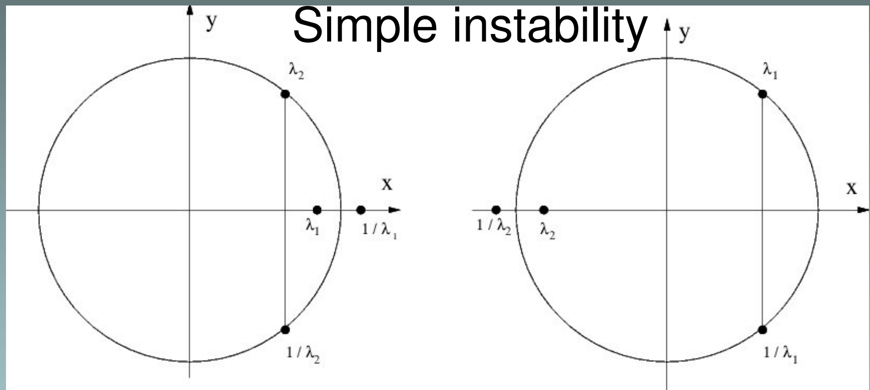

Complex instability

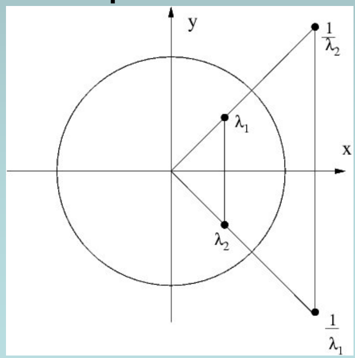

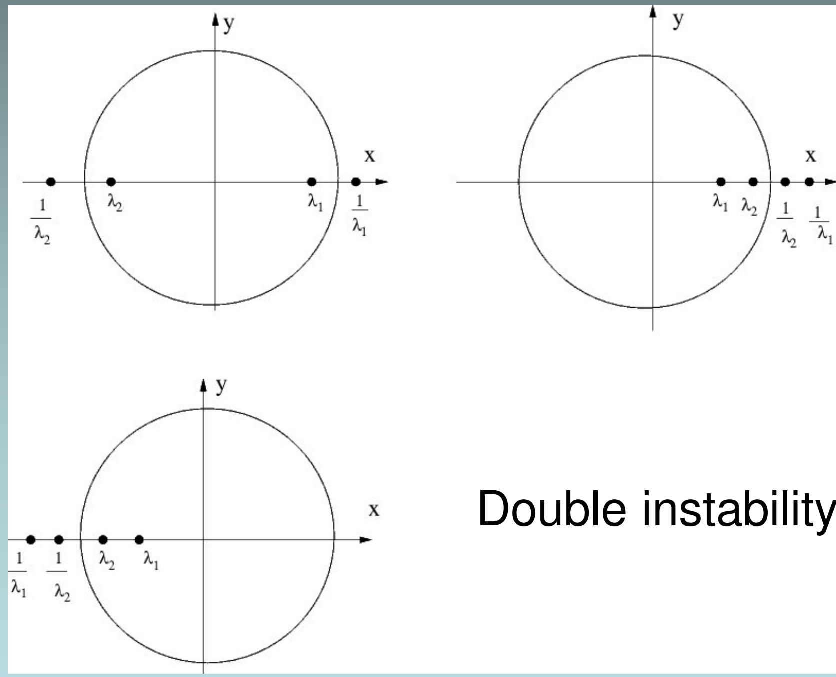

Double instability

Katsanikas et al. 2011-13, Int. J. Bif. Chaos

The structure of phase space
in the neighborhood of periodic orbits

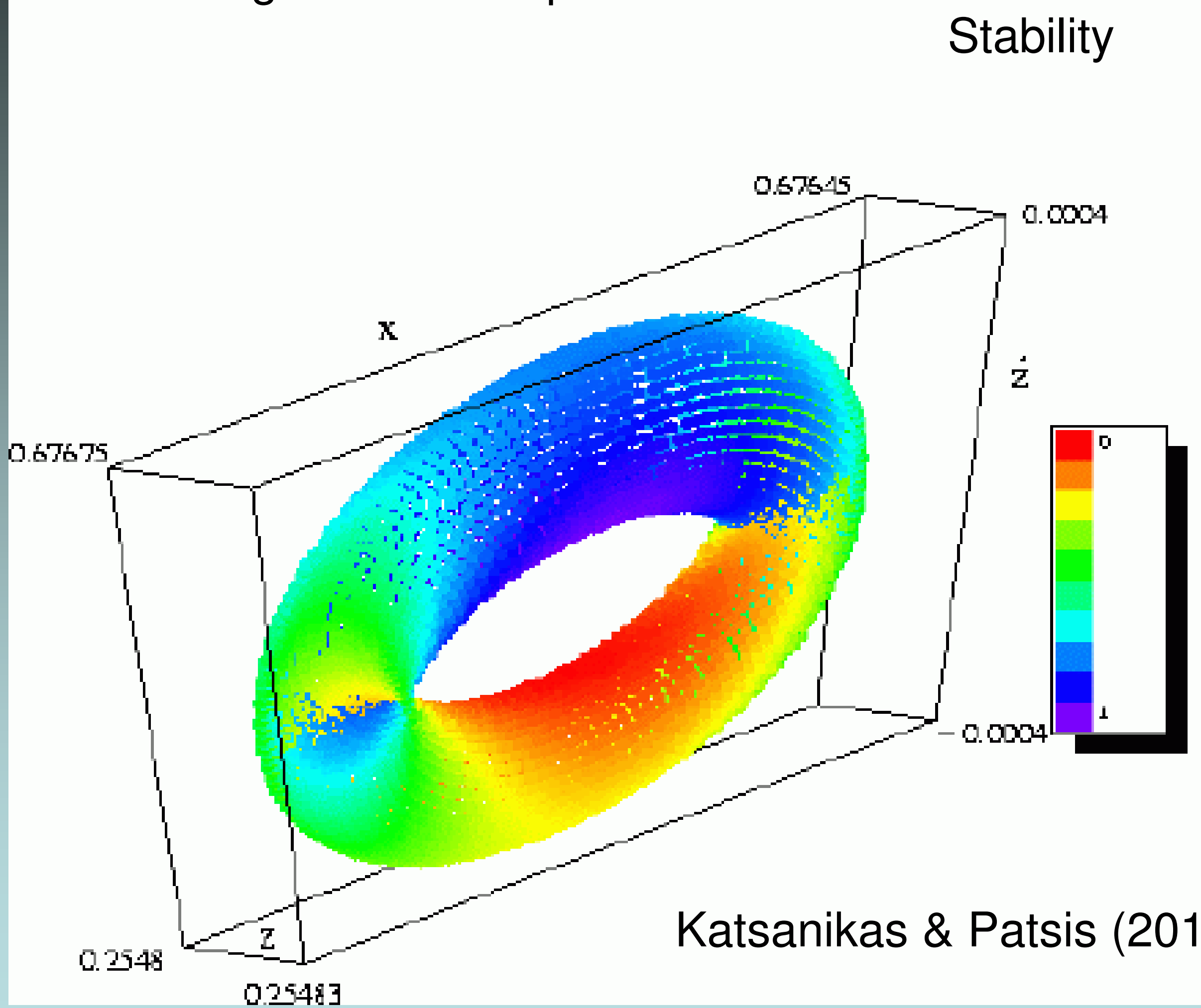

Katsanikas & Patsis (2010)

NGC 4710, α=12^h 49^m 38.9 , δ=+15° 9′ 56″

This natural-color photo was taken with the Hubble Space Telescope's Advanced Camera for Surveys on January 15, 2006

N-body peanuts I

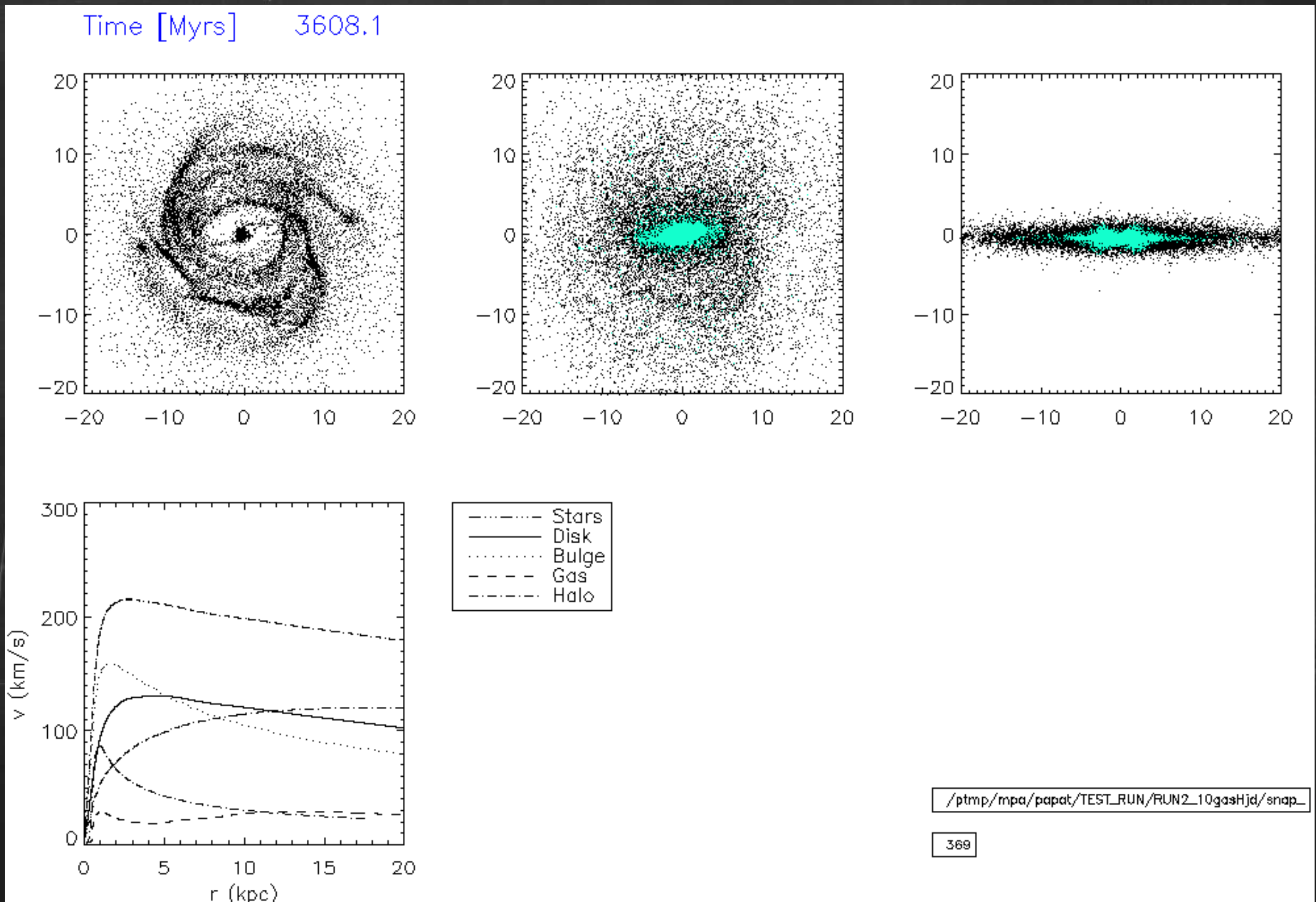

N-body peanuts II

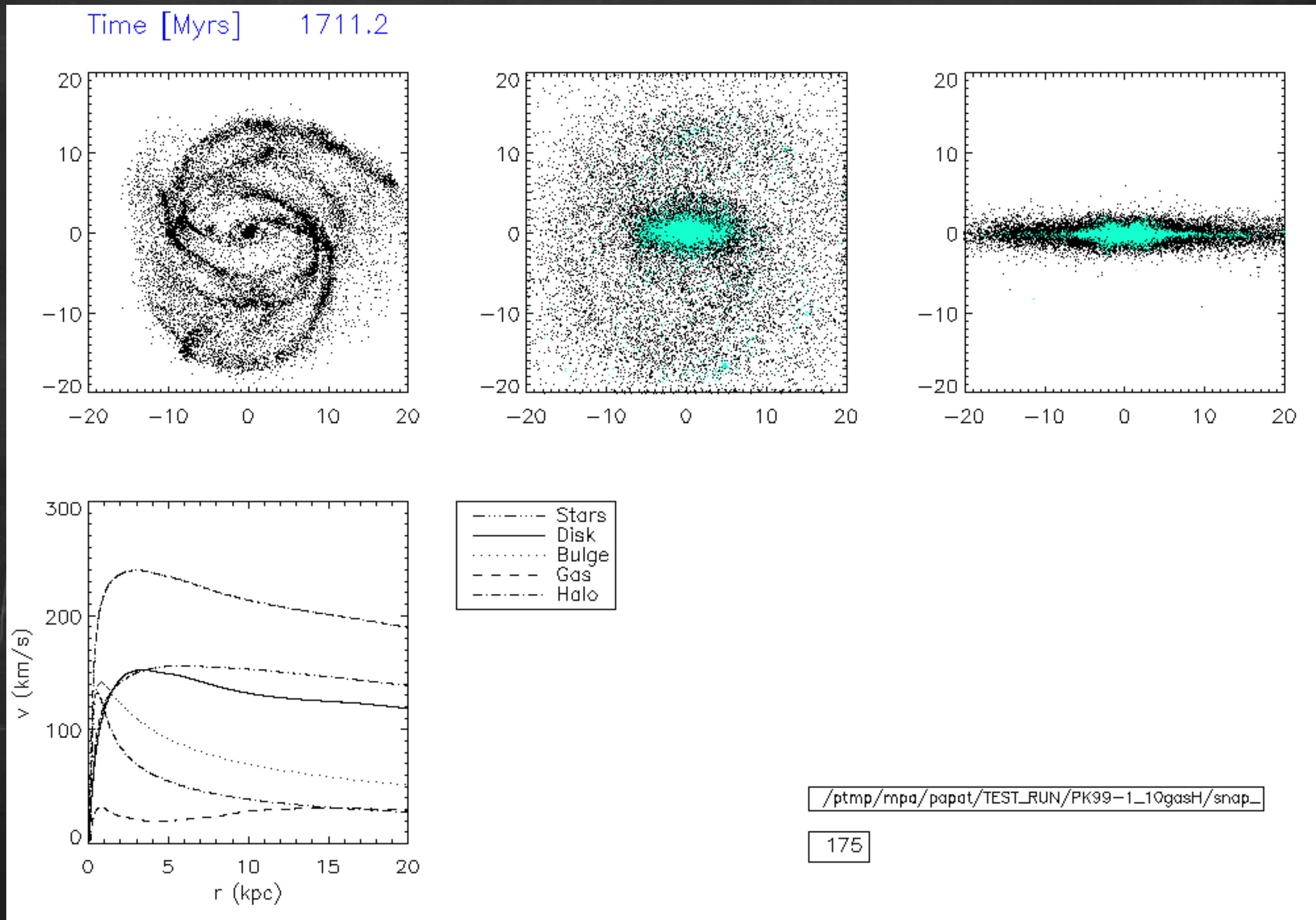

N-body peanuts III

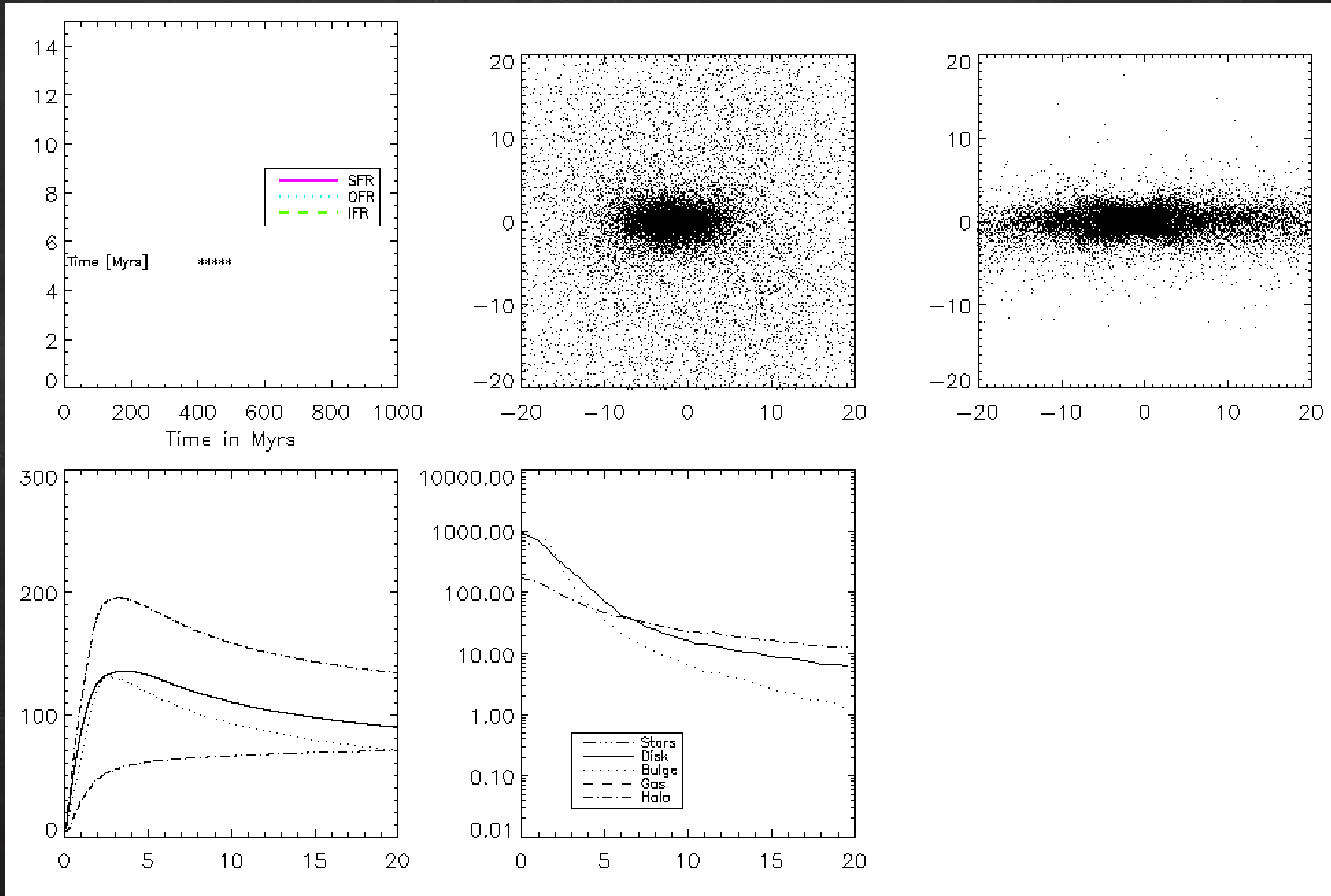

s/s from GADGET3 N-body simulation (Patsis & Naab 2018 – in preparation)

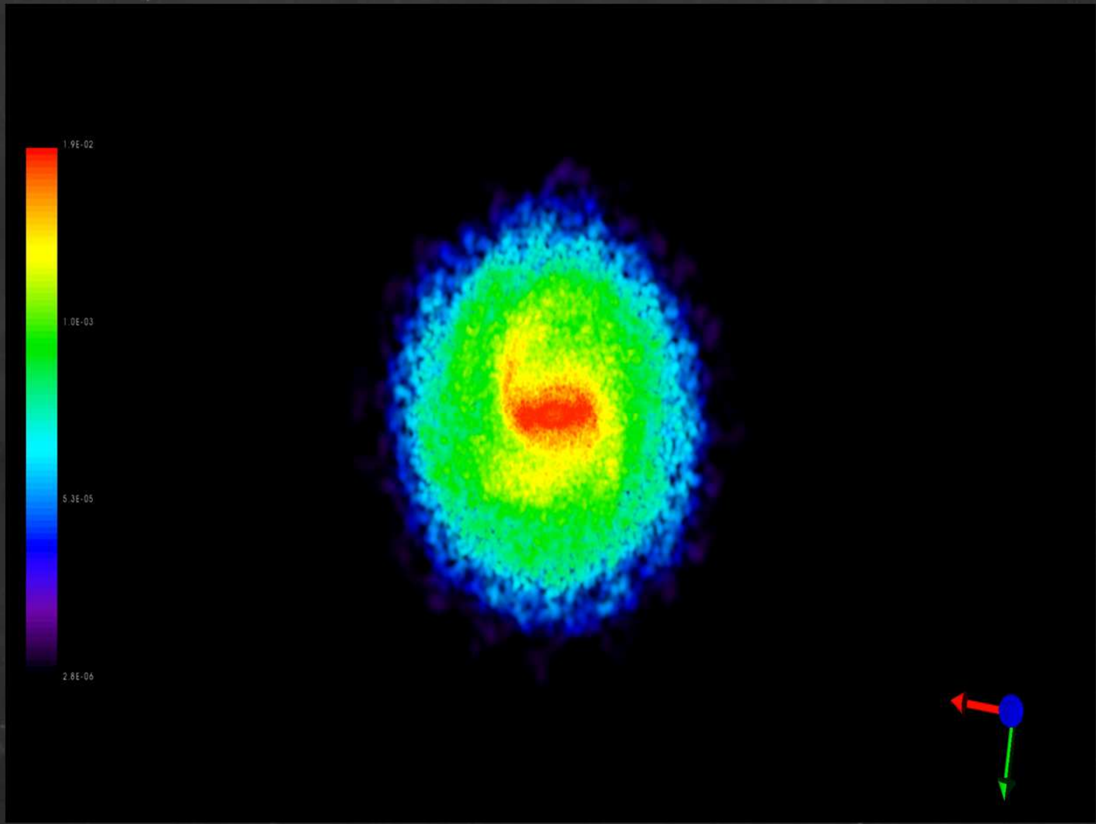

2 x 10^6 particles (DM, stars, gas, newborn stars)

NGC352 (Aristarchos telescope, Helmos, Greece)

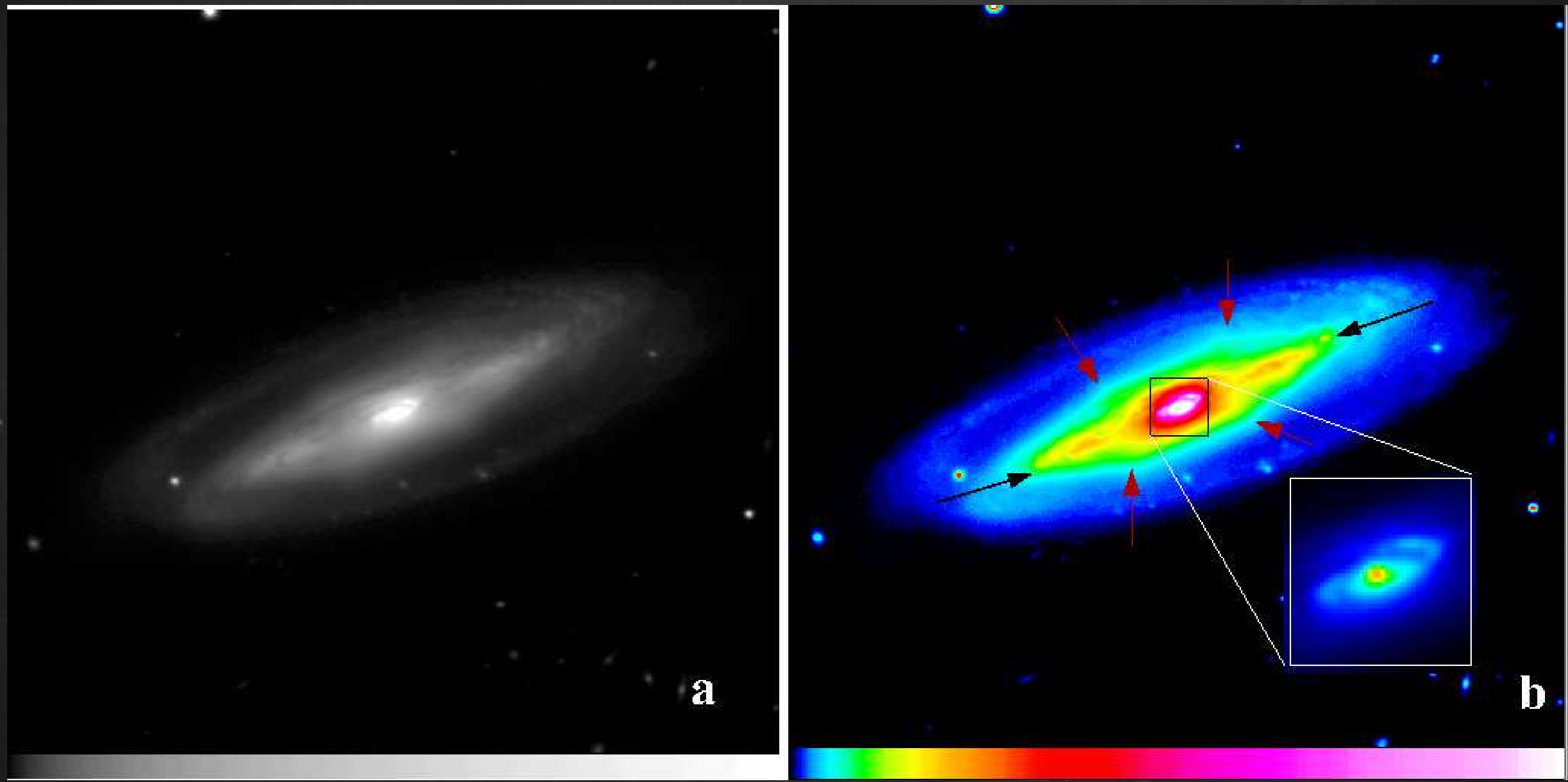

R filter. Patsis, Xilouris, Alikakos

N-body s/s (Athanassoula 2017)

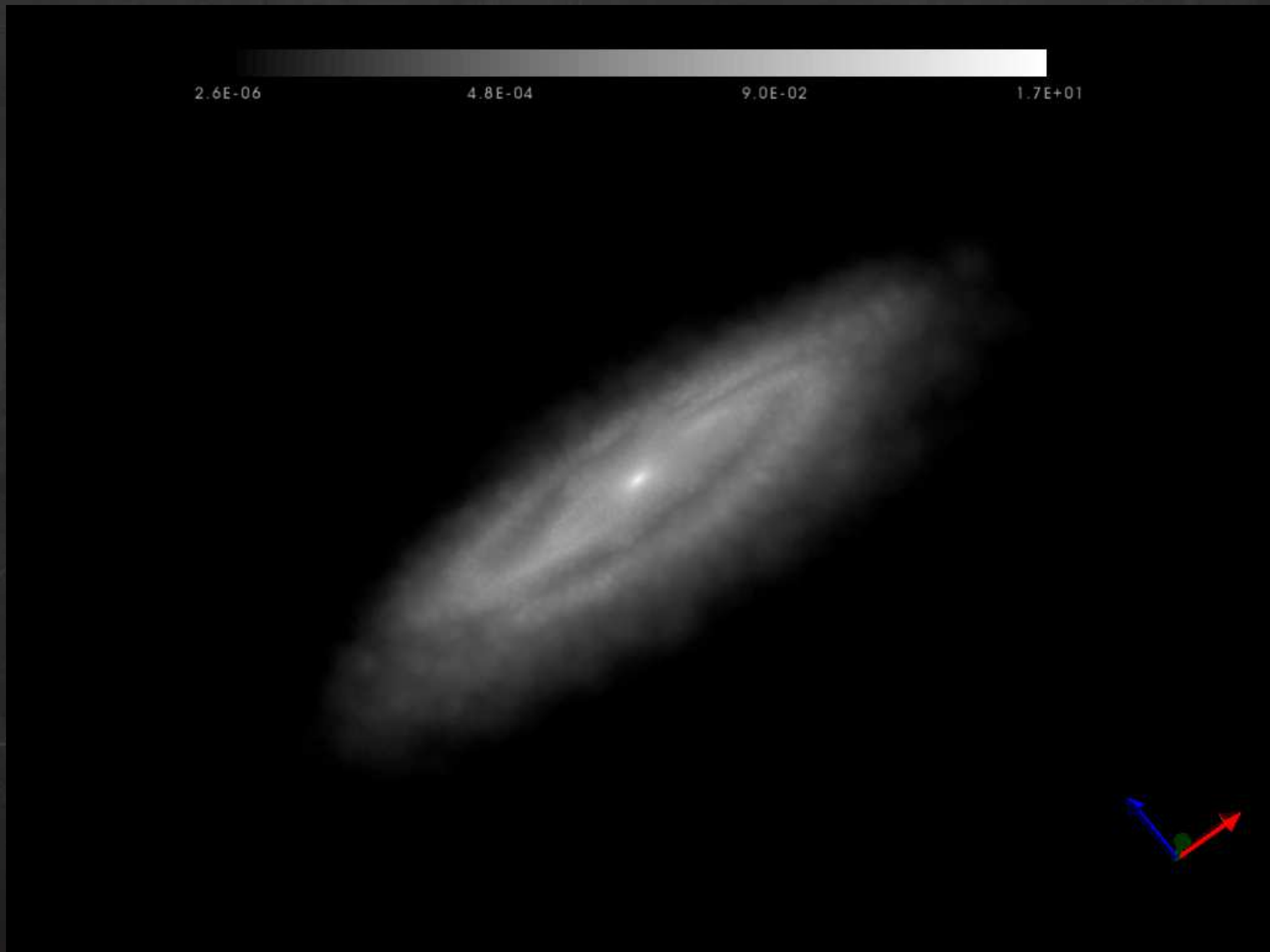

But also….

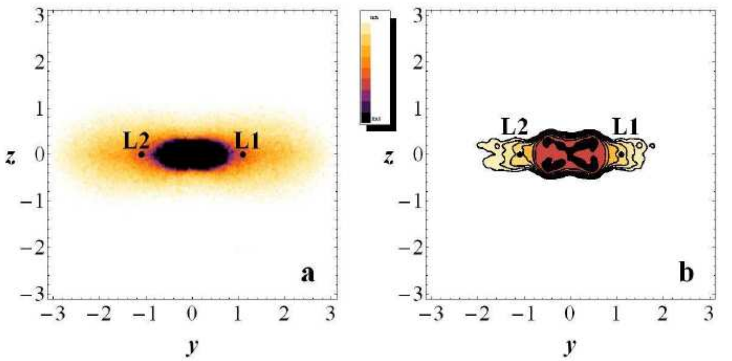

Fig. 2. (a) The side-on profile of the *N*-body model. (b) The side on profile consisting of orbits belonging to the 2:1 class in the corresponding frozen potential (Contopoulos & Harsoula 2013). The plotted isodensities in (b) emphasise the CX character of the profile. L1 and L2 indicate the location of the unstable Lagrangian points. Darker colour corresponds to more dense regions.

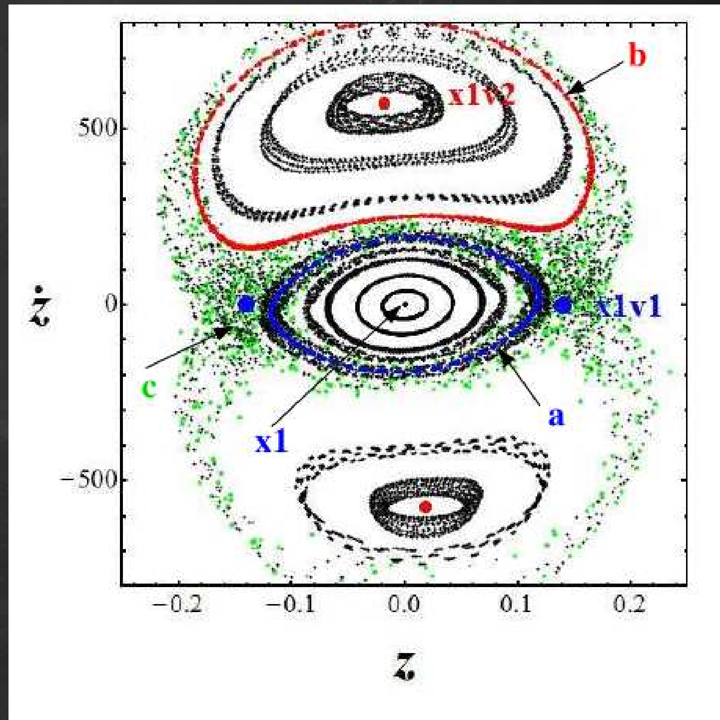

Patsis & Harsoula (2018)

1. Where does the b/p start?

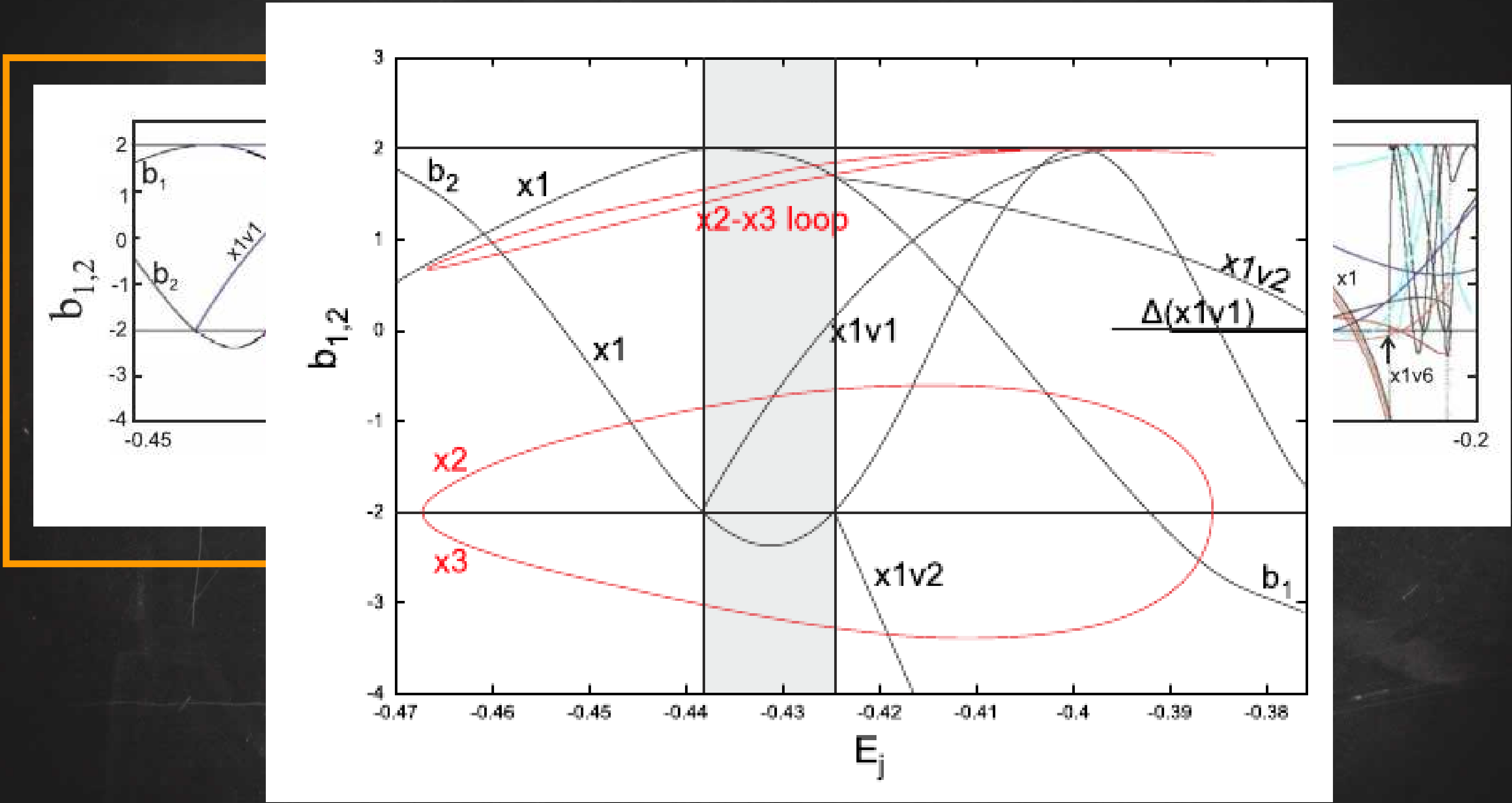

Bifurc … x1v1'

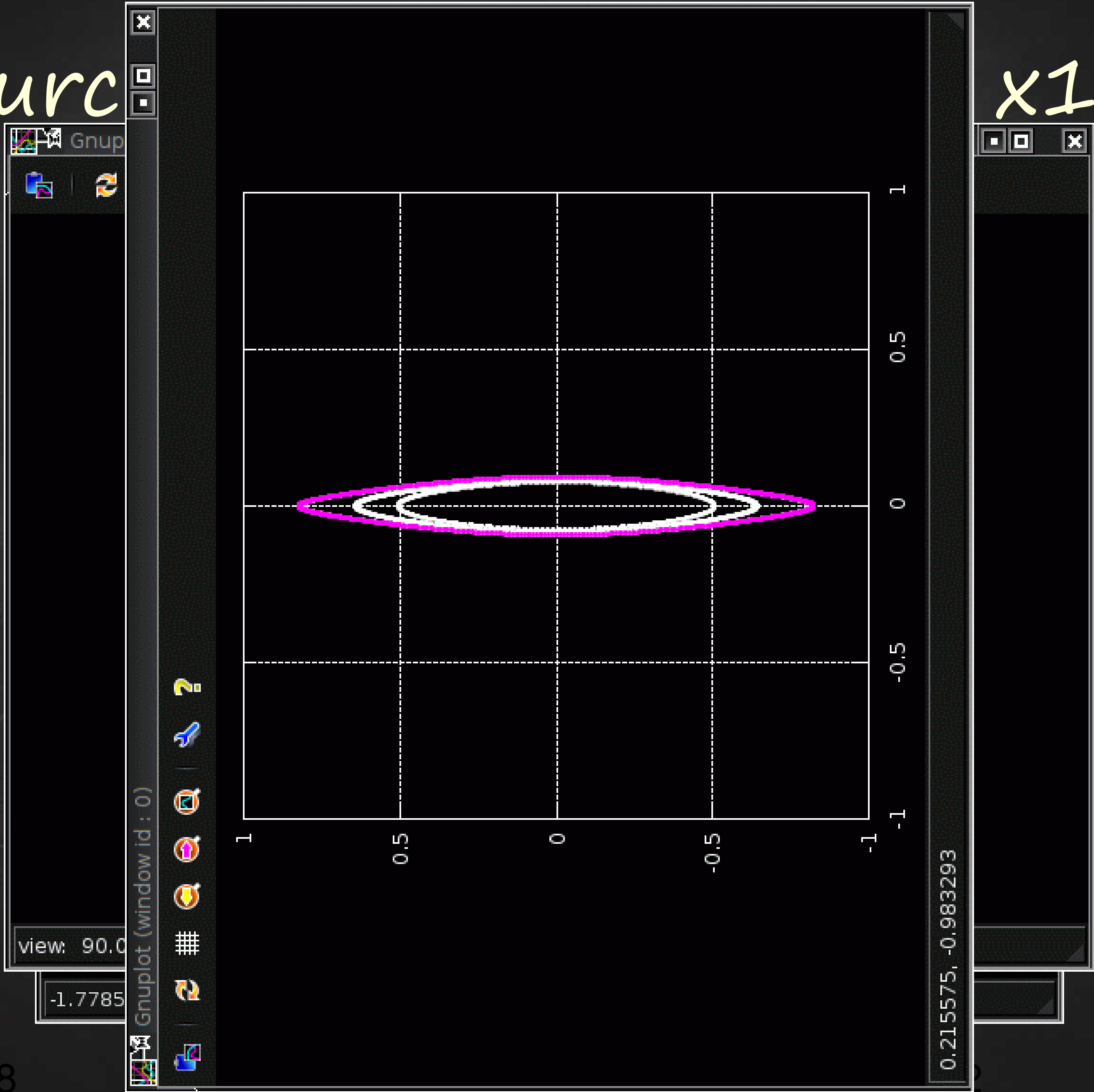

NGC1566-type response

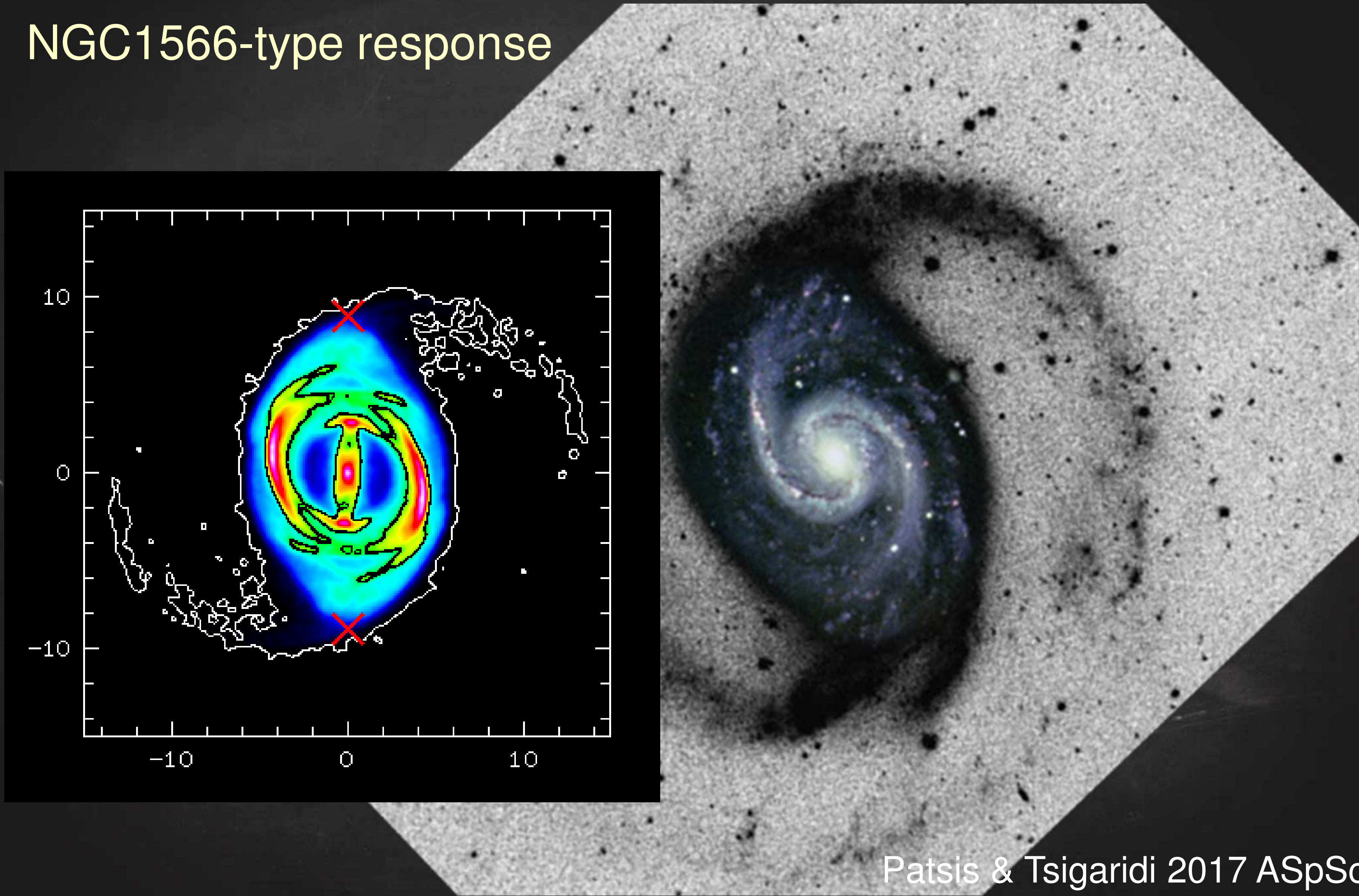

Patsis & Tsigaridi 2017 ASpSc

Summary

- p/b supporting orbital morphologies exist before the v-ILR. There is a continuity in the evolution of phase-space as Ej or perturbations vary approaching to/receding from the p.o.
- Dynamical mechanisms building peanuts: "x1v1 scenario", x1v1+x1v2, x1mul2

Summary

- Complex instability does not lead abruptly to chaos. In Galactic Dynamics chaotic orbits sticky to confined tori contribute to structure formation.
- Inner boxiness can be supported by q-p orbits and chaotic orbits sticky to x1v1 and x1v1' in the ILR region.

Ευχαριστώ για την προσοχή σας